March 2010

Reconfigurable Modular Mobile Robotic Platform (ReMMRP)

Daniel Raymond Garcia
Worcester Polytechnic Institute

Karl Bowen Wajcs
Worcester Polytechnic Institute

Matthew Richard Bienia
Worcester Polytechnic Institute

Reconfigurable Modular Mobile Robotic Platform

A Major Qualifying Project Report
Submitted to the Faculty
of the
WORCESTER POLYTECHNIC INSTITUTE
In partial fulfillment of the requirements for the
Degree of Bachelor of Science in
Robotics Engineering
on
3/16/10

by

Matt Bienia
mbienia@wpi.edu

Dan Garcia
dan.r.garcia@wpi.edu

Karl Wajcs
kwajcs@wpi.edu

proteanrobotics@wpi.edu

Approved:

_____

TaskinPadir

Project Number: RBE-TP1-RMP1

Acknowledgements

We would like to thank several people for their help throughout the duration of this project, without which this would not have been possible.

Atmel Corp. and The Fastener Source for their generous donation of electrical and mechanical components, respectively.

The Washburn Shops Faculty for the use of their time and resources.

Mike Niziol of MG Machine Co. for his generous donation of facilities and material for CNC machining.

Chip Bienia for his experience, time, and resources involving CNC manufacturing.

Ivo Dobrev for his knowledge and support in the development of robot kinematics.

Sam Kaplan and Kevin O'Brien for their dedicated work on the balance algorithm.

Professor Hugh Lauer for his expertise and instruction in distributed processing and data structures.

Professor Joseph Beck for his expertise and instruction in artificial intelligence.

And finally, Professor Taşkin Padir for continued support, ideas, and patience throughout the ups and downs that were encountered during this project.

Abstract

This project addresses the inflexibility of modern robotics by developing a modular robotic platform, capable of using various modules that can be added and removed to a base unit in a short amount of time. The scope of the project limited development of modules to a 3-DOF leg. The proof of concept was established by developing a main communications board capable of detecting attached peripherals, and individual leg circuit boards capable of full PID control utilizing inverse kinematics to precisely place the end of the leg. Mechanical issues prevented the leg constructed from being fully functional, however plans have been developed to address all issues found in the development of this platform.

Table of Contents

Acknowledgements ii

Abstract iii

Table of Contents iv

Table of Figures: vi

List of Tables: vii

Table of Equations viii

Table of Code Samples viii

Authorship ix

1. Introduction 1

1.1. Background 2

1.2. Report Organization 5

2. Methodology 6

2.1. Design Specifications 6

2.2. Robot Design: Mechanical 7

2.2.1. Leg Design 8

2.2.2. Gearbox 9

2.2.3. Hip Joint Design 12

2.2.4. Static Force Analysis 13

2.2.5. Chassis Design 15

2.3. Robot Design: Electrical System 16

2.3.1. Control System and Distributed Processing Overview 16

2.3.2. Leg Control Unit (LCU) Hardware 17

2.3.3. Main Communications Board (MCB) Hardware 23

2.3.4. Main Processing Unit (MPU) Hardware 26

2.3.5. Miscellaneous Electrical Considerations 28

2.4. Robot Design: Software and Control Systems 28

2.4.1. Communications Protocol 28

2.4.2. MPU Software & Operational Characteristics 37

2.4.3. LCU Software & Operational Characteristics 45

2.4.4. Software Model Diagrams 58

3. Results 63

3.1. Mechanical Design Revisions 64
3.1.1. Review of the Initial Design 65
3.1.2. Goals of the Revised Design 66
3.2. Electrical System Observations 74
3.2.1. LCU PCB Construction and Issues 74
3.2.2. MCB PCB Construction and Issues 75
3.3. Software Timing and Effective Control Frequencies 76
3.3.1. PID Loop Timing 77
3.3.2. Total Leg PID Loop Timing 77
3.3.3. Inverse Kinematics Timing 78
3.3.4. Forward Kinematics Timing 79
3.3.5. Total LCU Command Process Timing 79
3.4. Budget 80
3.4.1. Mechanical Budget 80
3.4.2. Electrical Budget 82
4. Future Work 84
5. Conclusion 85
6. References 86
7. Appendices 89
7.1. LCU Schematics 89
7.2. MCB Schematics 96
7.3. MPU Schematics 104

Table of Figures:

Figure 1: Kamimura Experimental Module (1) 2
Figure 2: Demonstration of Structural Disassembly and Reconstruction (3) 3
Figure 3: BigDog Robot (4) 4
Figure 4: Conceptual ReMMRP Illustration 7
Figure 5: Conceptual Leg Illustration 8
Figure 6: Conceptual Worm Gearbox Illustration 10
Figure 7: Conceptual Miter Gearbox Illustration 10
Figure 8: Miter Gearbox Design 12
Figure 9: Internal View of the Gearbox 12
Figure 10: Hip Joint Design 13
Figure 11: Static Force Calculation Figure. 14
Figure 12: The Robot Chassis 16
Figure 13: Labeled Top View of the LCU 17
Figure 14: Front and Back View of a Blank LCU PCB 22
Figure 15: Labeled Top View of the MCB 23
Figure 16: Front and Back Views of a Blank MCB PCB 26
Figure 17: Labeled Top View of the MPU 27
Figure 18: Front and Back Views of a Blank MPU PCB 28
Figure 19: Single Master / Single Slave Configuration 30
Figure 20: Single Master / Multiple Slave Configuration 30
Figure 21: Master / Slave Data Transfer 31
Figure 22: SPI Initial Single Byte Data Exchange 33
Figure 23: SPI Indexed Byte Transfer 33
Figure 24: Robot Coordinate Frame & Port Numbering 39
Figure 25: Base of Support and Robot Chassis Centroids 42
Figure 26: The Stabilizing Vector 43
Figure 27: Z-Constrained Leg Workspace 43
Figure 28: Leg Joint Coordinate Frames 46
Figure 29: PWM vs Analog Drive 53
Figure 30: Conceptual H-Bridge Diagram 54
Figure 31: Forward and Reverse Configurations of the Conceptual H-Bridge 55
Figure 32: PID Control Process Diagram 57
Figure 33: MPU Software Flow Diagram 59
Figure 34: LCU Software Flow Diagram 60
Figure 35: Integrated Software Control Flow Diagram 62
Figure 36: Completed Robot (1 Leg) 64
Figure 37: Conceptual Illustration of Revised ReMMRP Design 65
Figure 38: Side View Comparison of the previous gearbox (Top) and the new gearbox (Bottom) 67
Figure 39: Top view comparison of the previous gearbox (Left) and the new gearbox (Right) 67

Figure 40: Comparison between the old Thigh Plate (Top) and the new Leg Plate (Bottom) 68
Figure 41: Comparison View of the old HMA (Left) compared to the new design (Right) 69
Figure 42: Comparison View of the Current HCB (Left) and the Revised Design (Right). 70
Figure 43: Static Force Calculation for the Revised Design 70
Figure 44: Revised Chassis Short Plate CosmosXpress Results 72
Figure 45: Displacement of the Revised Short Chassis Plate 73
Figure 46: Chassis Long Plate CosmosXpress Results 73
Figure 47: Resulting Displacement of the Long Chassis Plate 74
Figure 48: Assembled LCU Board 75
Figure 49: Assembled MCB Board 76
Figure 50: Single PID Loop timing 77
Figure 51: Total PID Loop Timing 77
Figure 52: Inverse Kinematics Loop Timing 78
Figure 53: Forward Kinematics Loop Timing 79
Figure 54: Complete LCU Leg Motion Command Timing 79

List of Tables:

Table 1: Gearbox Trade Study 11
Table 2: Joint Motor Spec Comparison and Trade Study 19
Table 3: Graphic Comparison of LCU Connectors (11)(12)(13)(14)(15)(16) 21
Table 4: Comparison of ATMega164/324/644P Communication Modes 29
Table 5: Denavit-Hartenberg Parameters for ReMMRP Leg Modules 47
Table 6: Ziegler-Nichols Ultimate Gain Equations 57
Table 7: Design Specification Compliance 63
Table 8: Comparison of Current and Revised Motor Torques 71
Table 9: Mechanical Budget per Leg 81
Table 10: Single Purchase Material Budget 82
Table 11: LCU Itemized budget 83
Table 12: MCB Itemized Budget 83
Table 13: MPU Itemized Budget 84

Table of Equations

Equation 1: Motor 3 Torque 14
Equation 2: Motor 2 Torque 14
Equation 3: Motor 1 Torque 15
Equation 4: Minimum Joint 2 Angle for Horizontal Movement 15
Equation 5: Choose Function 41
Equation 6: Total Possible Leg Configurations of ReMMRP 41
Equation 7: Area of a Polygon 42
Equation 8: Polygon Centroid Equations (7) 42
Equation 9: Denavit-Hartenberg Homogeneous Transformation 46
Equation 10: Parameterized Sequential Homogenous Transformation Matrices 47
Equation 11: Homogeneous Transformation from Coordinate Frame 0 to Coordinate Frame 3 47
Equation 12: Transformation from Leg Coordinate Frame to Robot Coordinate Frame 48
Equation 13: Angular Position of the Horizontal Hip Joint 50
Equation 14: Angular Position of the Vertical Hip Joint 51
Equation 15: Angular Position of the Knee Joint 51
Equation 16: Linear Interpolation 55
Equation 17: Motor 3 Torque in Revised Leg 71
Equation 18: Motor 2 Torque in Revised Leg 71
Equation 19: Motor 1 Torque in Revised Leg 71

Table of Code Samples

Code Sample 1: Slave SBDE Communication Routine 36
Code Sample 2: Master SBDE Communication Routine 37
Code Sample 3: Forward Kinematics 50
Code Sample 4: Inverse Kinematics 52
Code Sample 5: PID Control 58

Authorship

Introduction..... All

Background..... KW

Methodology

Robot Design: Mechanical..... KW

Robot Design: Electrical System..... MB

Robot Design: Software and Control Systems..... DG

Results

Mechanical Design Revisions..... KW

Electrical System Observation..... MB

Software Timing and Effective Control Frequencies..... DG

Budget..... MB & KW

Future Work..... MB & KW

Conclusion..... All

1. Introduction

The development and control of (self-)reconfigurable and modular robotic platforms have emerged as a new research area in robotics within the past two decades. The field addresses new challenges that come with the design, modeling, implementation and control of autonomous robots whose kinematic structures can vary over time depending on the physical environment that they are in. The reconfigurable modular robots have two important features which make them desirable in applications; flexibility and robustness. They can adapt their shape and form with respect to changes in their environments and they can accommodate failures within modules provided that they possess redundancy.

A limitation to the field of robotics is that robots are designed to accomplish a specific task; this limits the versatility of these machines. The development of a modular robotics platform, specifically intended for rapid prototyping of autonomous systems, would promote the marketing of more products as well as the creation of more jobs in the assembly and testing of various configurations of the platform. Creation of various specialized units from a base of modular components would also allow any of these units to be quickly and easily repaired or reconfigured in the field.

The goal of this project is to design, construct, and demonstrate a reconfigurable mobile platform that addresses, at least in part, the issues outlined above. The project outcome will be a proof of concept for future development and commercialization of a reconfigurable mobile robot.

Within the scope of this project, the terms “reconfigurable,” “mobile,” and “modular” are defined as follows:

- A **reconfigurable** robot is one that is capable of attaining various configurations by the addition or removal of peripheral attachments (leg, arm, sensor, etc.) to predefined connection points existing on the robot chassis.
- A **mobile** robot is one that is capable of autonomous or controlled locomotion to change its relative position and orientation with respect to a global coordinate frame.
- A **modular** robot is one that is built using a variety of peripheral units employing standardized electrical and mechanical connections and communications.

1.1.Background

Reconfigurable robotics research has focused on design and implementation of multiple modules to work together to complete a goal. One recent work on reconfigurability focused on two blocks that are connected by a link that allows the two ends to rotate relative to the link (1)(2). On each surface of the module there are permanent magnets that connect two modules together into a robot. The module and an example configuration of modules is shown in Figure 1**.** The focus of the research was how the modules could combine to achieve a simple goal. A simple goal for the robot would be to walk on four legs or crawl along the ground. The results show how the robot can transform from the crawler configuration to the quadruped walker configuration. The robot does not dynamically calculate how it should configure itself or how to move itself. Instead a program was written that allows the robot's initial configuration and movements to be programmed into the robot. In addition the modules have zero sensing capability which means that the modules cannot adapt nor improve their movements (1).

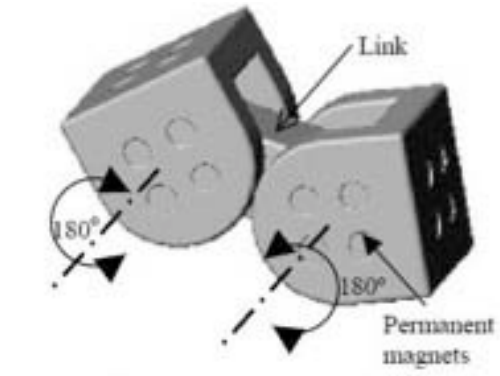

Figure 1: Kamimura Experimental Module(1)

A similar project, conducted at the Modlab of the University of Pennsylvania, demonstrates how a robot can detect an occurrence of structural disassembly and then proceed to repair itself(3). The entire robot consists of three modules using a Controller Area Network (CAN). Each module is controlled by a state machine with five states. The first state is connectivity where the module is able to communicate with other modules meaning that it is physically connected. The module will leave the first state if the system is structural deconstructed and enter the search state. The search state means that the module is looking for other modules to recombine with. The third and fourth states are the approach and dock states where two modules will eventually reconnect with each other. The final state is the walking state where all modules are combined and perform a walking gait. When the CAN was broken the robot would realize that it has undergone a structural disassembly. Using various range finders, a camera and LEDs, the modules can locate each other and come together. In this experiment the modules are identical in terms of function, which means that the modules do not have to be in their original configuration when reassembled. During this process, if two modules get reconnected, they share a master/slave control architecture. These modules will dock with the last module to complete the reconstruction and continue to perform its original task before the deconstruction occurred. This behavior is shown in Figure 2.

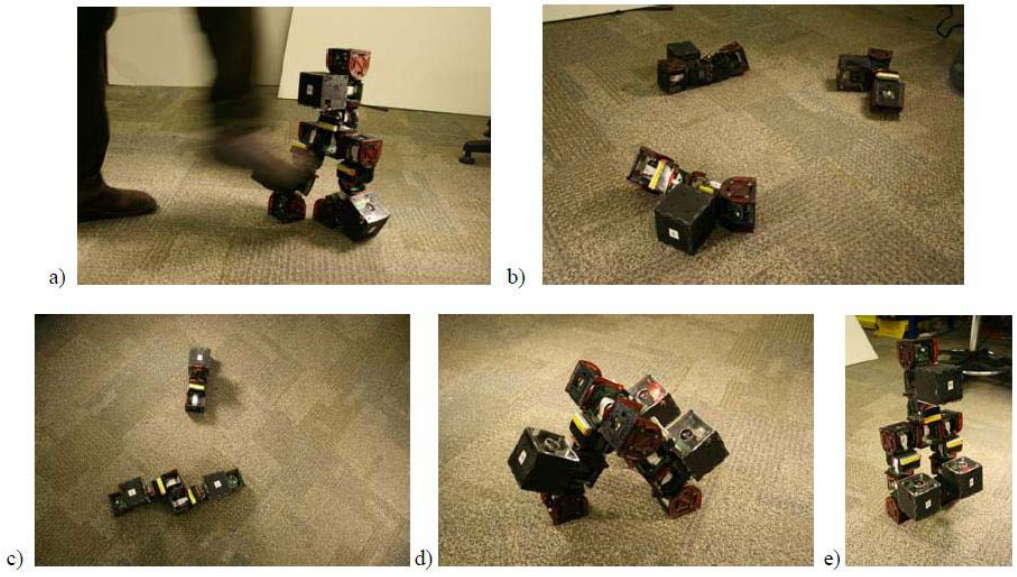

Figure 2: Demonstration of Structural Disassembly and Reconstruction(3)

BigDog is a quadruped robot being developed by Boston Dynamics for use in the United States military. BigDog is being designed for DARPA to function as a robotic pack mule for the US soldier. The robot must be able to navigate uneven and difficult terrain. The leg uses four hydraulic actuators to

control the position and movement. BigDog must be able to determine how it is interacting with its environment, how it is positioned in space and how to position its legs to achieve balance and the desired gait.

BigDog uses kinematics and the ground reaction forces generated by the robot as the basis for its control systems. BigDog uses 50 sensors to measure leg positions, accelerations and the various forces exerted and experienced by the robot. BigDog has different algorithms to handle different types of terrain like mud, snow or sand as well as handling different inclines. The robot must be able to uses its sensors to determine which type of algorithm to use and how to apply it. Although BigDog is controlled by a human, this is only used to give it a direction and speed of travel, all calculations for leg placement and balance is handled by the robot.

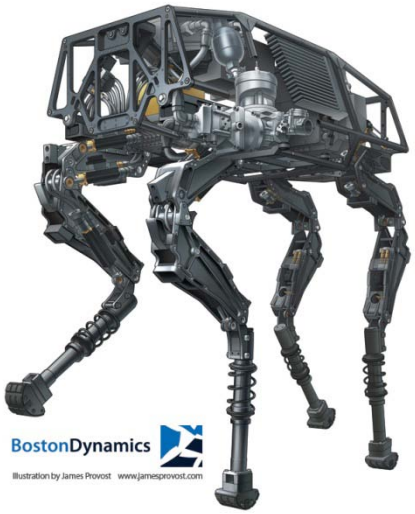

Figure 3: BigDog Robot(4)

The aforementioned robotic systems demonstrate reconfigurability, modularity, and mobility and illustrate the benefits of each idea as it applies to the advancing frontier of the robotics industry. The Reconfigurable Modular Mobile Robotics Platform (ReMMRP) takes the next logical step in innovation and combines these concepts into a robust, adaptive, plug-and-play robotic system. This report details the development of this platform and the integration of the mechanical, electrical, and software subsystems that make up the ReMMRP.

1.2. Report Organization

This report is broken down into the following sections:

- Methodology, separated into the following components:
  - mechanical
  - electrical
  - software
- Results
- Future Work
- Conclusions

2. Methodology

The ReMMRP explores the integration of the concepts of reconfigurability, modularity, and mobility in a single robotic platform. In order to achieve this goal, the robot must be able to accept peripheral leg modules, recognize their presence and location, and coordinate their actions. The ReMMRP must have:

- a base unit, or chassis, that serves as a common connection hub for all peripheral modules.
- leg modules capable of supporting the robot chassis and allowing mobility in three dimensions.
- the ability to detect addition or removal of peripheral modules in real time.
- the ability to control peripheral modules in real time.
- the ability to determine if the present configuration is balanceable, and if so balance.

2.1. Design Specifications

In order to meet the requirements outlined in Section 2, specifications for the mechanical, electrical, and software systems of the leg modules and chassis must be as follows:

- Chassis:
    - The chassis will have 12 connection points – 2 on each short side, 4 on each long side.
    - The chassis must contain a centralized power distribution and communications hub.
    - The chassis must contain a processor responsible for coordinating the actions of all peripheral modules, referred to as the Main Processing Unit (MPU).
    - The MPU must be interchangeable.
    - MPU software must determine actions for all peripheral modules and delegate commands to them in real time.
    - The chassis must have a dedicated processor responsible for detecting the addition or removal of peripheral modules in real time independently of the MPUs operation, referred to as the STATUS processor.
    - STATUS processor software must operate in real time, allowing MPU to have immediate knowledge of attached peripherals at any given time.
- Leg Modules:
    - The legs modules will have 3 degrees of freedom (DOF)
    - The leg must operate in 3-dimensional space.

- The leg must have position sensors integrated into each joint.
- The joint motors must be mounted internally in each leg link.
- Each leg module must have self-contained control system, referred to as a Leg Control Unit (LCU).
- The LCU must have a processor capable of handling the software controls.
- The LCU must distribute power to joint motors and read joint position sensors.
- The LCU must be able to relay signals to the main control system.
- LCU software must respond to commands from MPU with higher priority than any other task inherent to LCU software.
- Communications protocol must exist for data transfer among the MPU, STATUS processor, and LCUs).

2.2.Robot Design: Mechanical

Figure 4 is a conceptual illustration of the ReMMRP in a four-legged configuration. The chassis and legs can clearly be seen, as well as the 12 peripheral connection ports around the perimeter of the robot.

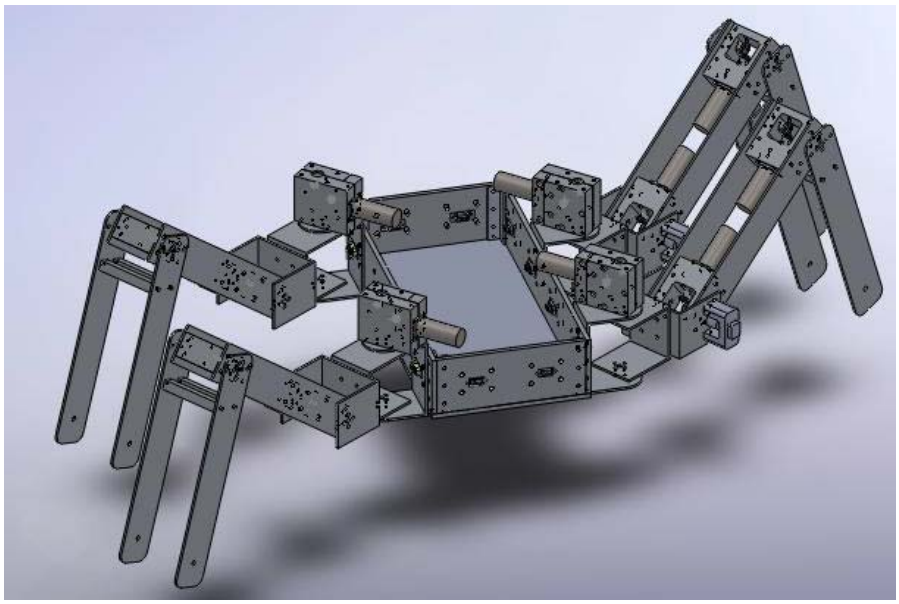

Figure 4: Conceptual ReMMRP Illustration

The leg modules have three degrees of freedom (DOF). The entire leg must be able to rotate horizontally with relation to the chassis, and the upper (thigh) and lower (calf) links must be able to

rotate vertically with relation to the chassis. The robot must be able to determine each link's position, therefore the leg must have sensors integrated into the design. The chassis will have 12 connection points around its perimeter. There will be two ports on each short side, and four on each long side. The long side of the chassis will be twice the length of the short side.

In order to provide the legs the greatest movement possible and to reduce collisions, the joint motors must be mounted internally in each leg link. However to achieve this specification, the motors will be perpendicular to the axis of rotation. In order to transfer the motor's rotation to the leg joint a gearbox is necessary.

2.2.1. Leg Design

The main peripheral design of the robot is a three DOF leg module and consists of a calf link, a thigh link, and a hip joint. The leg module is shown in Figure 5**.**

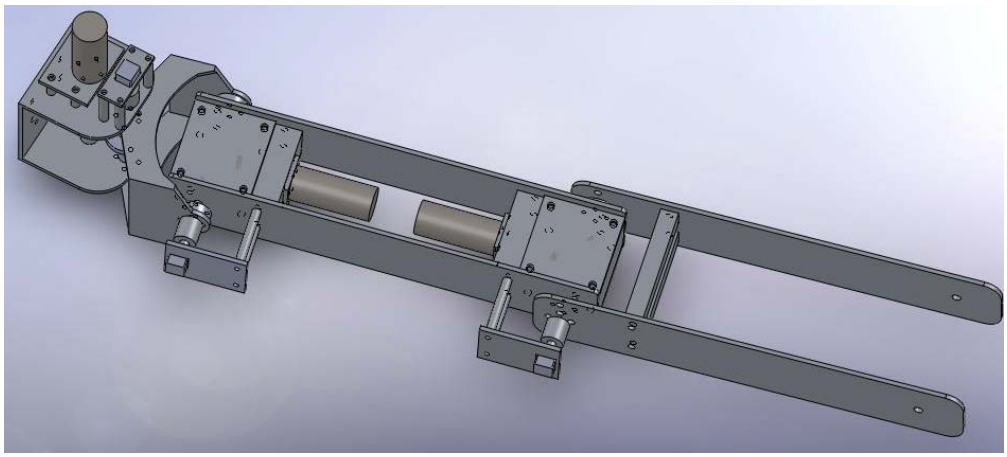

Figure 5: Conceptual Leg Illustration

The calf link is constructed out of two identical plates of sheet metal. Each plate is connected to the drive shaft exiting the gearbox by set screw hubs, which are mechanical connectors that attach to the calf plates and use a radial set screw to secure itself to the shaft. The calf link has braces to secure the two plates together and provide structural stability.

The thigh link contains two of the three leg motors. One motor is used to rotate the calf link and the other is used to rotate the thigh link. Two identical metal plates are used to join the two motors together. The thigh link is also used to secure the potentiometers (see Section 2.3.2.4 for sensor choice). The potentiometers are connected to the motors' output shafts using shaft couplers. The potentiometers on the two vertical joints are mounted to rectangular pieces of 1/8" sheet aluminum

which are secured to the thigh link by two #6-32 screws which use spacers to set the potentiometer at the correct distance from the thigh link.

The hip joint of the leg module is constructed from two machined pieces of aluminum tube stock. One piece is connected to the robot chassis and has the port connector. This piece allows for the horizontal rotation of the leg. The other piece connects the thigh link to the hip joint. This piece allows for the vertical rotation of the leg from the hip.

2.2.2. Gearbox

Commercial gearboxes fall into two distinct categories. The first are those designed for industrial applications, and the second are those designed for robotic hobbyists. The industrial gearboxes are typically large, weigh several pounds, and are designed for higher torque applications than required by the ReMMRP. The hobbyist gearboxes are designed for simple robots and made of cheap plastic. The gearboxes would break under the loads of this robot and are therefore unsuitable. As a result, ReMMRP uses a custom gearbox. Due to the fact that the gearboxes are a custom design, the leg will be designed around this gearbox. There are two types of gears that can be used for the gearbox: a worm gear and a miter gear. Each gear type has advantages and disadvantages as will be discussed below.

2.2.2.1. Worm Gearbox

The first gearbox design considered for the project is a worm gear system. The primary reason for the use of the worm gears is to make the legs non-backdriveable. The non-backdriveability would require less power to be consumed by the motors as the motors would not have to constantly be correcting the leg position of the robot. Worm gears typically have a high gear ratio, meaning that a weaker motor could be chosen when compared to a gear train with little or no gearing down.

This gearbox is made from two identical but mirrored parts forming a clamshell design. Figure 6 shows half of a conceptual gearbox design. Each half has two pockets to accommodate the gears. The machining required to make this design would be a series of pocketing operations. Given the precise nature of the gear set, the clearance holes for the axles require high tolerances (±0.0005 in.) which will add complexity to the machining process.

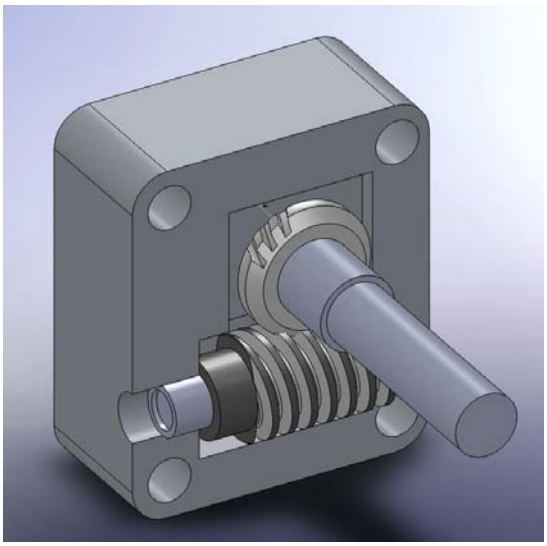

Figure 6: Conceptual Worm Gearbox Illustration

2.2.2.2. Miter Gearbox

The other choice for the gearbox is miter gears. Unlike the worm gears, miter gears allow the leg to be backdriveable. The use of miter gears will not limit the potential of the legs to explore other fields of research such as zero force control. During testing of the leg, the miter gears will also allow the leg to be manually positioned instead of being forced to drive the motors to the desired position. The manufacturing of this gearbox requires a single pocket for all the gears to be seated in which simplifies machining. Figure 7 shows a conceptual version of the miter gear box.

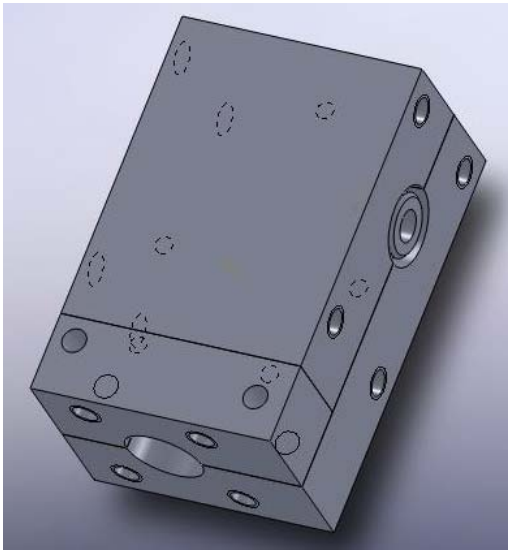

Figure 7: Conceptual Miter Gearbox Illustration

2.2.2.3. Gearbox Selection

In order to select the best type of gear for the design a trade study is conducted as shown in Table 1. The trade study has three categories for each gearbox type to be rated on. The categories are cost, torque and ease of manufacturing. Each of these categories is given a weight of 1-5 based on their importance. The two gearbox types are then given a rating on each category. The rating and the weight are multiplied together for the final score. These scores are then added together.

	Worm Gearbox	Miter Gearbox
Cost (2)	2 * 2 = 4	3 * 2 = 6
Torque (3)	4 * 3 = 12	3 * 3 = 9
Manufacturability (4)	2 * 4 = 8	3 * 4 = 12
Total	24	27

Table 1: Gearbox Trade Study

According to the trade study, the miter gear is the better gear choice for the gearbox. Both types of gears are close in price. The worm gear can have high gear ratio, but miter gears can also increase their torque output with a modified gear ratio. Manufacturing a miter gear box is also easier to do. Therefore, the miter gearbox will be used to construct the leg modules.

2.2.2.4. Gearbox Design

The gearbox consists of three parts. The design centers on a single piece of solid aluminum stock as seen in Figure 8. The other two parts are sheet metal covers, thus creating a sandwich design for the gearbox which is seen in Figure 9. The stock has a single pocket that goes through the entire piece of metal. The pocket allows both gears to be added to the pocket, but not in mesh. The gears can be moved into position and set into place once the entire gearbox is assembled. The two pieces of sheet metal seal the gearbox to keep the grease in and foreign particles out.

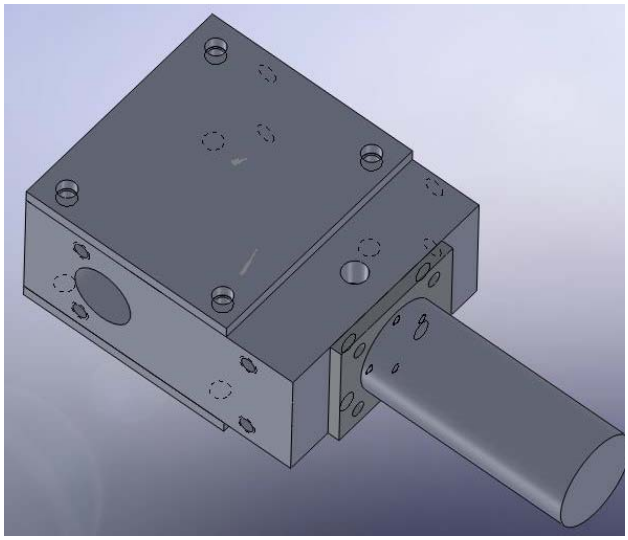

Figure 8: Miter Gearbox Design

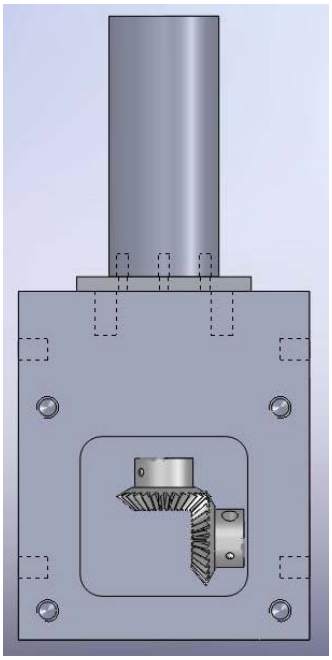

Figure 9: Internal View of the Gearbox

This gearbox has several advantages. The screw pattern on the top and bottom face of the gearbox gas only 4 screws for easy attachment of cover plates. The sizes of the screws are standardized to a single size of 6-32, which minimizes the number of different tools necessary to machine and assemble the part. The pocket of the gearbox also relies on looser tolerances. Often end-mill cutters will undercut the pocket which has the potential of forcing the gears out of their meshed position. By increasing the dimensions of the pocket it reduces the impact undercutting will have and decrease machining time. The gearbox design utilizes press fit ball bearings for easy manufacturing and assembly.

2.2.3. Hip Joint Design

The hip joint is responsible for the horizontal motion of the leg and is shown in Figure 10. The motor that controls horizontal motion of the hip joint is not constrained to fit within the confines of a leg link and is free to be mounted in any position. The motor can directly drive the axle to rotate the leg and no gearbox is necessary. Using a single axle to rotate the leg is ideal, however it makes the mounted potentiometer extend below the chassis. Mounting the potentiometer in this position will increase the chance that the potentiometer may be damaged during operation. The solution is to use two axles to achieve the motion. One axle is driven by the motor and this motion is transferred to a second axle via spur gears. The second axle then rotates the leg and is connected to the potentiometer on top of the joint. Using this configuration places the potentiometer in a position where it is least likely

to be damaged. The hip joint is made from two pieces of aluminum tube stock nested inside one another.

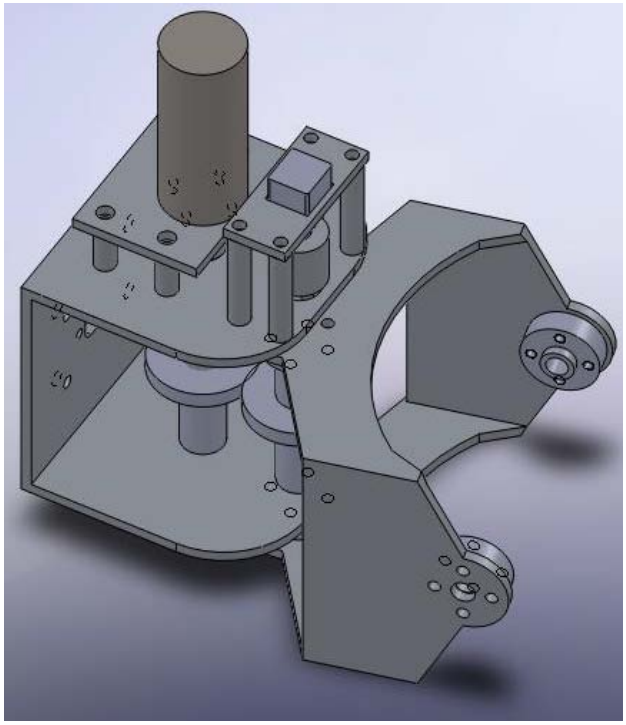

Figure 10: Hip Joint Design

2.2.4. Static Force Analysis

The forces involved must be known before the motors can be selected. The force calculations are done in units of oz-in. Also, the calculations will be done with each link fully extended and parallel to the ground, which means that the calculations will be for the maximum torque. Each plate has a length of 12 inches and weighs 4.64 oz. The gearboxes weigh 23.36 oz., and the center of mass is .75” from the axis of rotation towards the center of the thigh link. The axis of rotation is 7/8” from the end of the plate, giving the calf plate a functional length of 11.125” and the thigh plate a length of 10.25”. Figure 11 is given for a reference of the leg module.

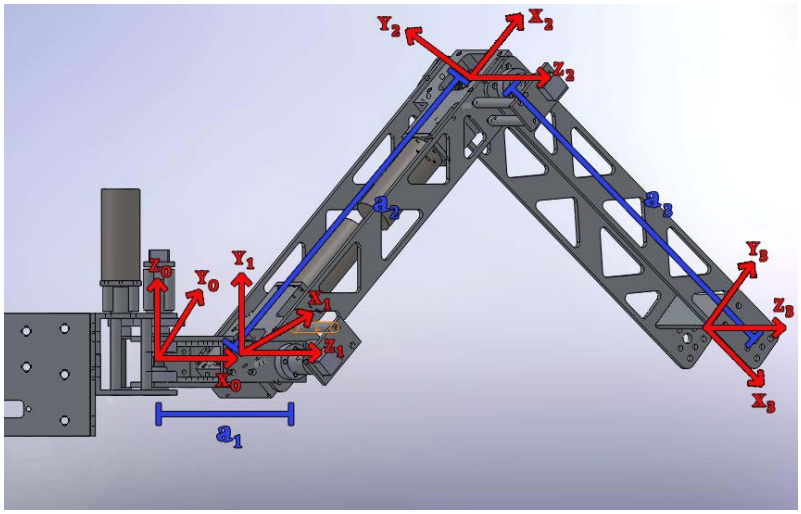

Figure 11: Static Force Calculation Figure.
Note: The leg shown is the revised version of the leg as described in Section 3.1.

The analysis starts by calculating the torque required to rotate the calf plate. The weight of the calf link is 9.28 oz and is 11.125" long. Assuming the force of the link is acting half of the length, the torque is:

Equation 1: Motor 3 Torque

$$M_2 = \frac{11.125}{2}\ in * 9.28\ oz$$

$$M_2 = 51.62\ oz\text{-}in$$

Continuing to coordinate frame 1, this motor has to rotate not only the thigh link but the calf link as well including a motor. Therefore:

Equation 2: Motor 2 Torque

$$M_1 = 51.62\ oz\text{-}in + \left[(23.36\ oz * 9.5\ in) + (\frac{10.25}{2} in\ * 9.28\ oz)\right]$$

$$M_1 = 51.62\ oz\text{-}in + 221.92\ oz\text{-}in + 47.56\ oz\text{-}in$$

$$M_1 = 321.1\ oz\text{-}in$$

The bracket that allows for the movement of the hip weighs 3.52 oz and the center of mass is 1.125 in away from the horizontal axis of rotation. The torque required is:

Equation 3: Motor 1 Torque

$$M_0 = 321.1\ oz\text{-}in + [(3.125\ in * 23.36\ oz) + (1.125\ in * 3.52\ oz)]$$

$$M_0 = 321.1\ oz\text{-}in + 73\ oz\text{-}in + 3.96\ oz\text{-}in$$

$$M_0 = 398.06\ oz\text{-}in$$

Based on the calculations performed, the Lynxmotion PGHM-04 is used. The motor selection is discussed in detail in Section 2.3.2.2. The motor is rated at 341.76 oz-in of torque and weighs 3.59 oz. Although this torque is below the maximum calculated torque for the thigh link, the specifications state that the leg does not have to be able to rotate the leg at maximum torque.

In order for the entire leg to be rotated the thigh and calf links must be at some angle with respect to the horizontal axis. Assuming that the calf and the thigh links are in line with each other and the motor is 85% efficient, which gives the motor a torque rating of 289.85 oz-in. The angle required is as follows:

Equation 4: Minimum Joint 2 Angle for Horizontal Movement

$$289.85\ oz\text{-}in = 3.96\ oz\text{-}in + (394.1\ oz\text{-}in * \cos\theta)$$

$$285.89\ oz\text{-}in = 394.1\ oz\text{-}in * \cos\theta$$

$$\frac{285.89}{394.1} = \cos\theta$$

$$\cos\theta = .725$$

$$\theta = 43.5$$

2.2.5. Chassis Design

The chassis, shown in Figure 12, is made up of four plates of aluminum connected by four angle brackets. There are two short sides containing two ports each and two long sides containing four ports each. Each port contains one connector, two holes to secure the connector, and four holes to mount each peripheral module. The holes used to mount the modules are ¼-20 threaded screw holes. The chassis has to be able to withstand the forces exerted on it by each leg, therefore the chassis is made out of .25” thick aluminum.

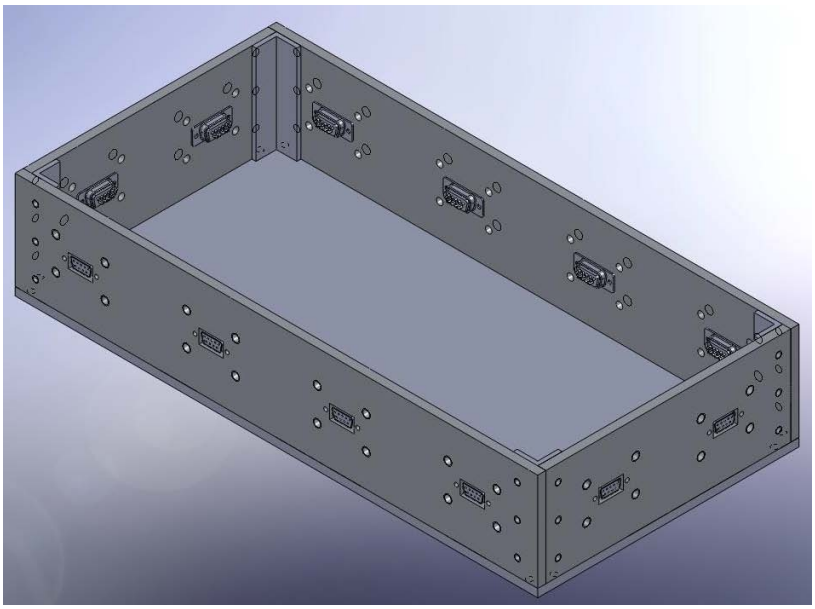

Figure 12: The Robot Chassis

Power and control signals must be distributed to the peripherals by an electrical subsystem, as discussed next.

2.3. Robot Design: Electrical System

The general specifications for the electrical system are outlined in Section 2.1. Here we will discuss the theory, design, and construction of the electrical system in detail, including component comparison and selection.

2.3.1. Control System and Distributed Processing Overview

In order to fully understand the electrical system, a brief overview of the control systems is necessary so that the need for certain components is clear. The control systems in ReMMRP are based on distributed processing. By utilizing multiple processors, the computational power needed for the robot to function, calculate kinematics, and control joints can be performed more efficiently through parallelization. Within this framework, the system can effectively work as well as be able to utilize using cheaper and less powerful microprocessors. This distributed processing also makes the programming modular, allowing the same code to be used in several processors.

Two structures for the tiered processing have been considered: a 2-tier and 3-tier approach. In the preliminary design, a 3-tier processing system is utilized. A processor on the main body (Tier-1) gives instructions all of the peripheral units. Each peripheral unit (Tier-2) has a communications and control processor. Each peripheral control processor directs its joint control modules (Tier-3). This design utilizes Serial Peripheral Interface (SPI) communication between Tier-1 and Tier-2, and uses serial

communication between Tiers 2 and 3. This structure effectively separates the two communication loops and prevents any cross-communication.

However, serial communications are not available on the processors that would be used in the Tier-3 modules, which would make it necessary to use 'over-qualified' processors for the Tier-3 modules to construct this system. Using SPI on both levels has been explored; however doing so requires the use of an elaborate gate system to prevent cross-communication between the Tiers. For this reason, a 2-Tier system is used in the final design. Tier-2 now functions as both the communications processor and the control unit for all three joints of the leg.

In the ReMMRP, every peripheral device has its own integrated processor. This allows the processing for that component to be confined to its own board, allowing the Main Processing Unit (MPU, Section 2.3.4) to do less work. Every peripheral chip must be capable of SPI communications for transfer of data between the MPU and the peripheral. The only peripheral unit currently being developed is a 3-DOF leg.

2.3.2. Leg Control Unit (LCU) Hardware

The Leg Control Unit is the board that handles all of the processing on the leg. This includes communication to the main board, calculating inverse kinematics, movement of the joints, and the maintenance of its health status. A completed LCU with labels is shown in Figure 13.

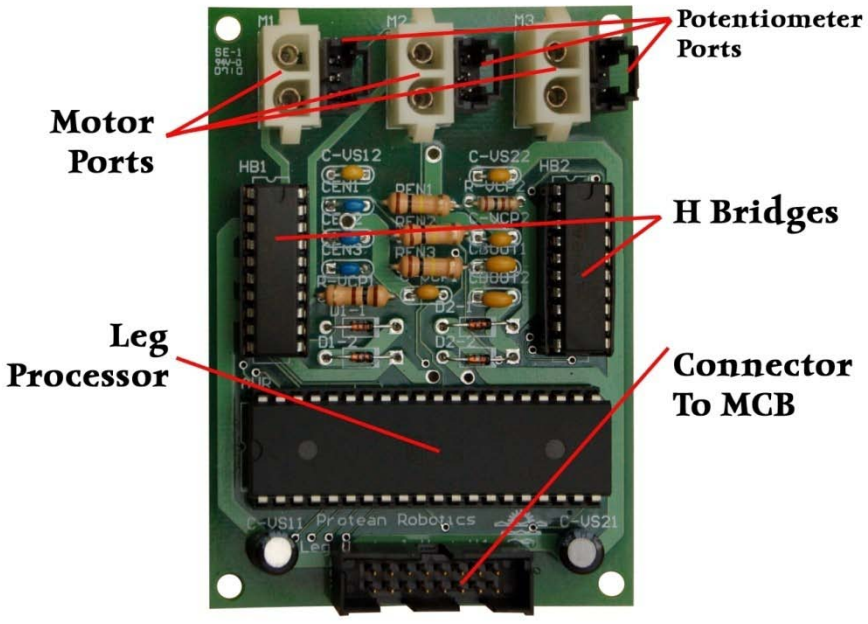

Figure 13: Labeled Top View of the LCU

2.3.2.1. Processor

The leg processor is selected to satisfy the following requirements:

1.) It must have SPI communications in order to communicate with the main processor.
2.) It must have 3 ADC ports to handle the potentiometer readings (see Section 2.3.2.4) from the joints.
3.) It must be capable of producing 6 PWM signals. Each of the three motors is controlled by two PWM signals, one to drive it forward, and one to drive it in reverse.
4.) It must have two I/O pins; one for a status signal to the main processor (output), one for a slave select (input).
5.) None of these pins can be shared on the chip.

An Atmel processor is used in the LCU because of the team's familiarity with the architecture, as well as the library of code that has been developed during the coursework prior to this project. Based on these requirements, the Atmel ATmega164/324/644P is used. It has Universal Serial Interface (USI) capabilities, including SPI. All of Port A (8 pins) are 10-bit ADC channels, and six PWM signals can be produced from 3 timers (2 8-bit, 1 16-bit). The 164/324/644P can have up to 32 I/O ports, so it can easily handle the 4 that are needed(5). This processor does not meet the specifications previously stated, as there is one pin overlap. The slave select pin for SPI communications is the same pin as one of the PWM signal outputs. The processor that meets the specifications for this application is the ATmega1281, however this IC is 3 times more expensive than the 164P ($14.96 compared to $4.73 (6)(7))and has 8 times the amount of memory, which is excessive(8). The cost of this IC outweighs its benefits, which is why it is not used. Because the 164/324/644P is used, the way that the motors are controlled is altered due to the SPI/PWM pin overlap. Instead of keeping the H-Bridge enabled at all times and pulsing the direction pins, the enable pin is pulsed with the PWM signal and the direction is controlled by 2 output pins connected to the direction pins on the H-Bridge. This means that 8 I/O pins are needed, however the 164/324/644P has more than enough. This also simplifies programming because the same code can be used for all PWM signals. All signals can use the 8-bit timers, while the 6-PWM configuration requires different code for the 16-bit timer.

Even though the ATmega164P has enough memory for performing the calculations necessary to control the leg effectively, an ATmega324P is used in the final design. This is because 324Ps are available through a sampling program, while the 164P is not. This processor functions the same as the 164P and has the same pinout, but has twice as much memory.

2.3.2.2. *Motors and Motor Driver*

The PWM signals that are output from the processor cannot source enough current to directly run the motors, nor are the signals the correct voltage. The maximum ratings for the I/O pins on the ATmega164P are 5V at 40mA. Therefore, a motor driver is necessary.

Based on the joint torque requirements for the leg discussed in Section 2.2.4, a motor torque of 321 oz-in is necessary. A low-current (<1A) motor is preferred for the robot in order to conserve battery life, however the majority of motors that can provide the necessary torque draw several amps. Two Lynxmotion motors were found that fit the requirements. Their specifications are outlined in Table 2. Their specifications are weighted, and the final scores show why motor 2 is chosen over motor 1. Although motor 1 more closely fit the desired specifications, its availability is a large deterrent to selecting it.

Table 2: Joint Motor Spec Comparison and Trade Study

	Motor 1 Specs.(9) 	Weight (1-10)	Motor 2 Specs.(10) 	Weight (1-10)
Voltage (V)	12	5	12	5
Stall Current (mA)	750	8	2710	5
Torque (oz-in)	295.34	6	341.76	8
Size (mm)	24 x 64.5	7	22 x 66.2	7
Shaft Speed (RPM)	31	7	64	6
Availability	Backorder (Unknown Time)	2	In Stock (Online Order)	8
Total		35		**39**

To drive these motors, the STMicroelectronics 6225N/6205N H-Bridge can be used as a motor driver. These chips are identical in pinout and function, but the 6205N is a higher current IC. This DIP20 has two full bridges per chip, and can handle 1.4/2.8A per channel. Each bridge has an enable pin, allowing full control over each individual bridge (11). Unfortunately, using this H-Bridge results in having a full bridge that is unused. This is a necessary concession.

2.3.2.3. Connection Ports

The LCU has several ports on it, shown in Table 3. This is mainly to increase the interchangeability of the components in the leg. Having ports allows the motors, potentiometers, and the board itself to be changed out if something breaks.

In the preliminary design, all of the ports were rectangular female headers with 0.1” pitch. These ports were rated for 3A per pin, making them suitable for most of the connections. After more development, they were insufficient for many others. The first reason is that they could not handle the current that would be travelling through the main connector on the LCU. Secondly, they did not have any lock between the male and female connectors, meaning that they could become unintentionally disconnected.

The main connector to the board in the preliminary design is an 8-pin 2x4 0.1” female rectangular header. Due to the chosen motors, transferring the necessary current is not possible with this setup. Ribbon cable is preferred for wire management, so a 16-pin 2x8 0.1” female rectangular header is used. The 12V power is distributed across four pins, and so is the ground. Due to financial considerations, the header is male instead of female. Also, keyed headers and ribbon cable connectors are used to ensure proper connections every time.

The motor connectors in the preliminary design are 2-pin 2x1 0.1” female rectangular headers. Due to the motors selected, and the lack of fasteners on the connectors, these are not acceptable for the final design. The rectangular headers are rated for 3A, but with motors that draw up to 2.71A, having a safety factor of 1.1 is not sufficient. Further, there is no assurance that the connection would not unintentionally become dislodged. Given these new considerations, a 2-pin 0.25” female header is used. It has two latches on the free hanging wire connector that attaches to the header on the board. The holes are irregularly shaped to ensure consistent connection every time it is plugged in.

Lastly, the potentiometer connection ports are insufficient in the preliminary design. While they meet all of the electrical specifications, there is no latch to prevent accidental disconnections. In order to have this feature and observe financial limitations, the board connector is a male header in the final design with a female connector on the free hanging wire.

Table 3: Graphic Comparison of LCU Connectors (12)(13)(14)(15)(16)(17)

	Motor Connector	Potentiometer Connector	Main Connector
Preliminary	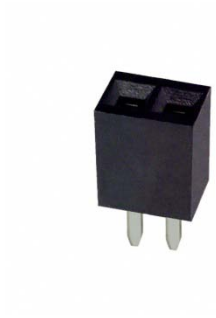		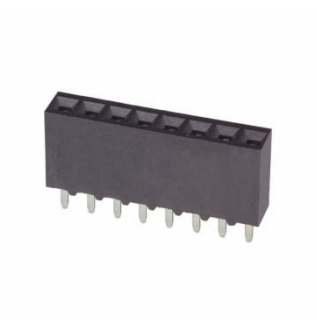
Final			

2.3.2.4. Joint Position Sensing

Each joint on the leg module needs a sensor to determine the location of the joint so that it can be moved to the appropriate location. There are two main options for absolute position sensing. The first is an absolute encoder. This sensor uses either optical or magnetic sensors to determine its angular position based on a binary code inside the sensor. The downside to this sensor is that it is very expensive to use at 10 bits of resolution, which is what the ATmega164/324/644P converts analog signals to using its ADC.

The other option is a potentiometer. This is an analog sensor that acts as a variable resistor, varying the output voltage linearly as the angular position changes. They also tend to be less expensive, and can be more accurate, depending on the quality of the potentiometer. For primarily the cost benefits, it was decided to use potentiometers.

High resistance potentiometers are used so that the current draw is minimized, conserving battery life. Also, a high quality potentiometer is desired for precision position sensing. Lastly, a small form factor is necessary so that it does not protrude very far from the leg.

For these reasons, a 10K, 20%, 1-Turn, 53 Series potentiometer from Bourns, Inc. is used on the leg module. It is in a small package, only 0.521" L x 0.492" W x 0.350" H (18). This potentiometer functions very well on the leg module.

2.3.2.5. PCB Design

Figure 14 shows the LCU design printed to accommodate the electronics necessary to operate the leg. Spatial limitations of the leg restrict the board to 2.5” wide by 11” long to ensure that it can fit inside the leg cavity. To accommodate the traces and form factor, it is necessary to have the boards printed on 2oz copper. The final board is 2.5” x 3.5”. The motor and potentiometer connections are paired together to keep connections organized. All IC’s are mounted on sockets for easy replacement in the event of burning one out or upgrading. The full schematics can be found in Appendix A.1.

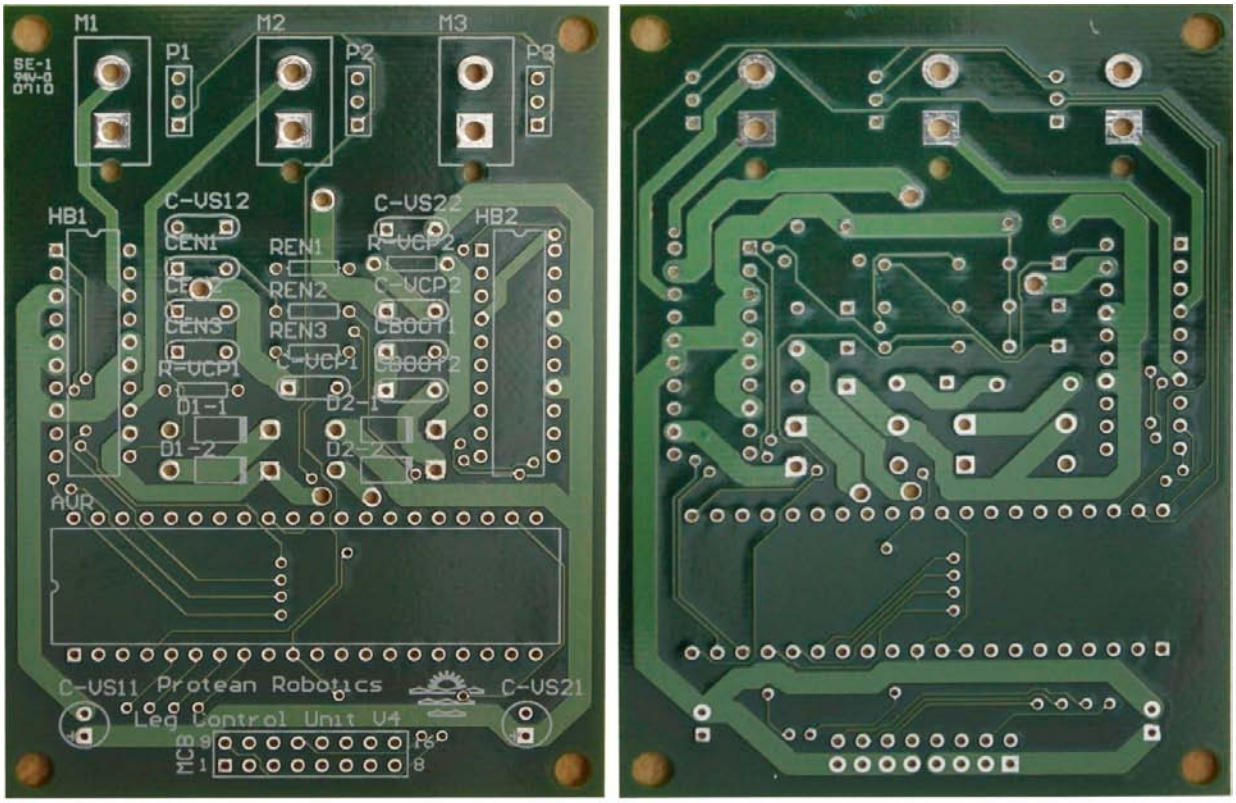

Figure 14: Front and Back View of a Blank LCU PCB

2.3.3. Main Communications Board (MCB) Hardware

Figure 15 shows a completed Main Communications Board with labels. The MCB has no decision-making power. It is essentially a communications hub for the Main Processing Unit (MPU, 2.3.4). Power management and distribution is also handled by the MCB.

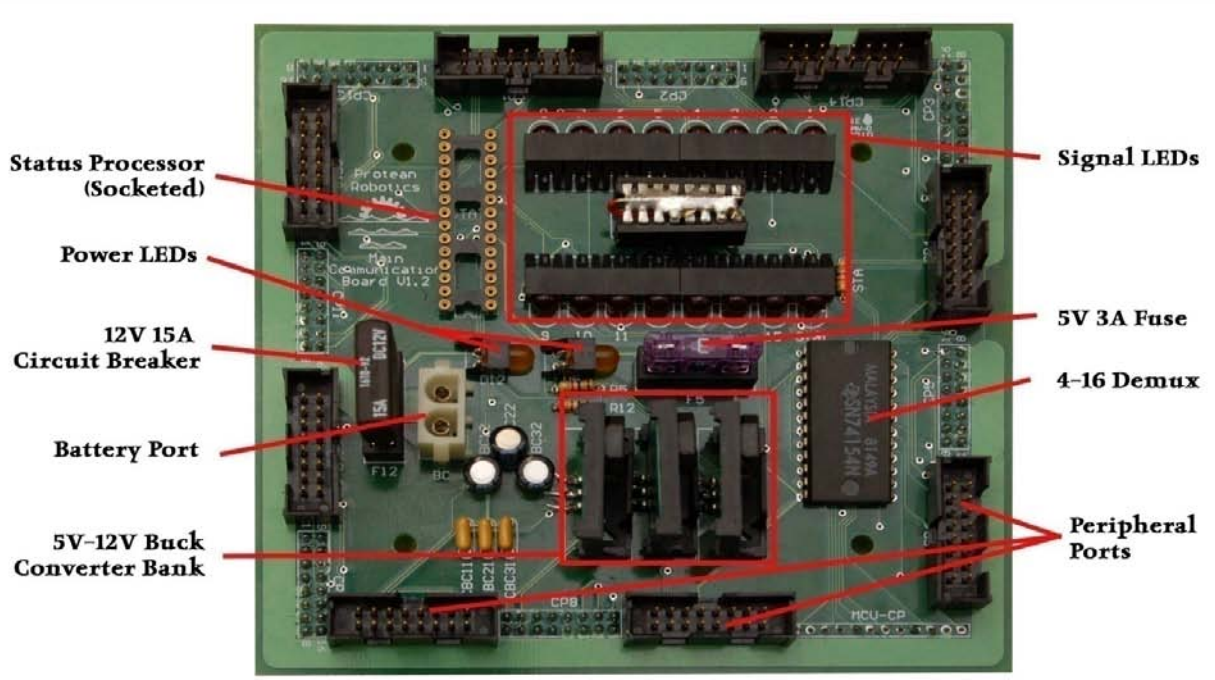

Figure 15: Labeled Top View of the MCB

2.3.3.1. Demultiplexer/Decoder

The MPU utilizes SPI communications to transfer data between itself and the Tier-2 processors. When using SPI, a slave select (SS) pin on the slave processor must be enabled by the MPU to establish which sub-processor it would like to communicate with. This means that it would require 16 separate I/O ports (15 peripherals, 1 STATUS processor (Section 2.3.3.2)) on the MPU to accomplish this. In an effort to maintain interchangeability of the MPU, it is necessary to reduce the number of pins required on the MPU. To do this, a line decoder, also known as a demultiplexer, or demux is used. This allows the number of SS lines from the MPU to be reduced to 4 (Section 2.4.1.1). By using a decoder, the MPU outputs the desired channel in binary to those 4 pins, and the decoder selects the appropriate slave chip.

The SN74154N from Texas Instruments is used as the decoder for the ReMMRP. It is a 4-16 decoder. It is also a 5V IC, which is the operating voltage of the other processors, and has a maximum current draw of 1µA, meaning low power consumption (19).

This decoder allows for the selection of one of 15 peripherals or the STATUS chip, for a total of 16 slaves. 12 of these peripherals will be along the outer edge of the body, and the remaining three will be available for Internal Connection Ports (ICP), intended for use with sensors internal to the chassis, such as inertial navigation sensors.

2.3.3.2. STATUS Processor

The STATUS (**ST**atus of **At**tached **U**nit**S**) processor is responsible for enumerating peripheral modules attached to the system and reporting any changes to the MPU. It also is used in the initialization sequence of the robot to establish which ports have peripherals attached. This processor has three requirements.

1.) It must have SPI communications for conveying data to the MPU.
2.) It must have 17 I/O ports; 15 for status inputs form the peripherals, one for slave select, and one for a status change pin to the MPU.
3.) None of these pins can be shared on the chip.

Due to the fact that 22 pins are necessary, a processor with extraneous features must be selected so that the requisite number of pins are available. The Atmel ATtiny48 meets the requirements outlined above, and is used as the STATUS chip. It has 24 I/O pins, and has SPI that does not interfere with the I/O ports for the status inputs (20).

2.3.3.3. Power Management

The motors will be running at 12 volts DC, so a 12V DC battery will be used as the power source for the robot. All of the ICs run at 5V DC, so power must be converted for these chips. The converter must:

1.) be efficient to conserve the battery life.
2.) be able to provide enough current to run the chips and potentiometers.
3.) reduce the voltage from 12v DC to 5v DC.

Using a step-down DC-DC (also known as buck) converter will help with the efficiency. A voltage regulator is very inefficient because it sheds the excess voltage as heat (21). For the ReMMRP, voltage will be reduced to 5V from 12V. Assuming the current is constant, a linear regulator operates at the following efficiency:

$$\frac{5V}{12V} = 41.6\%$$

The IV1205DA from XP Power is used for the power conversion in the preliminary design. It operates at 74% efficiency, and can supply up to 200mA of current (22). This specification meets the power to supply requirements by all of the ICs and the leg potentiometers. The leg potentiometers in a 12-leg configuration would consume 18 mA.

In order to account for future peripherals, three 1A DC-DC converters are used in parallel in the final design. This will allow for high draw peripherals to be developed without having to worry about not being able to source the necessary current. The Texas Instruments 5101N DC-DC converter is used on the MCB. It is 90%+ efficient, and can supply 1A of current and has very simple required external circuitry (23).

Both the 12-volt and the 5-volt lines have current protection. The 12-volt line has a 15A circuit breaker, and the 5V line has a 3A fuse. A fuse is used for the 5-volt line because it is much less likely that this line will have a surge of current. The 15A breaker is used because stalling motors can draw large amounts of current that could damage the board, and using a circuit breaker instead of a fuse saves time and money by not having to replace it every time it trips.

2.3.3.4. Connection Ports

The peripheral ports on the MCB need to meet the same requirements as the 16-pin keyed rectangular male pin headers on the LCU, and use the same component (Section 2.3.2.3). All 15 of the peripheral connection ports use this 16-pin header. The port to the MPU will be a 12x1 female header with 0.1” pitch. This header contains both power and communications lines. The battery connection port is identical to the one being used for the motors – a 0.25” 2-pin connector with two fastening latches. This can be used for the battery and the motors because it exceeds the current requirements for the motor application.

2.3.3.5. Signal LEDs

There are 18 signal LEDs on the MPU. These are used to display information to the user. 16 are status LEDs from peripherals. These are arranged in four 4-LED banks, using a bussed 10K resistor bank

as a pull-up resistor. An individual resistor had to be used for the 16th LED as a DIP16 resistor bank only has 15 available resistors. These LEDs are connected to the status lines from each peripheral port. This will tell the user which ports have connected peripherals. The other two LEDs are power LEDs, signaling whether the 5- and 12-volt lines are functioning properly. These also have 10K resistors as pull-up resistors.

2.3.3.6. PCB Design

The completed blank MCB board is shown in Figure 16. The final board size is 5" x 5". Due to the large amount of current that will be run through the traces and the desire to keep the form factor small, the MCB will be printed using 2oz copper. This will help to reduce the heat generated by the board. Also, the trace widths are significantly larger on this board than on others to further help with the heat generated by the high current. The connection ports are arranged around the perimeter to allow for easy access. The complete schematics can be seen in Appendix A.2.

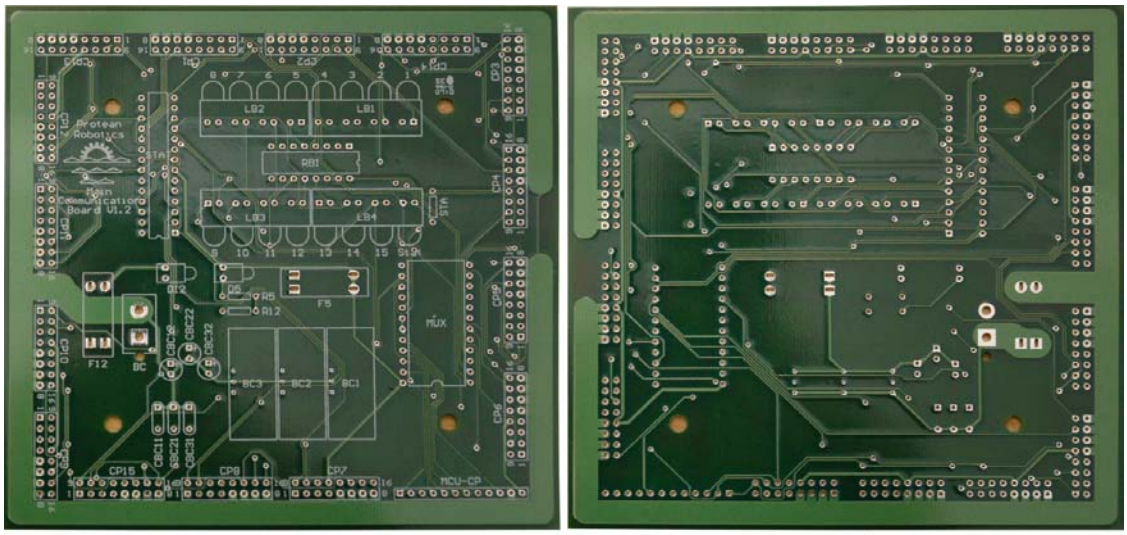

Figure 16: Front and Back Views of a Blank MCB PCB

2.3.4. Main Processing Unit (MPU) Hardware

A completed and labeled MPU is shown in Figure 17. The Main Processing Unit is designed to be interchangeable as the computational demands of the robot evolve. It is also designed to minimize the number of connection pins necessary to utilize all of the functionality of the MCB. The full schematic can be seen in Appendix A.3.

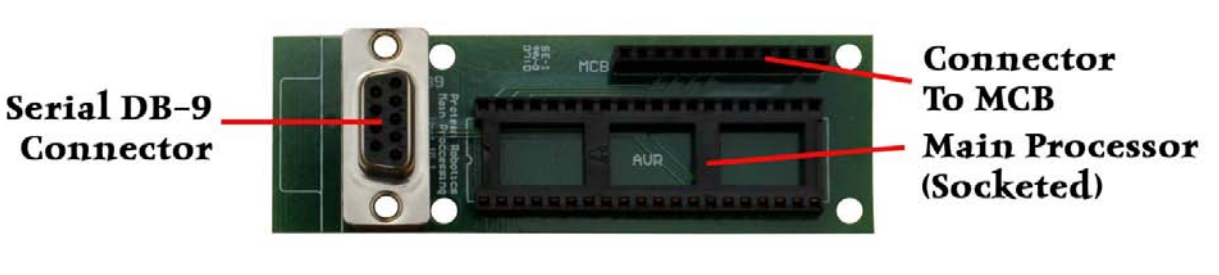

Figure 17: Labeled Top View of the MPU

2.3.4.1. Main Processor

The main processor has four requirements. It must have:

- enough memory to store a complex balance algorithm and the speed to execute it (discussed in Section 2.4.2).
- SPI capabilities
- 6 I/O pins (4 outputs for the SS demux, 1 output to enable the demux, and 1 input from the STATUS processor)
- serial communication to output data to a connected computer for data feedback during testing.

From these requirements, the Atmel ATmega644P is used as our main processor. It has the same specifications as the 164P/324P discussed in Section 2.3.2.1, except has 64k bytes of flash memory, 2k bytes of EEPROM, and 4k bytes of internal SRAM (5). This can handle the computational demands placed upon it.

2.3.4.2. Connection Ports

The only header used is identical to the 1x12 rectangular female header on the MCB. This is more than capable of handling the power and data going through it. The serial connector is a female DB-9 connector. It is perpendicular to the board for easy access once installed in the robot. The processor will be on a socket for easy replacement.

2.3.4.3. MPU PCB

The blank PCB is shown in Figure 18. There are only three components, and all three were placed and soldered without issue during assembly.

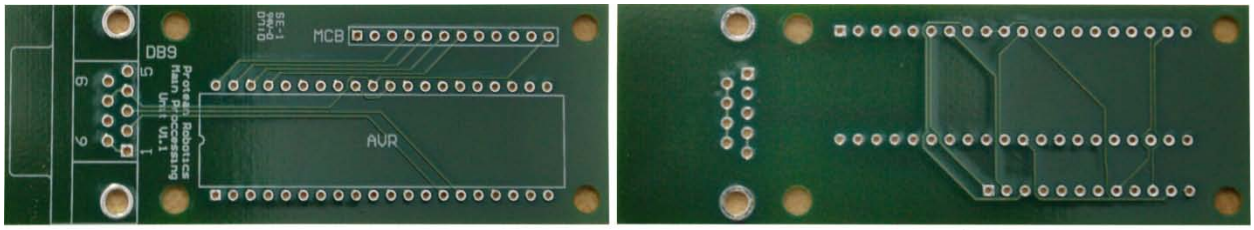

Figure 18: Front and Back Views of a Blank MPU PCB

2.3.5. Miscellaneous Electrical Considerations

All of the PCBs are 2-layer PCBs. The connection between the robot's chassis and the peripherals is done using a DB-15 HD connector, the male side being on the leg. Custom DB-15 HD to 8x2 header cables are used. One pin is left open on the DB-15 connector. The DB-15 HD connectors are fastened to the body and the peripherals so that the mechanical connection also contains the electrical connection.

2.4.Robot Design: Software and Control Systems

To determine and coordinate the actions of all peripherals attached to the ReMMRP so that it can accomplish a specified task (i.e., balancing, walking, etc.), control architecture and associated software are necessary. The following are the software design requirements for the ReMMRP:

1. Communications protocol must exist for data transfer among the MPU, STATUS processor, and LCUs (and other peripheral processors to be developed).
2. MPU software must determine actions for all peripheral devices (for the LCUs, desired coordinates of the leg's endpoint), and delegate commands to them in real time.
3. LCU software must respond to commands from MPU with higher priority than any other task inherent to LCU software.
4. STATUS processor software must operate in real time, allowing MPU to have immediate knowledge of attached peripherals at any given time.

2.4.1. Communications Protocol

The ATMega164/324/644P processors have four means of data transmission:

1. Serial Peripheral Interface (SPI)
2. Universal Synchronous and Asynchronous serial Receiver and Transmitter (USART)

3. USART in SPI mode
4. Two Wire Interface (TWI)

Each of these communication modes has different properties. Table 4 compares the following properties of each mode:

- Top speed – highest guaranteed data transmission rate in bits per second, assuming an 8 MHz processor clock speed. Higher data transmission rates are desired.
- Processor overhead – the total size of internal data registers, in bytes, required by the processor to use the communication mode. Lower processor overhead is desired.
- Full Duplex – whether the communication mode can simultaneously transmit and receive data. This increases effective data transfer rate; full duplex is desired.

Table 4: Comparison of ATMega164/324/644P Communication Modes

	SPI	USART	USART in SPI	TWI
Top Speed (bps)	2,000,000	500,000	2,000,000	400,000
Processor Overhead (bytes)	3	7	6	6
Full Duplex?	Yes	Yes	Yes	No

The SPI mode has the highest top speed, lowest processor overhead, and communicates in full duplex, and is subsequently the most appropriate choice for the ReMMRP communications scheme.

2.4.1.1. SPI Overview

Serial Peripheral Interface, or SPI, utilizes a master / slave hierarchy, where data transfer is initiated by the master device. Four data lines are inherent to this protocol, and are shown in Figure 19(24):

1. MISO (Master In / Slave Out): Bits are sent from the slave and received by the master.
2. MOSI (Master Out / Slave In): Bits are sent by the master and received by the slave.
3. SS (Slave select): Two modes-
    a. In Master Mode, this is used to select a slave.
    b. In Slave Mode, the slave is activated by this.
4. SCLK (Serial Clock): Timing signal generated by the master that synchronizes bit transfer.

Figure 19: Single Master / Single Slave Configuration

SPI only allows communication between the master and one slave at a time. The ReMMRP design incorporates multiple slaves (i.e., more than one LCU will be subject to commands from the MPU), so a more complex approach is needed. The SCLK, MOSI, and MISO lines can be shared between the master and all the slaves, as only the selected slave will be actively using these lines during communication. Each slave, though, needs its own SS line from the master. This could be configured as follows:

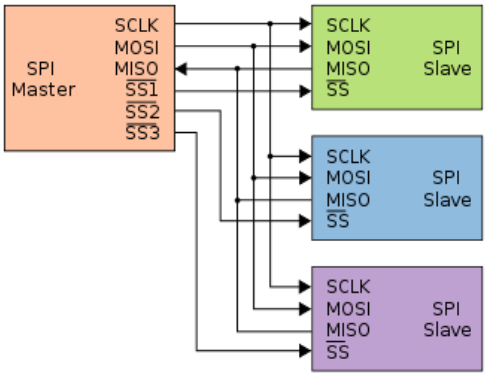

Figure 20: Single Master / Multiple Slave Configuration

The drawback to this configuration is the number of separate SS connections from the master; with twelve potential peripherals, three ICPs, and one STATUS processor as slaves in this design, nineteen pins (1 SCLK + 1 MOSI + 1 MISO + 16 SS) are required from the master to facilitate SPI communications with all ports.

A decoder can decrease the number of pins needed for slave selection purposes from the master. A decoder accepts input from a number of lines, or binary inputs, and has a number of outputs equal to:

$$n_{outputs} = 2^{binary\ \ inputs}$$

The decoder selected for this design (Section 2.3.3.1) has sixteen outputs, and will activate the output that corresponds to the value of the 4-bit input signal. This way, a four line signal can be used to activate one of sixteen peripherals, reducing the master's SPI pin requirements to seven (1 SCLK + 1 MOSI + 1 MISO + 4 Binary Signal to Decoder).

Once a slave is selected, the communications event can be viewed as in single master / single slave configuration. SPI is a full-duplex means of communication, which means that data between the master and the slave are exchanged simultaneously. SPI accomplishes this by treating the byte in the SPI data registers of each processor as a continuous two byte register and rolling, or performing a circular exchange of, the bits that comprise the two byte sequence. This means that:

1. The slave's Most Significant Bit (MSB) is stored in the MISO line, and the master's MSB is stored in the MOSI line.
2. The slave and master's remaining bits are all moved up one position.
3. The master's Least Significant Bit (LSB) assumes the value of the MISO line (whatever the slave's MSB was), and the slave's LSB assumes the value of the MOSI line (whatever the master's MSB was).

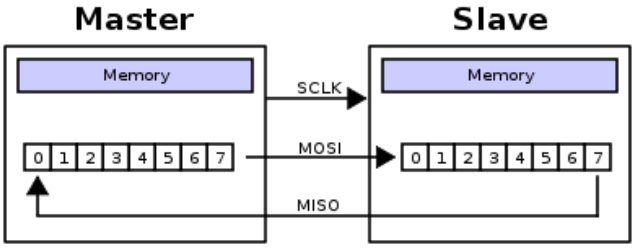

Figure 21: Master / Slave Data Transfer

This process is continued until the two bytes have been fully exchanged between the master and slave.

Under the SPI framework, the communications architecture can be divided into two general parts:

1. Master communications procedures: Those procedures utilized by the MPU to send data to the STATUS, LCU, or any other peripheral control processors with which the robot may be configured.

2. Slave communications procedures: Those procedures utilized by the STATUS, LCU, or any other peripheral control processors with which the robot may be configured, to send data to and receive data from the master processor.

Since SPI utilizes a full-duplex communications mode with a clock, sending and receiving are done not only simultaneously but also synchronously. The data exchange is quantified on the byte level, and initiated only by the master. Therefore, the above generalization defines a communication session as:

1. Master communications procedures:
    a. Select slave
    b. Choose byte to send
    c. Send byte, receive byte from slave
    d. Unselect slave
2. Slave communications procedures:
    a. Wait for selection from master
    b. Exchange current stored byte with incoming byte from master

In an episodic sense, these procedures do not appear to be an effective means of transferring information. Since communication between the master and slave at a given time involves the transfer of multiple bytes, an additional layer of abstraction over the SPI communication protocol is implemented.

2.4.1.2. Symmetric Data Buffer Exchange Protocol

In a multiple byte transfer scheme using SPI, the initial byte received from a slave processor is always undefined because its SPI data register has not been loaded with any pertinent information; the master can send valid data to the slave but will receive this undefined data, as shown in Figure 22.

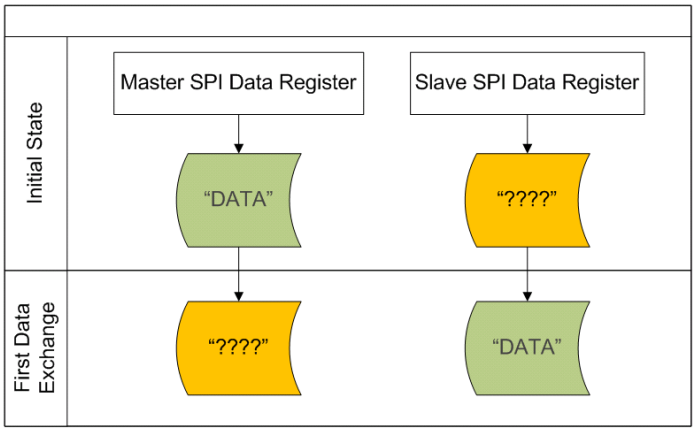

Figure 22: SPI Initial Single Byte Data Exchange

Alternatively, the data sent from the master can be utilized by the slave as an index to define the data on the next transmission. The master will receive undefined data (which is unusable) from the slave upon transmission of the index to the slave, but the index will cause the slave to load the usable data into its SPI register. Upon the next transmission from the master, the slave will send the usable data that corresponds to the index previously sent by the master. This process is shown in Figure 23.

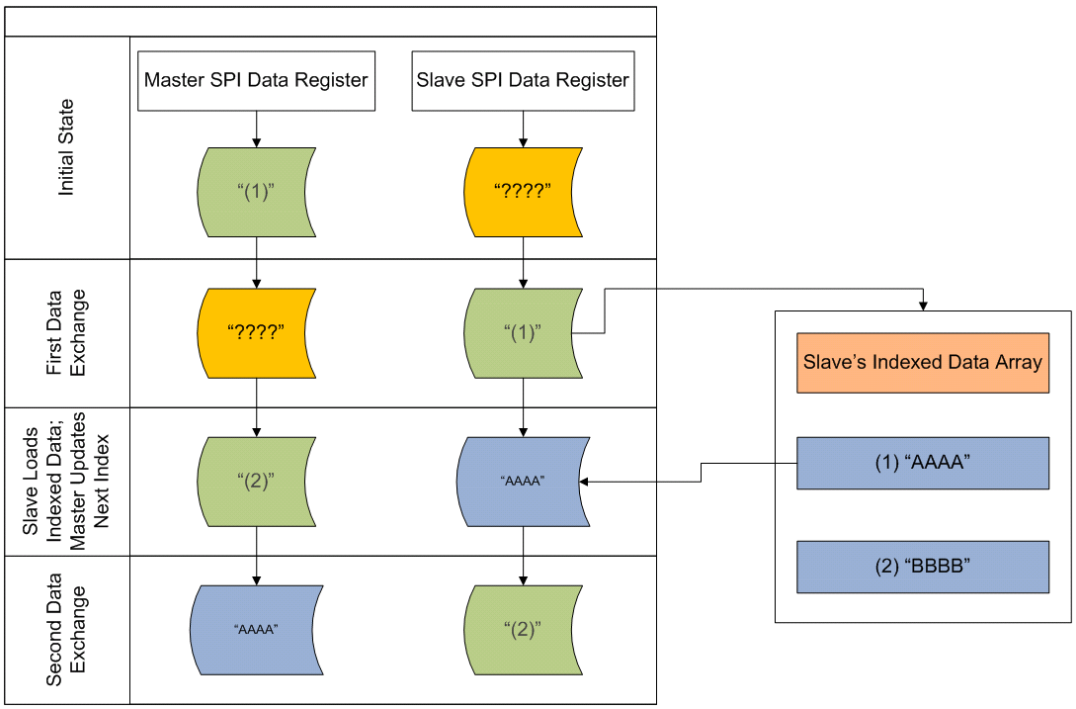

Figure 23: SPI Indexed Byte Transfer

This method can be extrapolated, where the master repeatedly sends indices to the slave. In this case, only the first byte the master receives from the slave will be unusable; the remaining bytes

received will be pertinent information from the slave. The last byte the master sends does not need any particular value in order to receive the last byte of indexed data from the slave. Note that this process results in a data offset between the master and slave; the master is always one byte behind the slave in terms of the byte sequence.

The indices sent from the master are useful in requesting data from the slave, but have no particular meaning to the overall operation of the robot other than to ensure the proper data is received from the slave processor. The communications session would be better exploited if more pertinent data were exchanged as often as possible. To accomplish this, data buffers must exist on both the master and slave processors in the following manner:

1. Each element in the data buffer must be a single byte, commensurate with the size of the SPI register.
2. The data buffers present on the slave must be known by the master and each buffer must have an index that explicitly identifies it.
3. The size of the data buffers on both processors must be known by the master before transmission begins. The data buffers to be exchanged must be of equal size; this criterion is fundamental to the symmetric aspect of this protocol.
4. One buffer is chosen on each processor as a “send” buffer, and one buffer is chosen on each processor as a “receive” buffer.

With these rules in place, the master and slave can simultaneously transfer information blocks of equal size. This process will be referred to as Symmetric Data Buffer Exchange (SDBE).

In the following example, the MPU simultaneously sends the LCU new coordinates and receives from the LCU its last known coordinates using SDBE. The assumption will be made that both processors have a data buffer called “Command Coordinates,” and the LCU has an additional buffer called “Current Coordinates.” The data exchange will occur as follows:

1. The MPU designates its “Command Coordinates” as a send buffer, and initializes an index variable that will correspond to successive bytes of its send and receive buffers.
2. The MPU initiates an SPI communication session with the LCU by enabling the decoder and sending it the bit pattern that corresponds to the chassis port where the LCU is attached.

3. The MPU sends the LCU a byte indicating that the LCU must designate its “Command Coordinates” as a receive buffer.
4. The MPU sends the LCU a byte indicating that the LCU must designate its “Old Coordinates” as a send buffer; at this point the LCU will load the first byte of its “Command Coordinates” into its SPI register, and initialize an index variable that will correspond to successive bytes in its send and receive buffers.
5. The MPU enters a loop where:
    a. The byte of the send buffer corresponding to the index variable is transmitted. This causes the MPU to receive the first byte from the LCU.
    b. Once the bytes have been exchanged, each processor copies the new data from its SPI register into its respective receive buffer at the index indicated by their respective index variables.
    c. Index variables on both processors are incremented after the copy.
    d. Steps (a) through (c) are repeated until the index variables are equal to the size of the data buffers.
6. The MPU ends the SPI communication session with the LCU by disabling the decoder / multiplexer.

At the end of this procedure, the MPU’s “Command Coordinates” buffer will contain the LCU’s last known coordinates, and the LCU’s “Command Coordinates” buffer will contain the new set of coordinates from the MPU. SBDE control code for each processor can be seen in Code Sample 1 and Code Sample 2.

```
ISR(SPI_STC_vect)
{

	//Interrupt trigger when a byte is written to the SPI (ie, transfer is finished)
	//SPIF flag in SPSR should be set at this time

	int i, packetLen;
	unsigned char* SendBuffer;
	unsigned char* ReceiveBuffer;
	//Global variable commandReceived is used in this procedure
	//Global array instructionSet[] is used in this procedure

	//Read SPSR then SPDR;
	//This will clear the SPI interrupt flag.
	//Now commandReceived is set to first transmission byte.
	commandReceived = SPSR;
	commandReceived = SPDR;

	//Second byte indicates data requested by master
	while (!(SPSR & (1 << SPIF))) {
		//wait for receive byte 2
	}
	//Designate send buffer as proper array
	SendBuffer = instructionSet[commandReceived].data[SPDR];

	//Third byte indicates data coming from master
	while (!(SPSR & (1 << SPIF))) {
		//wait for receive byte 3
	}
	//Designate receive buffer as proper array
	ReceiveBuffer = instructionSet[commandReceived].data[SPDR];

	//Fourth byte indicates how many bytes will be transferred
	while (!(SPSR & (1 << SPIF))) {
		//wait for receive byte 4
	}
	//Set packet length to proper number of bytes
	packetLen = SPDR;

	for (i = 0; i < packetLen; i++) {
		//Load transmit byte
		SPDR = *(SendBuffer + i);

		while (!(SPSR & (1 << SPIF))) {
			//wait for receive byte
		}

		//Write received byte to receive buffer
		*(ReceiveBuffer + i) = SPDR;
	}

}
```

Code Sample 1: Slave SBDE Communication Routine

```
void SBDExchange(unsigned char toPort, char cmd, xData *sendData, xData *rcvData) {

	int i;
	char temp;

	//Enable demux and enable SPI communications with peripheral device
	SelectSlave(toPort);

	//Send command to peripheral, received data byte irrelevant
	temp = SPI_Transmit(cmd);

	//Request data set from peripheral, received data byte irrelevant
	temp = SPI_Transmit(rcvData->identifier);

	//Indicate incoming data set to peripheral, received data byte irrelevant
	temp = SPI_Transmit(sendData->identifier);

	//Indicate length of transfer, received data byte irrelevant
	temp = SPI_Transmit(sendData->length);

	//Initiate data exchange loop
	for (i = 0; i < sendData->length; i++) {
		//Simulataneously send and receive pertinent data
		rcvData.buffer[i] = SPI_Transmit(sendData.buffer[i]);

	}

	//Disable demux, ending communication session
	Unselect();
}
```

Code Sample 2: Master SBDE Communication Routine

Other means of data buffer exchange can be utilized over an SPI data link, and for certain peripherals or procedures this may be advantageous. SDBE can also be modified slightly to accommodate an asymmetric data buffer exchange. However, the LCUs function primarily by the use of SDBE protocol, and only do so otherwise upon the receipt of single byte commands; therefore an asymmetric data exchange protocol is unnecessary.

2.4.2. MPU Software & Operational Characteristics

The MPU software is the uppermost level of the control architecture of the robot. The MPU must:

1. Validate peripherals as enumerated by the STATUS processor, both on startup and in real time as the robot operates.
2. Guarantee collision-free communication. Physical communications collisions are not possible due to the serial and full-duplex nature of SPI communication, but logical collisions can still occur, and the MPU must prevent this.
3. Guarantee continuous operation in the event of an unexpected peripheral loss, provided that redundancy exists in the current configuration.
4. Determine the degree of interaction among peripherals. The MPU will determine that any number of legs, or peripherals with an LCU, will function together towards the locomotion of the robot. A different configuration may have multiple legs, but also a wireless communications

beacon. In this situation the MPU must still determine the cooperative relationship that the legs share, but also determine that the wireless peripheral has a separate and independent function.

5. Control peripherals at their degree of interaction.

The above functions will now be discussed in further detail.

2.4.2.1. Peripheral Validation

On startup, the MPU must wait for a "ready" signal from the STATUS processor. After receiving this signal, the MPU can poll the STATUS processor for information regarding what ports on the robot chassis have peripheral devices attached to them. Once the MPU is aware of which ports are active, it can then poll these ports for information.

Every peripheral device will have a serial number written directly into its memory, either as a constant term in the embedded software, or stored in its permanent EEPROM memory. This serial number identifies the peripheral as a particular type of device, and the MPU will have a list of every possible peripheral. The MPU will initially request this information from each peripheral, and create a data structure for each port that corresponds to the device that is attached there.

2.4.2.2. Communications

The MPU acts as the master in communications with all other processors in the robot architecture. As such, it is responsible for initiating any and all communications. In a multiprocessor environment, care must be taken to avoid collisions in data transfer. The primary type of data collision in computer networking is a physical collision; this occurs when data transfer occurs simultaneously between more than two processors (25). The SPI protocol is free from this concern in a single master / multiple slave environment.

A secondary type of collision will be referred to hereafter as a logical collision. This is likely inherent to other architectures, but for the purposes of this paper it will pertain solely to the robotic design of this project. Logical collision potential exists when the MPU attempts to exchange data with a peripheral before that peripheral has utilized the most recent data that was exchanged.

In the case of the SDBE protocol, this might occur if:

- The MPU exchanges a number of bytes of data with an LCU, indicating a set of coordinates.
- The LCU begins using this new data, but the master sends another set of coordinates half way through the LCU's procedures having to do with said data.

In the event of this situation, the LCU would see data that was the first half of the old set of coordinates, and the second half of the new set of coordinates. This might range in issues from simply a wrong coordinate set or, if the bytes in the data were actually subdivisions of a larger data type such as a floating point decimal, completely erroneous or unusable data. Given the speed of the processors involved, the speed at which SPI functions, and the size of the data, it is unlikely that this would occur. However, because the potential exists it must be mitigated.

The solution employed by this architecture is to calculate how long each command that the MPU issues to a particular peripheral will take to execute on that peripheral. This way, the MPU can check the system time when a particular command is issued to a peripheral, and not send further commands to that peripheral until enough time has passed to ensure that no logical collision will occur.

2.4.2.3. Control Algorithms

The MPU is responsible for correlating the movement of the legs in such a manner as to cause the entire robot to balance. To do so, the MPU must be able to produce sets of coordinates where the end-effector of each leg will be located when the robot is balanced. All such algorithms, since they are based on the geometry of the robot, use the same convention for port numbering and coordinate assignment, as shown in Figure 24:

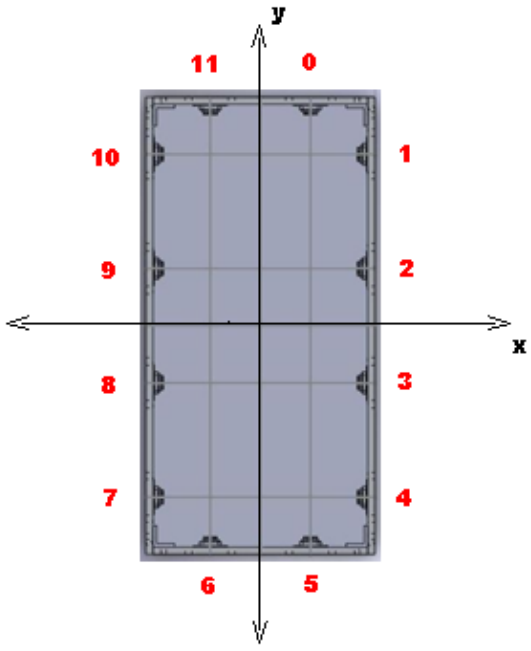

Figure 24: Robot Coordinate Frame & Port Numbering

The robot coordinate frame's origin is positioned at the geometric center of the robot chassis, with the long edges parallel to the y-axis, and the short edges parallel to the x-axis, as viewed from above the robot. Using the right-hand rule, the z-axis extends skyward from the robot chassis center. The ports are numbered beginning with "0" at the topmost right in this orientation and increasing clockwise until "11". Any positional coordinate of the robot's peripherals can ultimately be expressed in terms of this system, and the balancing algorithms described below use that fact advantageously.

Combined Static Stability and Mobility (CoSSMo) Balancing Method

This method of balancing is done without the benefit of accelerometers or gyroscopic devices. The only data utilized is the number of legs attached to the robot and where they are. The following assumptions are then made:

- The center of gravity of the robot is the geometric center of the chassis.
- The robot is on a flat surface.
- The robot is not in motion.
- The robot has been commanded to a set height. This will fix the z-coordinate of the robot chassis, and calculate a configuration for the robot to stand at the desired height.

This balancing algorithm has two separate goals. These are:

- Maximize Stability**:** Determine most stable configuration as defined by the area of the base of support, or the polygon made by defining each leg's end-effector as the vertex of a polygon in the x-y plane, and the position of the robot's center of gravity, or mass centroid, when projected onto this polygon.
- Maximize Mobility: Determine the greatest potential for motion from the balanced configuration, i.e., how much each end-effector is able to move within its workspace from the balanced position.

The mobility and stability of the robot both depend on the position of the end-effectors, but in most cases improving one will tend to worsen the other. Therefore the algorithm must find a compromise between the stability and mobility metrics, where a configuration is found in which the robot is both statically balanced and has some ability to move each leg in any direction.

One approach to this involves calculating and storing optimal or sufficient solutions for each possible configuration. However, even with the presumption that the robot cannot balance with less than three

legs, the possible configurations can be numbered using the "choose" function. The function $\binom{n}{x}$, read as "n choose x," determines the number of ways that x elements from an equal or larger set of n elements can be arranged. This function is calculated as follows:

Equation 5: Choose Function

$$\binom{n}{x} = \frac{n!}{x!\,(n-x)!}$$

Since the ReMMRP has a twelve-port chassis, n will always be fixed to 12 (the number of ports cannot be changed). The variable x will denote how many legs are attached in a given configuration. The robot cannot physically balance with less than 3 legs attached; therefore 1 and 2 leg configurations will not be explored.

In the interest of examining search space for the algorithm, the choose function can be utilized to express the number of configurations the robot can have with different numbers of legs. Beginning with the least allowable number of legs, the number of different configurations possible can be stated as "12 choose 3," and calculated as:

$$\binom{12}{3} = \frac{12!}{3!\,(12-3)!} = 220$$

Extrapolating this to the remaining possible number of legs (4 through 12) and summing the results, the total configurations possible for the range 3 to 12 legs is:

Equation 6: Total Possible Leg Configurations of ReMMRP

$$\sum_{i=3}^{12} \binom{12}{i} = \sum_{i=3}^{12} \frac{12!}{i!\,(12-i)!} = 4017$$

Pre-calculating, optimizing, and storing this amount of possible configurations would still be a heavily time consuming and storage intensive task. The robot uses an 8MHz main processor with 4K of RAM, so the space and time complexity of the algorithm must remain very small in order to function at all. Therefore, the candidate algorithm must be small enough to fit in the 64K of processor memory, and fast enough to calculate a "good" balance scheme in a small amount of time, with a processor that is very slow by modern standards. The CoSSMo algorithm is a rudimentary but effective solution to the compromise between stability and mobility.

The stability metric is defined as a function of the distance between the centroid of the robot chassis and the centroid of the base of support. To calculate the area of the base polygon, the following formula is used:

Equation 7: Area of a Polygon

$$A = \frac{1}{2}\sum_{i=0}^{n-1}(x_i y_{i+1} - x_{i+1} y_i)$$

where $X_{0..i}$ and $y_{0..i}$ are the XY coordinate pairs of the vertices of the base polygon in order of adjacency, and A is the area of the base polygon. Once A has been calculated, the centroid of the base of support can be calculated using the formula,

Equation 8: Polygon Centroid Equations (7)

$$C_x = \frac{1}{6A}\sum_{i=0}^{n-1}(x_i + x_{i+1})(x_i y_{i+1} - x_{i+1} y_i)$$

$$C_y = \frac{1}{6A}\sum_{i=0}^{n-1}(y_i + y_{i+1})(x_i y_{i+1} - x_{i+1} y_i)$$

where C_x and C_y are the coordinates of the centroid, and X_i and Y_i are defined similarly to the Area equation.

In Figure 25, the red outline indicates the base of support. The red point indicates the centroid of the base of support, and the blue point indicates the centroid of the robot chassis:

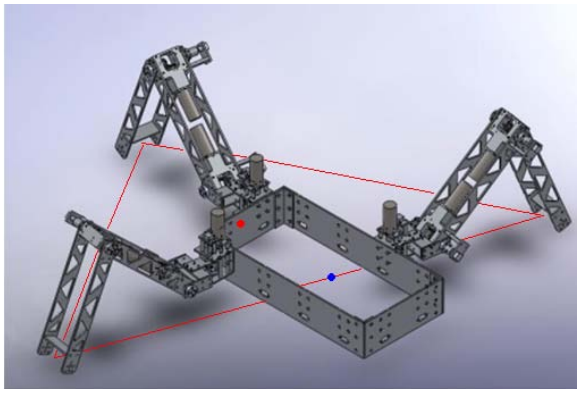

Figure 25: Base of Support and Robot Chassis Centroids

The robot is balanced when the robot centroid lies inside the base of support. In order to achieve “perfect” balance, the centroid of the robot chassis and the centroid of the base of support must be aligned. Figure 26 shows the vector (in green) along which the base of support centroid must move in order to most efficiently maximize balance. This vector will be referred to as the stabilizing vector:

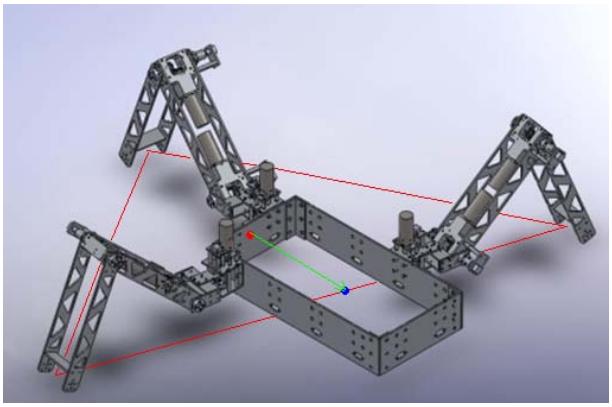

Figure 26: The Stabilizing Vector

As previously discussed, each leg must move within its physical workspace given the height at which the robot is commanded, referred to as the z-constrained leg workspace. Given each leg’s constraints for joint range of motion and link length, this workspace will resemble that of the following image, with the boundaries denoted by red lines or arcs, and the centroid, or best mobility/manipulability position (26), denoted by the red point in Figure 27:

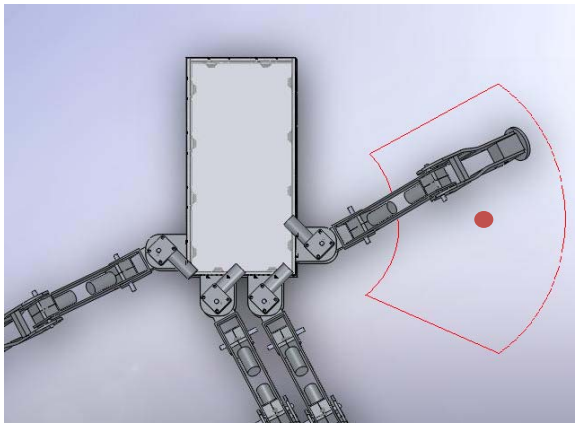

Figure 27: Z-Constrained Leg Workspace

The CoSSMo algorithm is a continuous simulation; it does not physically move the robot legs until it has produced an answer. CoSSMo works by first hypothetically placing all end-effectors in their

optimal position for mobility, or the centroid of their respective workspaces. CoSSMo then iterates through adjacent end-effectors and moves them incrementally along the stabilizing vector inside their workspace boundaries. This results in one edge of the base of support moving in such a direction as to cause an increase in overall stability of the robot. At each incremental move, a metric is calculated both for mobility and stability, and these metrics are combined into a total score. The current highest scoring configuration's end-effector positions are stored, and the process repeats until the algorithm is stopped. In this way, CoSSMo can be set to run for a fixed time, and allowed varying amounts of time to determine a stable and mobile configuration. Start-up configurations (i.e., connecting legs to the robot and powering it) will be allowed larger amounts of time to reach a more optimal configuration, but other situations (such as losing a leg) may require that less time is spent on determining a configuration and must use a less optimal but still "sufficient" answer.

Sensor Assisted Balancing

In the event that the MPU detects devices that generate data about the robot's gravitational orientation, such as a gyroscope or an accelerometer, other balancing methods can be employed without making the assumptions used by the CoSSMo method. Furthermore, sensor assisted methods do not necessarily need to operate by maximizing geometric symmetry or centroid positioning, allowing the robot more freedom in its motions, and the ability to dynamically balance. While sensor assisted balance methods have not been attempted on the current platform, future work will be done in this area so a general discussion involving sensor assisted balancing follows.

The CoSSMo method can still be employed with sensors to arrive at a starting point for balance and mobility. However, utilizing devices that can determine the robot's acceleration can balance the robot by means that do not force the chassis to remain parallel to the ground.

A three-axis accelerometer can report acceleration in the x, y, and z directions. This reported acceleration can be viewed as a vector, indicating the speed and direction in which the robot is moving. Assuming that the robot is not currently moving itself, any non-zero vector would indicate that the robot is falling or sliding in the direction of that vector, so this vector will be referred to as the falling vector. If the falling vector is made to be a ray originating from the centroid of the robot chassis (which would simply involve the correct placement of the accelerometer), then it must at some point cross a boundary of the base of support. Legs that are adjacent to where this intersection occurs can move in the direction of the falling vector, weighted by their distance to the intersection point, and cause the robot to stabilize.

In any method of balance control, the MPU must send coordinates to the LCUs. It is expected that the LCUs will use these coordinates to position end feet of their respective legs in these locations. Next, we will discuss how this is achieved by the LCU.

2.4.3. LCU Software & Operational Characteristics

The individual LCUs will help the ReMMRP exploit the multiprocessor environment presented by the attachment of multiple peripherals. Were the MPU the only processor in the robot, it would have to perform every calculation necessary for the actuation of each motor in each leg. These calculations can be both processor-intensive and time sensitive. The amount of calculations will increase linearly with each leg, and eventually the demand on the MPU would cause noticeable effects on the performance of the robot, either by sheer consumption of computing cycles or decreased ability to update leg positions at the desired frequency (also due to consumption of computing cycles.) To lessen the load on the MPU, every peripheral will be required to perform its own joint position calculations, and the MPU will only perform those calculations that correlate data from the peripherals.

Individual LCUs exchange relevant data with the MPU in the form of floating point three-dimensional coordinates. The LCU is responsible for:

- Converting the end-effector coordinates into angular values between its links.
- Reading the angular position of its links, and converting that data into a three-dimensional coordinate.
- Controlling all three of its motors in such a fashion that the angular values derived from coordinates are reached in a reliable and timely fashion.

2.4.3.1. Kinematics

The process by which joint angles are converted to leg end-effector coordinates, and vice versa, falls under a branch of classical mechanics referred to as kinematics (27). Each joint of the robot leg can be defined in its own coordinate frame**,** where the initial coordinate frame n_0 (at the first joint of the leg) is defined in the same z-direction as the robot coordinate frame, but the x-axis is oriented away from the chassis. The y-direction is defined as the vector cross product of z and x, respectively. Coordinate frames of the individual joints in a leg module are illustrated in Figure 28.

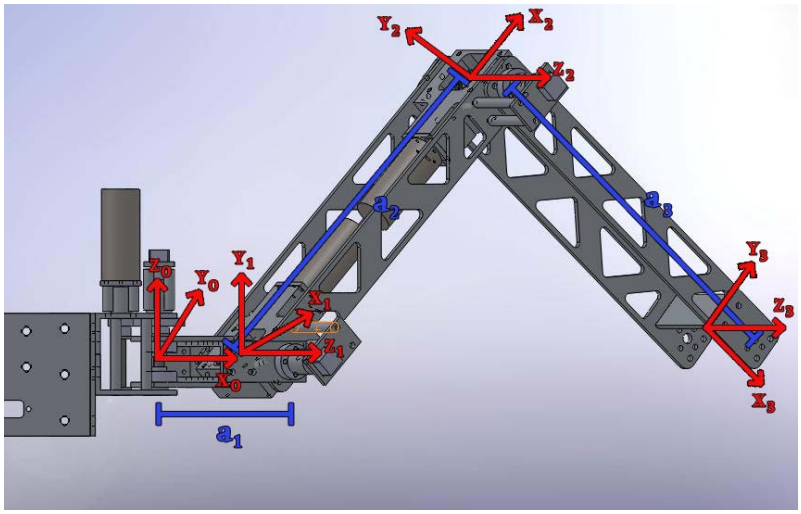

Figure 28: Leg Joint Coordinate Frames
Note: The leg shown is the revised version of the leg as described in Section 3.1.

The Denavit-Hartenberg Convention

The Denavit-Hartenberg convention is used to describe the complete shift, or homogeneous transformation, from coordinate frame *n-1* to coordinate frame *n,* and is defined as the product of four basic transformations, using four parameters:

- **d** – link offset
- **Θ** – joint angle
- **α** – link twist
- **a** - link length

The homogeneous transformation from *n-1* to *n*, denoted as T_n^{n-1}, is then described as:

Equation 9: Denavit-Hartenberg Homogeneous Transformation

$$T_n^{n-1} = Trans_{z_{n-1}}(d_n) \cdot Rot_{z_{n-1}}(\theta_n) \cdot Trans_{x_n}(a_n) \cdot Rot_{x_n}(\alpha_n)$$

In linear algebraic terms, this is:

$$T_n^{n-1} = \begin{bmatrix} 1 & 0 & 0 & 0 \\ 0 & 1 & 0 & 0 \\ 0 & 0 & 1 & d_n \\ 0 & 0 & 0 & 1 \end{bmatrix} \begin{bmatrix} \cos\theta_n & -\sin\theta_n & 0 & 0 \\ \sin\theta_n & \cos\theta_n & 0 & 0 \\ 0 & 0 & 1 & 0 \\ 0 & 0 & 0 & 1 \end{bmatrix} \begin{bmatrix} 1 & 0 & 0 & a_n \\ 0 & 1 & 0 & 0 \\ 0 & 0 & 1 & 0 \\ 0 & 0 & 0 & 1 \end{bmatrix} \begin{bmatrix} 1 & 0 & 0 & 0 \\ 0 & \cos\alpha_n & -\sin\alpha_n & 0 \\ 0 & \sin\alpha_n & \cos\alpha_n & 0 \\ 0 & 0 & 0 & 1 \end{bmatrix}$$

$$= \begin{bmatrix} \cos\theta_n & -\sin\theta_n \cos\alpha_n & \sin\theta_n \sin\alpha_n & a_n \cos\theta_n \\ \sin\theta_n & \cos\theta_n \cos\alpha_n & -\cos\theta_n \sin\alpha_n & a_n \sin\theta_n \\ 0 & \sin\alpha_n & \cos\alpha_n & d_n \\ 0 & 0 & 0 & 1 \end{bmatrix}$$

The following table illustrates Denavit-Hartenberg values for each coordinate frame *n* of the leg. By substituting these values into the general homogeneous transformation derived above, a specific homogeneous transformation can be determined between each joint in the leg.

Table 5: Denavit-Hartenberg Parameters for ReMMRP Leg Modules

n	Θ_n	α_n	d_n	a_n
1	Θ_1	90°	0	a_1
2	Θ_2	0°	0	a_2
3	Θ_3	0°	0	a_3

Equation 10: Parameterized Sequential Homogenous Transformation Matrices

$$T_1^0 = \begin{bmatrix} \cos\theta_1 & 0 & \sin\theta_1 & a_1\cos\theta_1 \\ \sin\theta_1 & 0 & -\cos\theta_1 & a_1\sin\theta_1 \\ 0 & 1 & 0 & 0 \\ 0 & 0 & 0 & 1 \end{bmatrix}$$

$$T_2^1 = \begin{bmatrix} \cos\theta_2 & -\sin\theta_2 & 0 & a_2\cos\theta_2 \\ \sin\theta_2 & \cos\theta_2 & 0 & a_2\sin\theta_2 \\ 0 & 0 & 1 & 0 \\ 0 & 0 & 0 & 1 \end{bmatrix}$$

$$T_3^2 = \begin{bmatrix} \cos\theta_3 & -\sin\theta_3 & 0 & a_3\cos\theta_3 \\ \sin\theta_3 & \cos\theta_3 & 0 & a_3\sin\theta_3 \\ 0 & 0 & 1 & 0 \\ 0 & 0 & 0 & 1 \end{bmatrix}$$

Computing the homogeneous transformation from coordinate frame 0 to coordinate frame 3 is then:

Equation 11: Homogeneous Transformation from Coordinate Frame 0 to Coordinate Frame 3

$$T_3^0 = T_1^0 T_2^1 T_3^2$$

$$= \begin{bmatrix} \cos\theta_1 & 0 & \sin\theta_1 & a_1\cos\theta_1 \\ \sin\theta_1 & 0 & -\cos\theta_1 & a_1\sin\theta_1 \\ 0 & 1 & 0 & 0 \\ 0 & 0 & 0 & 1 \end{bmatrix} \begin{bmatrix} \cos\theta_2 & -\sin\theta_2 & 0 & a_2\cos\theta_2 \\ \sin\theta_2 & \cos\theta_2 & 0 & a_2\sin\theta_2 \\ 0 & 0 & 1 & 0 \\ 0 & 0 & 0 & 1 \end{bmatrix} \begin{bmatrix} \cos\theta_3 & -\sin\theta_3 & 0 & a_3\cos\theta_3 \\ \sin\theta_3 & \cos\theta_3 & 0 & a_3\sin\theta_3 \\ 0 & 0 & 1 & 0 \\ 0 & 0 & 0 & 1 \end{bmatrix}$$

In the interest of brevity, the following notations will be used for trigonometric functions:

- $\mathbf{C}_n = \cos(\Theta_n)$; $\mathbf{C}_{nm} = \cos(\Theta_n + \Theta_m)$
- $\mathbf{S}_n = \sin(\Theta_n)$; $\mathbf{S}_{nm} = \sin(\Theta_n + \Theta_m)$

The following trigonometric sum-difference identities are also used for simplification:

- $\sin(\alpha \pm \beta) = \sin\alpha\cos\beta \pm \cos\alpha\sin\beta$
- $\cos(\alpha \pm \beta) = \cos\alpha\cos\beta \mp \sin\alpha\sin\beta$

Accordingly, the final product is:

$$T_3^0 = \begin{bmatrix} \boldsymbol{C_1C_2C_3 - C_1S_2S_3} & \boldsymbol{-C_1C_2S_3 - C_1S_2C_3} & \boldsymbol{S_1} & a_1\boldsymbol{C_1} + a_2\boldsymbol{C_1C_2} + a_3\boldsymbol{C_1C_{23}} \\ \boldsymbol{S_1C_2C_3 - S_1S_2S_3} & \boldsymbol{-S_1C_2S_3 - S_1S_2C_3} & \boldsymbol{-C_1} & a_1\boldsymbol{S_1} + a_2\boldsymbol{S_1S_2} + a_3\boldsymbol{S_1C_{23}} \\ \boldsymbol{S_2C_3 + C_2S_3} & \boldsymbol{-S_2S_3 + C_2C_3} & 0 & a_2\boldsymbol{S_2} + a_3\boldsymbol{S_{23}} \\ 0 & 0 & 0 & 1 \end{bmatrix}$$

Note that this transformation only results in the end-effector of the leg with respect to the initial coordinate frame; each port on the ReMMRP chassis has a predefined transformation $T_{n_0}^r$, which is used to find the location of leg *n*'s initial coordinate frame with respect to the robot coordinate system. The position of leg *n*'s foot with respect to the robot coordinate system is then calculated as:

Equation 12: Transformation from Leg Coordinate Frame to Robot Coordinate Frame

$$T_{n_3}^r = T_{n_0}^r T_{n_3}^{n_0}$$

Linear algebra procedures, such as the matrix multiplication used in the above equations, are very time and memory consuming when performed on the ATMega164/324/644P processor. However, the matrices derived from the general equation can be condensed to produce a closed form solution, and this can be converted almost directly into usable, efficient code.

Forward Kinematics

Forward kinematics will allow the LCU to generate a three dimensional coordinate that describes the position of its end-effector as a function of its joint angles, or simply:

$$(\theta_1, \theta_2, \theta_3) \rightarrow (x, y, z)$$

The final product, T_3^0, from the Denavit-Hartenberg equations results in what is known as a homogeneous transformation matrix from coordinate frame *n-1* to coordinate frame *n* (26):

$$\begin{bmatrix} \begin{pmatrix} & R_n^{n-1} & \end{pmatrix} & \begin{pmatrix} P_x \\ P_y \\ P_z \end{pmatrix} \\ 0 \quad 0 \quad 0 & 1 \end{bmatrix}$$

As shown above, the homogeneous transformation matrix consists of:

- R_n^{n-1}, a 3x3 matrix describing the rotation from *n-1* to *n*, and
- P, a 1x3 matrix describing the translation from *n-1* to *n*, or coordinates of *n* with respect to *n-1.*

Recall the homogenous transformation matrix T_3^0, shown below with the translation portion P highlighted:

$$T_3^0 = \begin{bmatrix} \boldsymbol{C_1C_2C_3 - C_1S_2S_3} & \boldsymbol{-C_1C_2S_3 - C_1S_2C_3} & \boldsymbol{S_1} & \boldsymbol{a_1C_1 + a_2C_1C_2 + a_3C_1C_{23}} \\ \boldsymbol{S_1C_2C_3 - S_1S_2S_3} & \boldsymbol{-S_1C_2S_3 - S_1S_2C_3} & \boldsymbol{-C_1} & \boldsymbol{a_1S_1 + a_2S_1S_2 + a_3S_1C_{23}} \\ \boldsymbol{S_2C_3 + C_2S_3} & \boldsymbol{-S_2S_3 + C_2C_3} & 0 & \boldsymbol{a_2S_2 + a_3S_{23}} \\ 0 & 0 & 0 & 1 \end{bmatrix}$$

End-effecter positions of the leg with respect to its initial coordinate frame can simply be extracted from this matrix, and are:

$$x = a_1 \cos\theta_1 + a_2 \cos\theta_1 \cos\theta_2 + a_3 \cos\theta_1 \cos(\theta_2 + \theta_3)$$

$$y = a_1 \sin\theta_1 + a_2 \sin\theta_1 \cos\theta_2 + a_3 \sin\theta_1 \cos(\theta_2 + \theta_3)$$

$$z = a_2 \sin\theta_2 + a_3 \sin(\theta_2 + \theta_3)$$

Control code used to perform these calculations can be seen in Code Sample 3.

```
void ForwardKinematics(Angles *angle, Coordinate *coords) {

	//Scratchpad variables
	double q1, q2;

	//Calculate and store z coordinate
	q1 = sin(angle->theta2);
	q1 += sin(angle->theta2 + angle->theta3);
	q1 *= LINK_LENGTH;
	coords->z = q1;

	//Calculate and store x coordinate
	q1 = cos(angle->theta2);
	q1 += cos(angle->theta2 + angle->theta3);
	q1 *= LINK_LENGTH;
	q1 += A1;
	q2 = cos(angle->theta1);
	coords->x = q1 * q2;

	//Calculate and store y coordinate
	q2 = sin(angle->theta1);
	coords->y = q1 * q2;

}
```

Code Sample 3: Forward Kinematics

In order for the LCU to derive joint angles from a set of coordinates, a different strategy is needed, and is discussed next.

2.4.3.2. Inverse Kinematics

Inverse kinematics equations will allow the LCU to generate a set of joint angles from a set of coordinates that will cause the end-effector to be in the position indicated by the coordinates:

$$(x, y, z) \rightarrow (\theta_1, \theta_2, \theta_3),$$

Where (x,y,z) denotes the three-dimensional coordinate of the end-effector.

The horizontal angular position of the hip joint, or θ_1, is does not depend on the position of the other two joints in the leg, as it has no effect on the z position of the end-effector. This angle can be calculated using the inverse tangent function and the desired x and y position of the end effector:

Equation 13: Angular Position of the Horizontal Hip Joint

$$\tan\theta_1 = \left(\frac{y}{x}\right) \rightarrow \theta_1 = \tan^{-1}\left(\frac{y}{x}\right)$$

For the angle to be in the correct quadrant, the function **atan2** must be utilized:

$$\theta_1 = atan2(y, x),$$

where **atan2** will return the angle in the correct quadrant by using the signs of the x and y coordinates.

Unlike θ_1, the vertical hip angle θ_2 depends on the knee angle θ_3. Therefore, θ_3 must be calculated first:

Equation 14: Angular Position of the Vertical Hip Joint

$$\theta_3 = \cos^{-1}\left(\frac{\left(\frac{x}{\boldsymbol{C}_1} - a_1\right)^2 + z^2 - a_2^2 - a_3^2}{2a_2a_3}\right)$$

Since the ReMMRP's link lengths a_2 and a_3 are identical, they will be referred to as *L*, and the above equation can be simplified to:

$$\theta_3 = \cos^{-1}\left(\frac{\left(\frac{x}{\boldsymbol{C}_1} - a_1\right)^2 + z^2 - 2L^2}{2L}\right)$$

Finally, θ_2 can be calculated using θ_1 and θ_3:

Equation 15: Angular Position of the Knee Joint

$$\theta_2 = -\tan^{-1}\left(\frac{a_3\boldsymbol{S}_3}{a_2 + a_3\boldsymbol{C}_3}\right) + \sin^{-1}\left(\frac{z}{\sqrt{(a_2 + a_3\boldsymbol{C}_3)^2 + a_3^2\boldsymbol{S}_{23}^2}}\right)$$

This equation must again utilize the **atan2** function to return the angle in the proper quadrant, and can be rewritten as:

$$\theta_2 = -atan2\left(\frac{a_3\boldsymbol{S}_3}{a_2 + a_3\boldsymbol{C}_3}\right) + \sin^{-1}\left(\frac{z}{\sqrt{(a_2 + a_3\boldsymbol{C}_3)^2 + a_3^2\boldsymbol{S}_{23}^2}}\right)$$

Control code used to perform these calculations can be seen in Code Sample 4.

```
void InverseKinematics(Coordinate *coords, Angles *angle) {

	//Scratchpad variables
	double q1, q2, b;

	//Calculate and store hip angle (theta 1)
	angle->theta1 = atan2(coords->y, coords->x);

	//Calculate knee (y) angle (theta 3)
	q2 = (coords->x / cos(angle->theta1));
	q2 -= A1;
	q2 *= q2;
	q2 += (coords->z * coords->z);

	q2 -= (2.000 * LINK_LENGTH * LINK_LENGTH);
	q1 = 2.000 * LINK_LENGTH * LINK_LENGTH;
	q2 /= q1;

	//Store theta3
	angle->theta3 = acos(q2); //2-26 4:38pm

	//Calculate hip vertical angle (theta 2)
	b = A3 * cos(angle->theta3);
	b += A2;
	q1 = A3 * sin(angle->theta3);
	q2 = atan2(q1, b);
	q2 *= -1;

	b = A3 * cos(angle->theta3);
	b += A2;
	b *= b;
	q1 = A3 * A3;
	q1 *= (sin(angle->theta3) * sin(angle->theta3));
	b += q1;
	q1 = sqrt(b);
	b = coords->z / q1;

	angle->theta2 = q2 + asin(b);

}
```

Code Sample 4: Inverse Kinematics

Now that leg coordinates can be converted into control angles, and vice versa, the robot control functions can be abstracted to the Euclidean coordinates of the robot base frame.

2.4.3.3. Motion Control

The LCU contains the central processing unit for the entire leg peripheral. As such, it is responsible for distributing power to each of three motors and interpreting data from each of three potentiometers. Each motor is paired with a unique potentiometer as a means of measuring joint position. The LCU must integrate the control of the motor with the interpretation of the potentiometer signal in a meaningful way.

Motor Functions

Any electric motor can be controlled by varying the input voltage, which is referred to as analog drive. However, for a digital processor to process an analog signal, it must have a digital-to-analog converter, or DAC, to produce a usable output signal to the motor. Additionally, most processors do not function at the voltage nor can source the amperage required by an electric motor. This means that any voltage signal directed to a motor must be amplified, usually by means of an operational amplifier, or op-amp. These requirements for analog drive require a large amount of accessory hardware for simple motor control.

Another means of control is referred to as pulse width modulation, or PWM (28). In this method, the control signal to a motor will always be a constant voltage. This signal is high (on) or low (off) for subsequent portions of a predefined time increment, referred to as the PWM period. The inverse of the PWM period defines the PWM Frequency. The portion of the PWM period that is occupied by a high signal is referred to as the duty cycle.

PWM will approximate an analog signal, as seen in Figure 29, by accelerating the motor to a certain velocity during the duty cycle, and allowing it to decelerate during the low signal portion of the PWM period:

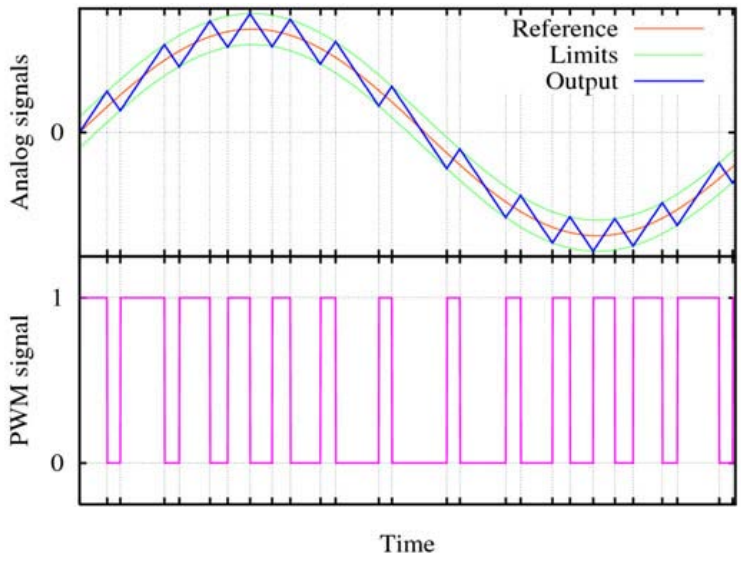

Figure 29: PWM vs Analog Drive

The PWM signal can be used to drive a simple H-bridge that will supply the motor with its necessary power, and no DAC or op-amp is necessary. The conceptual H-bridge, shown in Figure 30, has the following switches:

- E: Enable switch. Allows the H-bridge to operate by sourcing the motor voltage.
- 1 through 4: Combinations of these switches direct the flow of current through the h-bridge to ground. The combinations (1,4) and (2,3) will allow current to flow through the motor

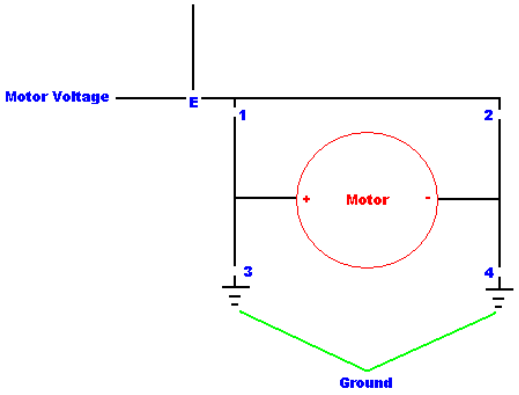

Figure 30: Conceptual H-Bridge Diagram

The ATMega164/324 /644P processors are equipped with three internal timers that are each capable of generating two PWM signals separately from each other and independent of any other internal processing. This feature is exploited in the LCU software by initializing two timers to the same PWM frequency. One of these timers is used to control the PWM signal to two motors, and the other timer controls the PWM signal to the third motor. The ATMega164/324/644P PWM timer function can then be controlled by simply augmenting the duty cycle with the software.

The only remaining aspect of motor control is directionality, where it is determined in which direction the motor will rotate. The LCU is configured in such a fashion as to enable the H-bridge on the "high" PWM signal, and disable the H-bridge on the "low" PWM signal. The actual motor signal in the software is represented as a signed value, which indicates whether the motor should be moving in forward or reverse rotation. The sign of this value will cause the H-bridge to be configured in one of two ways:

- Forward, where current across the motor flows from the positive motor terminal to the negative motor terminal, and

- Reverse, where current across the motor flows from the negative motor terminal to the positive motor terminal.

These are illustrated below:

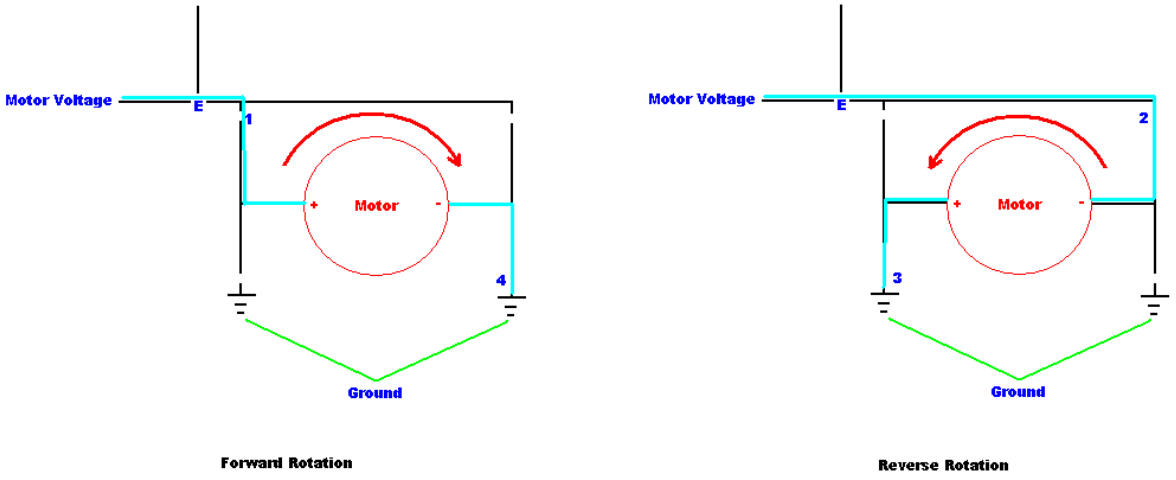

Figure 31: Forward and Reverse Configurations of the Conceptual H-Bridge

Now that the motor can be commanded to rotate in either direction at varying speeds, a means of detecting the corresponding joint's position must be employed. This is done through the use of variable resistors, or potentiometers, connected to the joint axis.

Potentiometer Functions

The potentiometers will produce a voltage signal that is commensurate with their angular position. They have a physical range of 270°, and their voltage output ranges from 0V to the input voltage (in this application, 5V). Tests on the potentiometers used for this application showed a linear correlation between potentiometer position and voltage output. Using linear interpolation, the start and end voltages are referred to as x_0 and x_1 respectively, and the start and end angle values are referred to as y_0 and y_1 respectively. An angular value y is then determined from the equation,

Equation 16: Linear Interpolation

$$y = y_0 + (x - x_0)\frac{y_1 - y_0}{x_1 - x_0}$$

This still renders an analog voltage; the resulting value must be converted into one that can be used by the ATMega164/324/644P processor.

The ATMega164/324/644P processors have a built-in analog to digital converter, or ADC. The ADC functions by approximating a voltage input to a certain resolution; on the ATMega164/324/644P this resolution is 10 bits. The input voltage is converted into a digital value in the range of 0 to $(2^{resolution})$-1, or 0 to 1023.

The same linear interpolation can be used by replacing the voltage range of 0V to 5V with the digital range of 0 to 1023.

2.4.3.4. PID Control

In order to control the motor to arrive and stay at a given angle, a continuous means of control must be implemented. Simply running the motor until it reaches a certain point will not work, since the inertia of the motor and leg will continue to carry the axis past the desired point after the motor is shut off. A controller must be used that monitors the relationship between the desired joint position and the actual joint position, the difference in which is referred to as the error, and adjusts the motor's behavior to minimize the error.

Proportional-Integral-Derivative (PID) control uses the summation of three terms to monitor and control the signal to a motor (29):

1. Proportional Term: the difference between the current motor position and the desired position. Greater errors will cause a larger control signal to the motor. Proportional control alone is typically subject to oscillations in the motor output.
2. Integral Term: the sum of the positional errors over time. The role of the integral term is to decrease the oscillation caused by the Proportional control. By using the Integral control the arm will eventually settle into the desired position.
3. Derivative Control: the rate of change in the error, used to balance the Integral control by dampening the decaying oscillations from proportional-integral control.

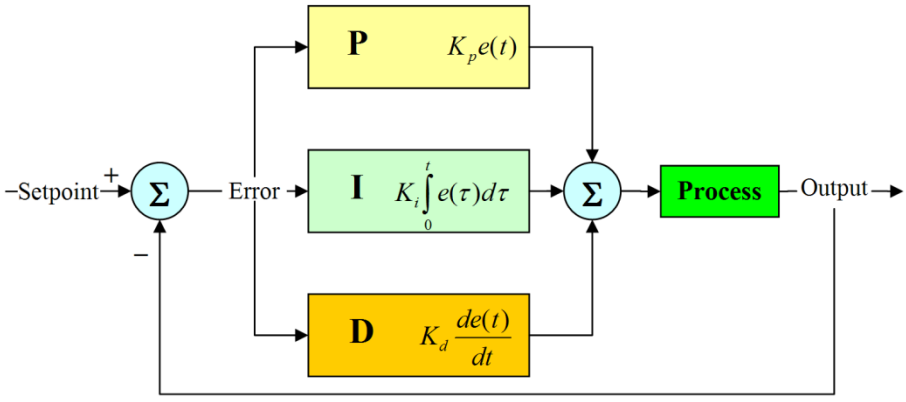

Figure 32: PID Control Process Diagram

As can be seen in Figure 32, each term is typically expressed with a constant coefficient that will give weight to the term in the overall equation. The constants for proportional, integral, and derivative terms are referred to as K_p, K_i, and K_d, respectively. The values of these constants will vary from application to application, and in each robot leg from joint to joint, due to the different masses and torques associated with each joint.

To tune the PID equations for the robot leg motors, the Ziegler-Nichols Ultimate Gain method is employed (30). This is a simple method, using only four steps:

1. Initialize PID with all constants set to zero.
2. Increase K_p until a steady oscillation is reached.
3. Once oscillation is reached, the value of K_p is referred to as K_c, or the ultimate gain, and the period of the resulting oscillation is referred to as P_c.
4. Calculate the PID constants using the following formulae:

Table 6: Ziegler-Nichols Ultimate Gain Equations

K_p	K_i	K_d
0.60 K_c	$2K_p / P_c$	$K_p P_c / 8$

Control code used to perform PID control can be seen in Code Sample 5.

```
int PIDController(int setPoint, int processValue, pidData_t *pid_st) {
	float p_term, d_term, i_term, ret, error;
	int err, output;

	err = setPoint - processValue;
	if (err > 1024) {
		err = 1024;
	} else if (err < -1024) {
		err = -1024;
	}
	error = err;

	//P TERM
	p_term = pid_st->P_Factor * error;

	//I TERM
	pid_st->sumError -= pid_st->errHistory[pid_st->curError];
	pid_st->curError++;
	pid_st->curError %= ERROR_WINDOW;	//Use fixed number of previous errors

	if ((error <= DEADZONE) && (error >= -DEADZONE)) {
		pid_st->errHistory[pid_st->curError] = 0;
	} else pid_st->errHistory[pid_st->curError] = err;

	pid_st->sumError += pid_st->errHistory[pid_st->curError];

	i_term = pid_st->I_Factor * (float)pid_st->sumError;


	//D TERM
	d_term = pid_st->D_Factor * (float)(pid_st->lastProcessValue - processValue);

	pid_st->lastProcessValue = processValue;

	ret = (p_term + i_term + d_term) * pid_st->scalingFactor;
	if (ret > MAX_INT) {
		ret = MAX_INT;
	} else if (ret < -MAX_INT) {
		ret = -MAX_INT;
	}

	output = ret;
	return output;
}
```

Code Sample 5: PID Control

Through the use of kinematics and PID control, each robotic leg can now be reliably commanded to a desired orientation in the robot coordinate frame.

2.4.4. Software Model Diagrams

The following section outlines the general behavior of the MPU, LCU, and integrated ReMMRP control system during their operational cycles.

2.4.4.1. MPU Flow Diagram

The MPU software behaves continuously in the following manner:

1. On power up, initialize internal hardware (communications, timers, etc.), and wait for a “ready” signal from STATUS processor.
2. Determine available peripherals and select proper control algorithm(s).

3. Command peripherals using control algorithms and real-time feedback data from peripherals. At any time during this process, if there is a change in peripheral attachments as indicated by the STATUS processor, return to step 2.
4. Return to step 3.

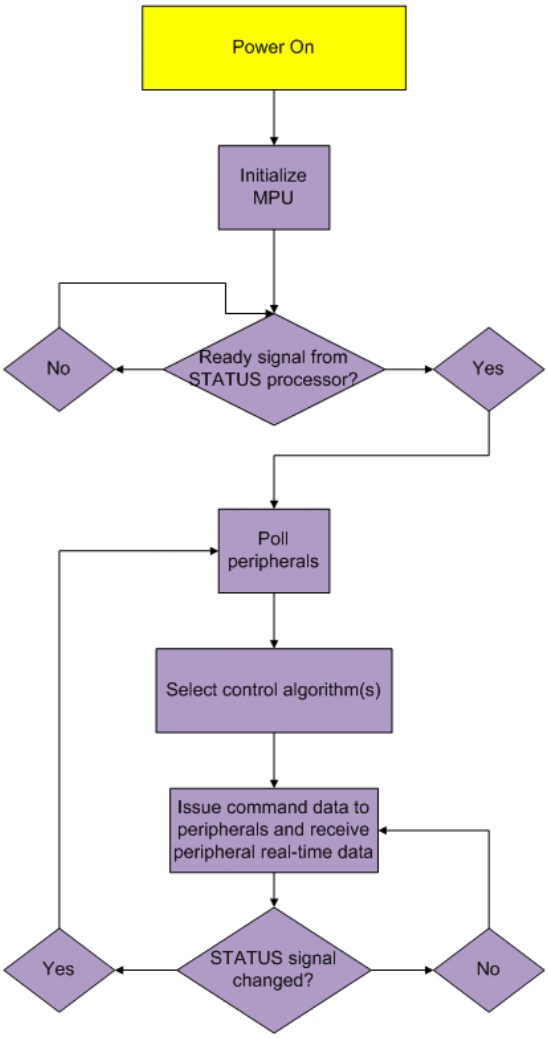

Figure 33: MPU Software Flow Diagram

2.4.4.2. LCU Flow Diagram

The LCU software behaves continuously in the following manner:

1. On power up, initialize internal hardware (communications, timers, ADC, etc.), and produce a "ready" signal to the STATUS processor.
2. Wait for a command from the MPU, causing simultaneous transfer of real-time feedback data to MPU.

3. Perform command from MPU until either:
    a. A new command is received, or
    b. A software or hardware error in the LCU occurs; then disable “ready” signal to STATUS processor to indicate malfunction. Operation is terminated in this event.
4. Return to step 3.

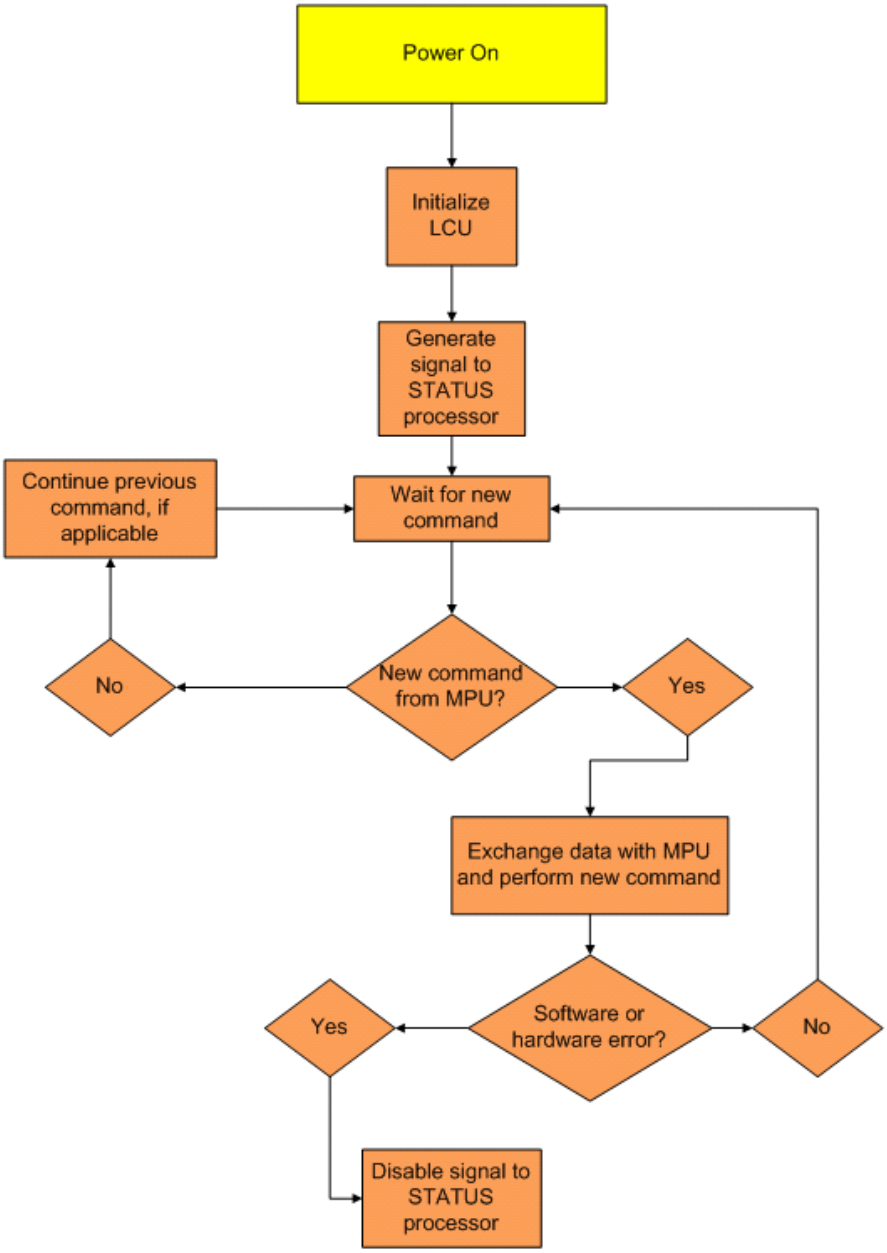

Figure 34: LCU Software Flow Diagram

2.4.4.3. Integrated Flow Diagram

The complete software model of the robot behaves continuously in the following manner:

1. On power up, MPU, LCUs, and STATUS processors initialize.
2. LCUs (and other peripherals) send “ready” signal to the STATUS processor.
3. STATUS processor determines which ports have attached peripherals, or active ports, and communicates this information to the MPU.
4. MPU polls active ports for identification information and creates a list of peripheral devices based on type.
5. MPU groups similar peripherals and selects control algorithm to employ accordingly.
6. MPU utilizes control algorithm(s) to generate command data for peripherals.
7. Command data is distributed to peripherals while real-time configuration data is simultaneously returned to the MPU.
8. Real-time peripheral configuration data is fed into the control algorithm(s) on the MPU to generate new command data for the peripheral devices.
9. In the event of a change in peripherals, go to step 3.
10. Return to step 5.

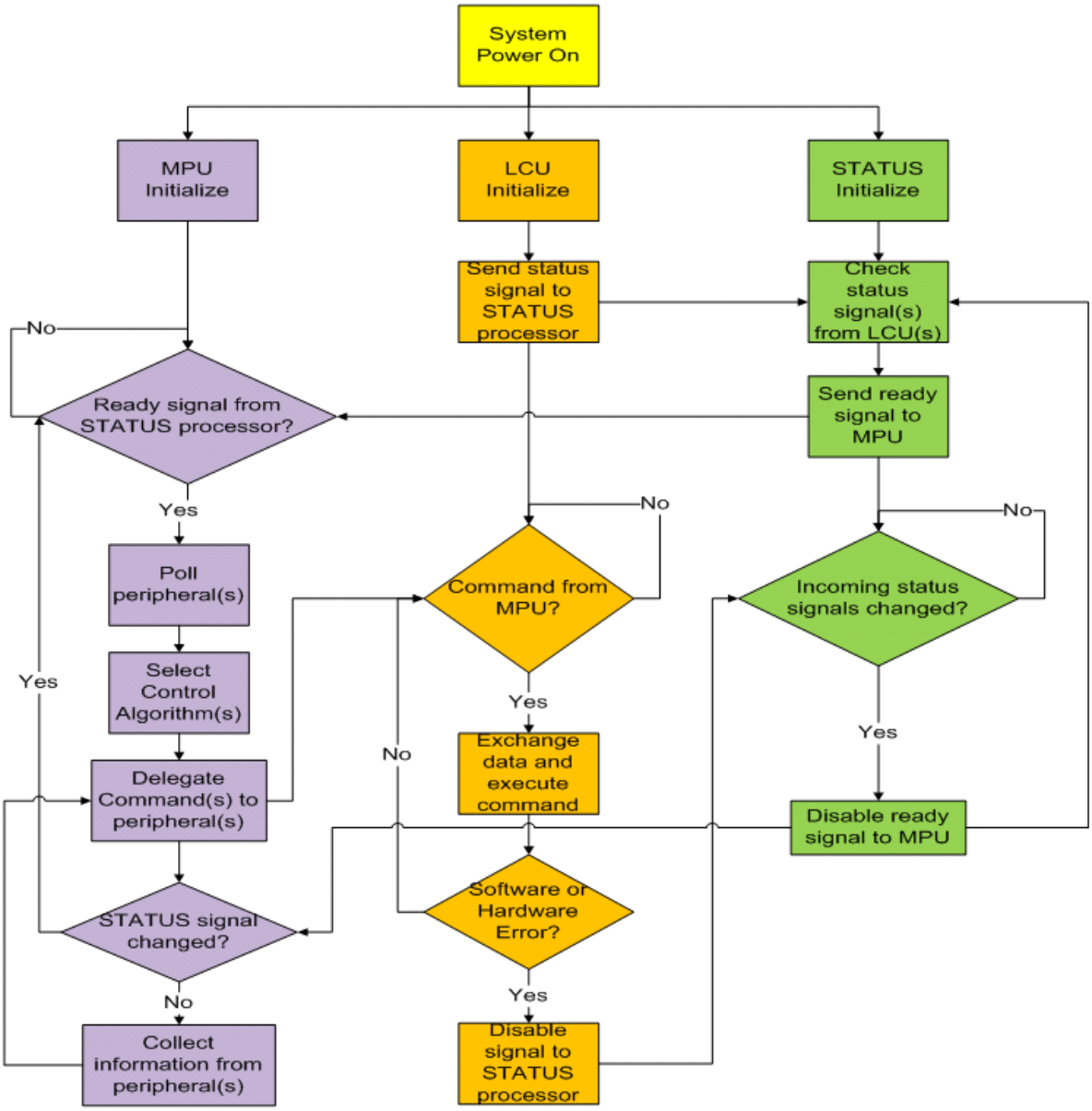

Figure 35: Integrated Software Control Flow Diagram

3. Results

The primary specifications outlined in Section 2.1 were reevaluated at the conclusion of the project. The success of each specification is rated according to the following key:

- ☺ - Design Specification Met; needs little to no revision or additional work
- 😐 - Design Specification Met; needs revision or additional work
- ☹ - Design Specification Not Met

Table 7: Design Specification Compliance

The chassis will have 12 connection points – 2 on each short side, 4 on each long side.	☺
The chassis must contain a centralized power distribution and communications hub.	☺
The chassis must contain a processor responsible for coordinating the actions of all peripheral modules.	☺
The MPU must be interchangeable.	☺
MPU software must determine actions for all peripheral modules and delegate commands to them in real time.	😐
The chassis must have a dedicated processor responsible for detecting the addition or removal of peripheral modules in real time independently of the MPUs operation.	☺
STATUS processor software must operate in real time, allowing MPU to have immediate knowledge of attached peripherals at any given time.	😐
The legs modules will be 3 degree of freedom (DOF) links	☺
The leg must operate in 3-dimensional space.	😐
The leg must have position sensors integrated into each joint.	☺
The joint motors must be mounted internally in each leg link.	☺
Each leg module must have self-contained control system.	☺

The LCU must have a processor capable of handling the software controls.	☺
The LCU must distribute power to joint motors and read joint position sensors.	☺
The LCU must be able to relay signals to the main control system.	☺
LCU software must respond to commands from MPU with higher priority than any other task inherent to LCU software.	☺
Communications protocol must exist for data transfer among the MPU, STATUS processor, and LCUs).	☺

While all of the design specifications were met, the fully assembled robot did not perform as desired. Solutions to the issues that affect the current version are discussed next. The robot at the completion of this project is shown in Figure 36.

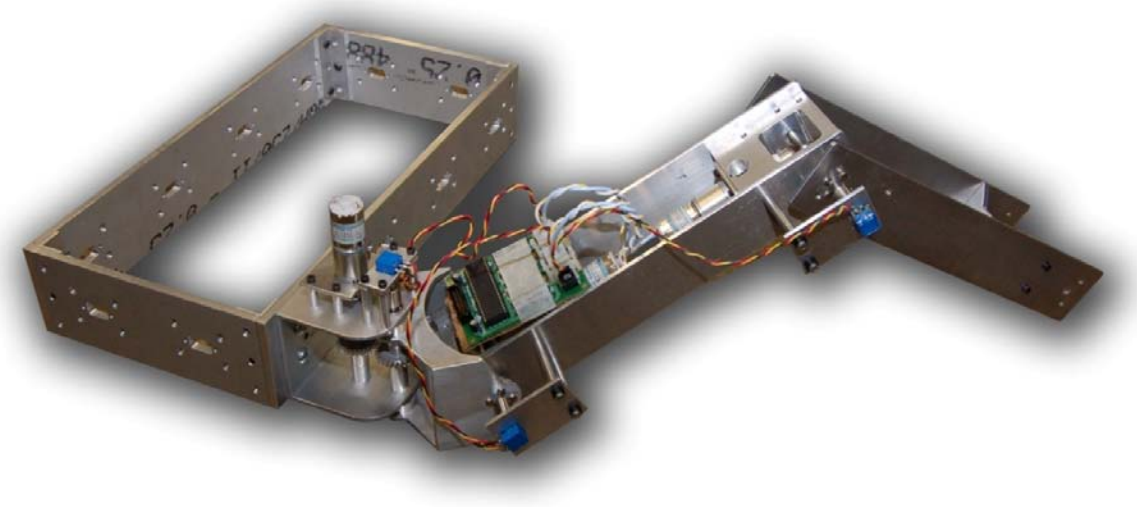

Figure 36: Completed Robot (1 Leg)

3.1.Mechanical Design Revisions

Once the leg was constructed, several problems became apparent and areas for improvement were noticed. In order to improve robot performance, an increase in complexity in the new version of the robot is needed. However before a new robot is designed, the initial design must be reviewed.

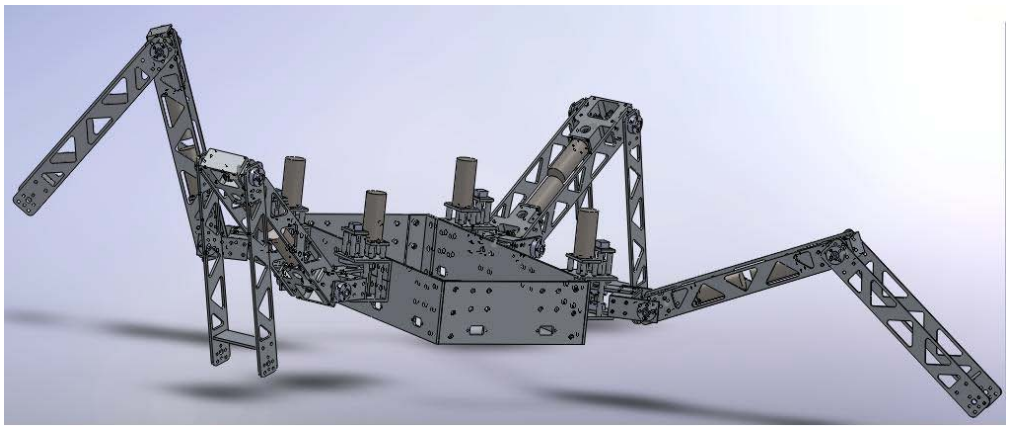

Figure 37: Conceptual Illustration of Revised ReMMRP Design

3.1.1. Review of the Initial Design

The main problem of the legs was caused by the miter gears used at the joints. The miter gears generate substantial axial forces that pushed the gears out of mesh. The solution to the problem was to ensure that washers were placed so that the gears could not force each other out of mesh. The other problem with the gears was the fact that the set screws would be forced out of place, which would allow the gears to spin freely. Holes were drilled through the gears and axles to pin them together and thus ensure that gears and axles will always rotate together.

Another problem experienced in the original design was the couplers between the motors and the shafts. The motor's output shaft is 4mm in diameter and the shaft used is 0.25 inches. The closest standard size diameter for a coupler is 0.375". The difference in diameters is 0.03 inches, which is enough to allow an unacceptable gap between the coupler and the shaft. A commercial coupler does not exist for the 4mm to 0.25" conversion; therefore a custom coupler was manufactured. The coupler was designed to use a 4-40 set screw, however the set screws proved insufficient against the forces of the gearbox. New holes were drilled into the coupler to accommodate an 8-32 set screw. These screws were more effective, but still frequently failed to prevent slippage.

The bracket design for the hip joint posed significant manufacturing challenges since it is made from tube stock. The main problem came from the through holes for the shaft. These holes need to be concentric to one another, which means that the holes should be drilled at the same time, however that requires a long carbide drill. The problem introduced by the long drill is deflection, which means that the drill bit will tend to be pushed off axis as the drill is pressed into the part. This phenomenon could result in the through holes not aligning with each other. All of the brackets made for the initial leg

suffered from drill bit deflection. Although the deflection was minimal, it is not desirable, and the effects were noticeable during construction of the leg.

The weight of the initial design could be lowered to reduce the forces needed to move the leg. There are two key places that could see weight reduction: the gearboxes, and the plate metal that forms the legs and the chassis. The current design of the gearboxes has significant excess metal. In addition, the placement of holes and the dimensions of the pocket could be optimized to further reduce the weight of the gearbox.

The plates that form the leg are currently solid sheet aluminum and weigh 0.16 lbs per plate, with a combined four-plate-per-leg weight of 0.64 pounds. Reducing the weight of each plate will reduce the torque required to move each leg, which will produce smaller forces on the various components in the leg.

The chassis is another source of substantial weight of the robot. The chassis is made of 0.25" sheet aluminum. An analysis will be conducted to see if the chassis can be manufactured from 0.125" thick aluminum.

3.1.2. Goals of the Revised Design

There are two main considerations for the revised design of the robot. The first consideration is to reduce the overall weight of the legs and chassis. The second consideration is to simplify the manufacturing process and assembly of the robot's components. Addressing these two areas will make the robot perform better, put less stress on the connection points, and eliminate the slippage in the gearbox that affected the previous design. Several components are targets to reduce the weight of the robot, namely the gearbox, the leg plates, and the chassis. The hip assembly is to be redesigned to be simpler to manufacture and assemble.

3.1.2.1. Gearbox Redesign

The current gearbox contains significant portions of unused metal. Figure 38 and Figure 39 show comparison images of the current and the revised gearboxes. The bolt holes that mount the gearbox to the leg are closer to the output shaft. The holes that secure the cover plates are shifted closer to the pocket to minimize the material in the gearbox. The pocket that holds the miter gears is reduced in size so that it will require fewer washers to mount the gears. The mounting holes that secure the motor are moved to reduce the size of the motor mounting plate. The movement of the mounting holes allowed for the removal of material on either side of the drive shaft. In addition, the front wall of the gearbox (the topmost edge in Figure 39) is reduced in thickness from 0.25" to 0.125". The thickness

of the gearbox was also reduced by 0.25”. These changes in the gearbox design reduced the weight of the gearbox from 1.46 lbs to 1.03 lbs, which is a 29.5% reduction in weight.

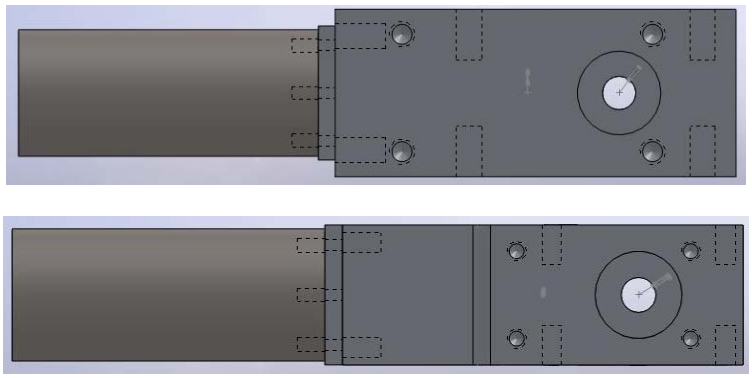

Figure 38: Side View Comparison of the previous gearbox (Top) and the new gearbox (Bottom)

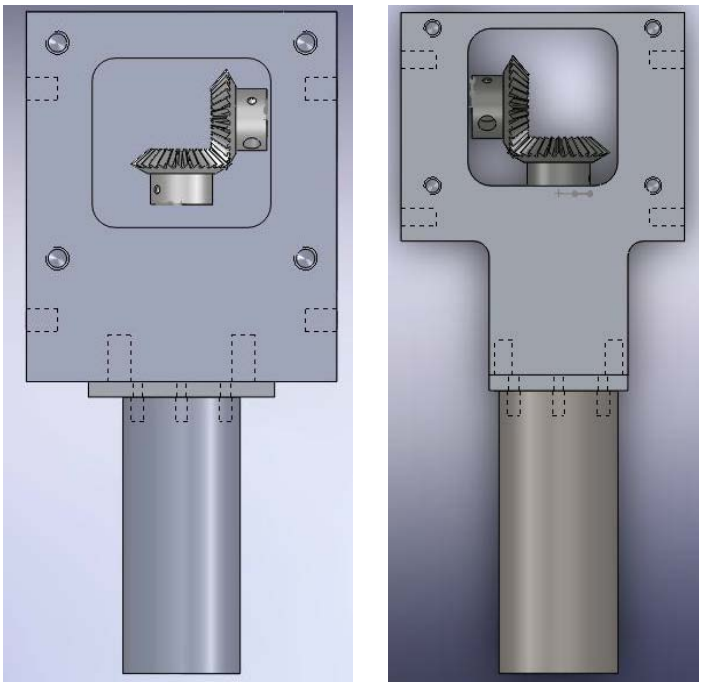

Figure 39: Top view comparison of the previous gearbox (Left) and the new gearbox (Right)

3.1.2.2. Leg Plate Redesign

In the current design there are two separate designs for the leg plates: one for the thigh and one for the calf. However, the only functional difference between the two plates is that the calf plate lacks the mounting holes for the gearboxes. In terms of manufacturing, this increases the time of manufacturing because two separate CAM files need to be created and two separate production runs need to be made. There is also no benefit to having a design like this. In the revision, the plates are

unified into a single design that can serve either as a calf plate or as a thigh plate. Figure 40 shows a comparison between the current thigh plate and the revised leg plate.

With the reduction in size of the gearbox, the leg plate was scaled down to fit the revised gearbox design. This leg plate is 11" long, compared to the 12" of the current design, and 1.25" wide compared to the 2" wide of the current design. The revised plate has all of the hole patterns necessary to connect a gearbox or mount the set screw hubs. The current thigh plate is solid plate metal with no pockets to reduce weight. The revised leg plate has cutouts to reduce the weight of the plate. The current thigh plate weighs 0.29 lbs while the revised leg plate weighs 0.11 lbs, which is 62% reduction in the weight of the plate.

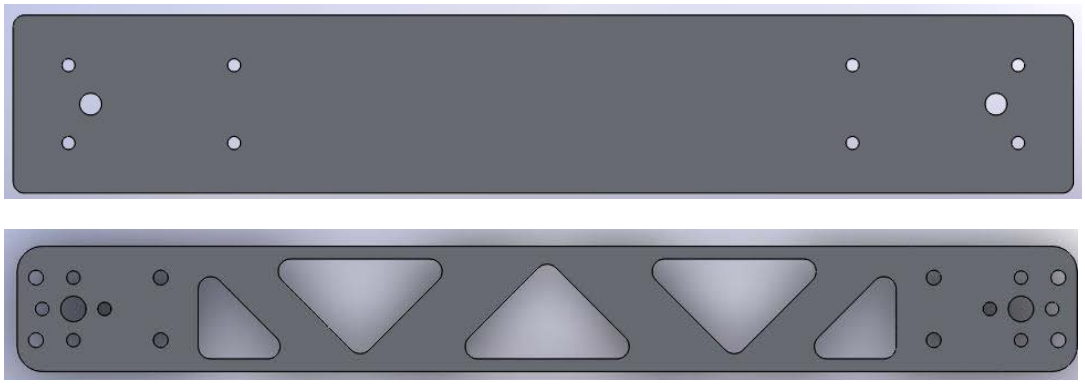

Figure 40: Comparison between the old Thigh Plate (Top) and the new Leg Plate (Bottom)

3.1.2.3. Hip Assembly

The main problem with the current design of the hip assembly is the difficulty of ensuring that the holes are concentric. The Horizontal Movement Assembly (HMA) is designed around a piece of aluminum tube stock; however in the revision the tube stock is used to mount plates which hold the set screw hubs. Figure 41 shows a comparison of the new and old brackets. Using plates makes it easier to ensure that the holes for the various shafts are concentric and do not require special machining. In addition, the bracket is smaller than the current one. The height of the part has been reduced to 1.25" from the original 3". The part wasn't redesigned to be lighter, but easier to manufacture, so the overall weight hasn't changed drastically. The weight has dropped from .25 lbs to .22 lbs.

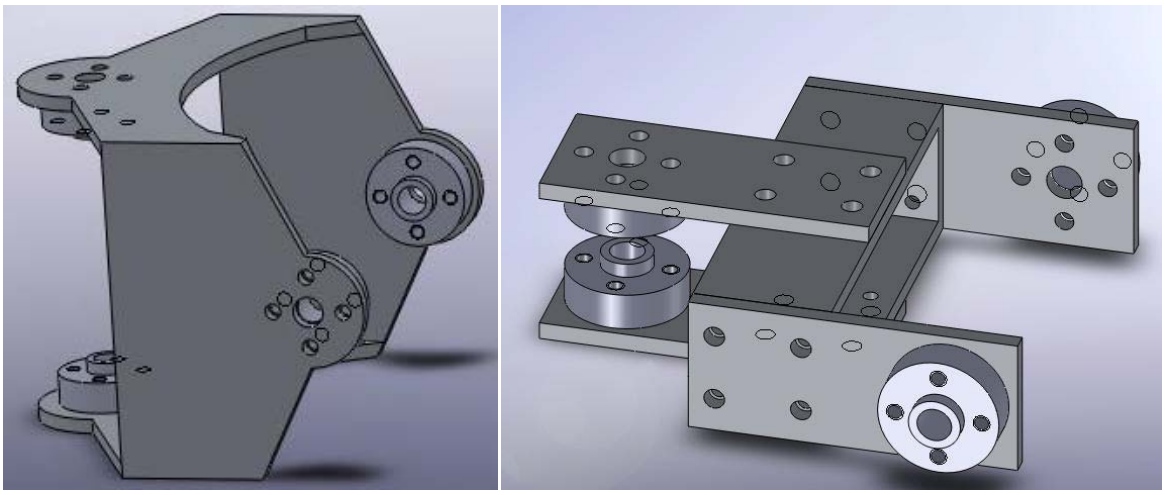

Figure 41: Comparison View of the old HMA (Left) compared to the new design (Right)

The current Hip Connection Bracket (HCB) is one piece of cut tube stock, but the revised design is made of two separate pieces of angle aluminum. There are two reasons for the two piece design. The primary reason is the resolution of the problem of concentric holes. The secondary reason is so that the design isn't limited by the dimensions of commercially available tube stock. Commercially available tube stock comes in a limited set of sizes, which would force the part to be designed around it. The use the angle aluminum allows for more flexibility in terms of length and depth of the assembly.

The electrical connector was removed from the part so that the assembly of the components and the wiring wouldn't interfere with each other. Also by removing the electrical connection from the part, the HCB can become smaller and easier to assemble. A comparison is shown in Figure 42. The weight of the original design is 0.69 lbs while the new design weighs 0.56 lbs, which is a 19% reduction in weight.

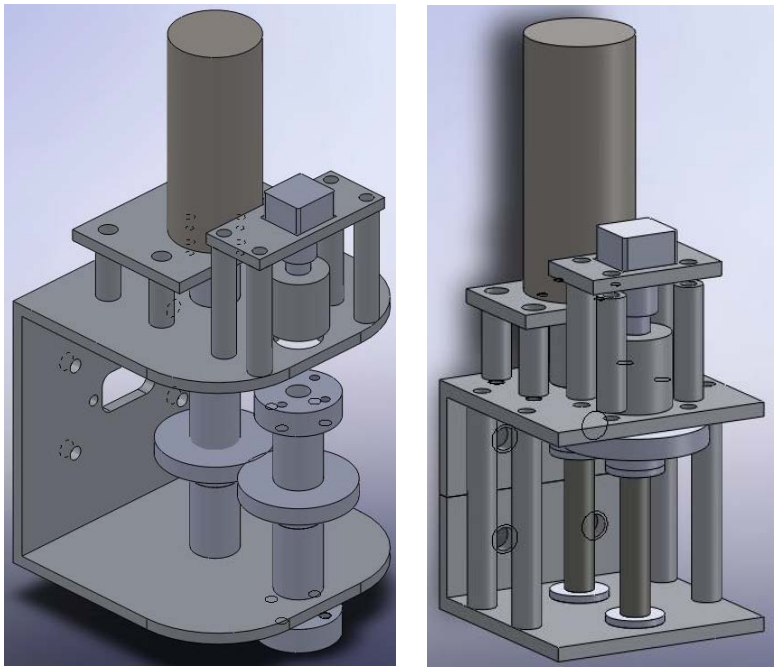

Figure 42: Comparison View of the Current HCB (Left) and the Revised Design (Right).

3.1.2.4. Force Analysis of the New Design

The revised leg design is significantly lighter compared to the current design and slightly shorter as well. A new force analysis will show the additional benefits of the revised design. Once again, the calculations are done in oz-in. Each plate has a length of 11 inches and weighs 1.76 oz. The gearboxes weigh 16.48 oz and the center of mass is 0.75" from the axis of rotation towards the center of the thigh link. The mounting hole for the drive shaft is 0.5625" from the end of the plate, giving the calf plate a functional length of 10.4375" and the thigh plate a length of 9.875".

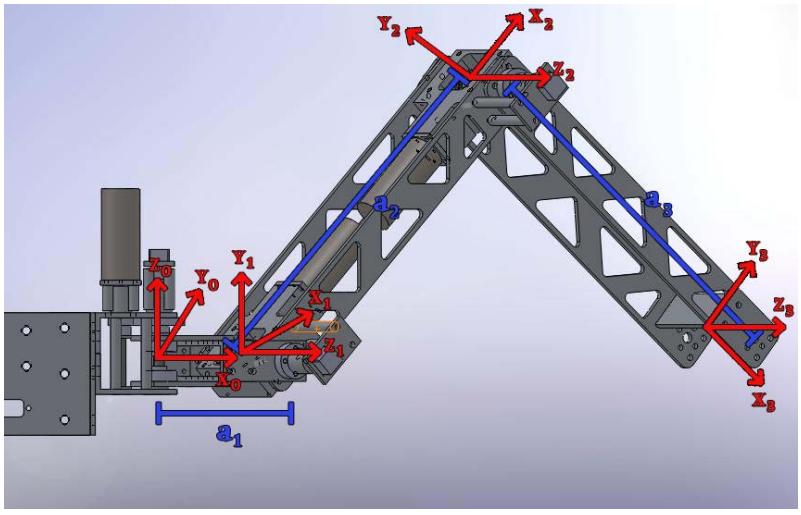

Figure 43: Static Force Calculation for the Revised Design

The analysis will start by calculating the torque required to rotate the calf plate. The weight of the calf link is 3.52 oz and is 10.4375" long. Assuming the force of the link is acting at the midpoint of the length of the calf, the torque is:

Equation 17: Motor 3 Torque in Revised Leg

$$M_2 = \frac{10.4375}{2} in * 3.52\ oz$$

$$M_2 = 18.37\ oz\text{-}in$$

Continuing to coordinate frame 1, this motor has to rotate not only the thigh link but the calf link as well including a motor. Therefore:

Equation 18: Motor 2 Torque in Revised Leg

$$M_1 = 18.37\ oz\text{-}in + \left[(16.48\ oz * 9.6875\ in) + \left(\frac{9.875}{2}\ in * 3.52\ oz\right)\right]$$

$$M_1 = 18.37\ oz\text{-}in + 159.65\ oz\text{-}in + 17.38\ oz\text{-}in$$

$$M_1 = 205.4\ oz\text{-}in$$

The bracket that allows for the movement of the hip weighs 3.52 oz and the center of mass is 1.125 in away from the horizontal axis of rotation. The torque required is:

Equation 19: Motor 1 Torque in Revised Leg

$$M_0 = 205.4\ oz\text{-}in + \left[(3.125\ in * 16.48\ oz) + (1.125\ in * 3.52\ oz)\right]$$

$$M_0 = 205.4\ oz\text{-}in + 51.5\ oz\text{-}in + 3.96\ oz\text{-}in$$

$$M_0 = 260.86\ oz\text{-}i$$

Table 8 compares the torque requirements of the current and revised designs:

Table 8: Comparison of Current and Revised Motor Torques

	Motor 1	Motor 2	Motor 3
Current (oz-in)	398.06	321.1	51.62
Revised (oz-in)	260.86	205.4	18.37
Reduction	34.47%	36.04%	64.42%

As Table 8 shows, the revised design results in a significant torque reduction for all motors. This will in turn save power and extend the battery life of the robot.

3.1.2.5. The Chassis

The main modifications to the chassis are accommodating the changes in the HCB and the new placement of the electrical connection port. In addition, the types of bolt holes in the chassis plates were reduced. Originally there were several types of holes: ¼-20, 10-24 and 5-40. The ¼-20 holes were used to mount the leg to the chassis, the 10-24 holes were used to bolt the chassis plates together and the 5-40 holes were to mount the electrical connection. Having 3 different bolt types complicates manufacturing as a different operation, drill and tap must be used for each type of hole. This adds time and complexity to the part. In the new design the 10-24 holes have been replaced with ¼-20 bolt holes.

The other change to the chassis is switching from 0.25" aluminum to 0.125" aluminum. This change is to save weight on the chassis. The current chassis weighs 3.41 lbs, while the new chassis weighs 1.92 lbs. This is a 44% reduction in weight. The main concern about switching to a thinner plate is that the plate would bend under the load of a configured robot.

The CosmosXpress feature in SolidWorks was used to study how the chassis plates would react to various forces. The first test was conducted on the short chassis plate. The plate was restrained around the bolt holes and a 15 pound force was applied to the front face of the plate. After running the analysis, the lowest safety factor was 6.46. Figure 44 shows the distribution of safety factor across the plate. The blue areas are where the safety factor is higher than the entered value, which in this case is 15, and the red areas are where the safety factor is lower than the entered value.

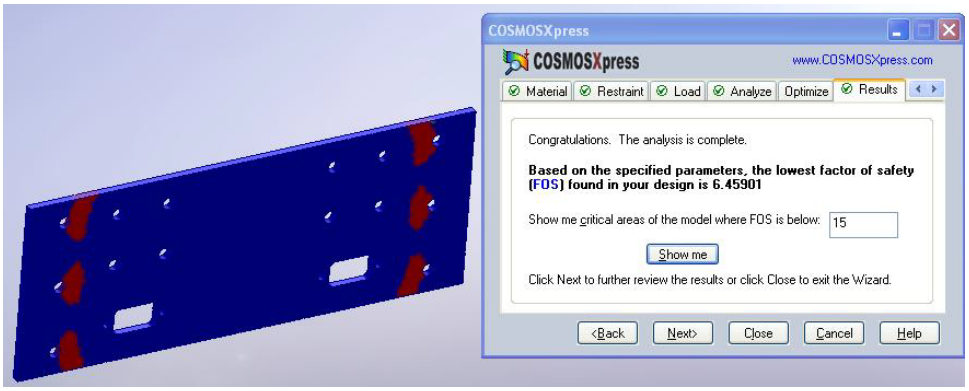

Figure 44: Revised Chassis Short Plate CosmosXpress Results

Figure 45 shows the maximum displacement of the part under the 15 pound load. The part appears to bend significantly under the load, however the greatest displacement of the part (shown in red) is 0.0018 inches.

Figure 45: Displacement of the Revised Short Chassis Plate

The long plate underwent a similar analysis using the CosmosXpress feature. Again, the plate was restrained around the bolt holes and a 15 pound force was applied to the front of the face plate. The red areas shown in Figure 46 are where the safety factor of the part is below 15.

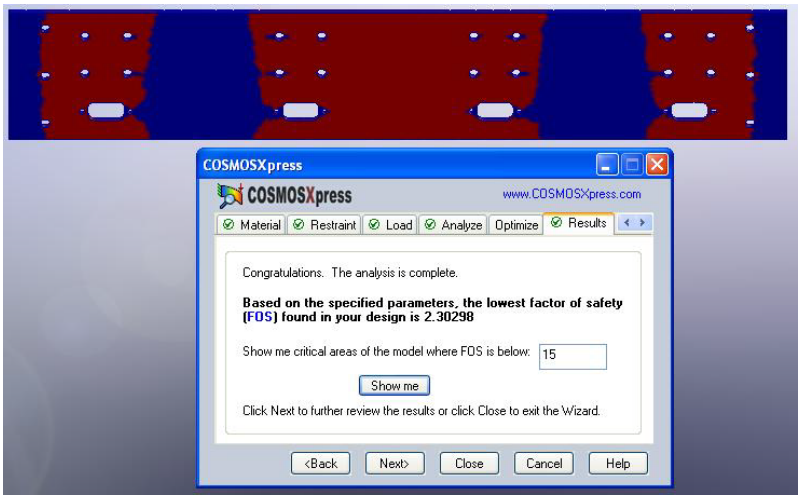

Figure 46: Chassis Long Plate CosmosXpress Results

The red area is far larger in the long plate than in the short plate, however the minimum safety factor is still above 2. The maximum displacement that the plate experiences under the force is 0.023 inches. The various displacements of the plate can be seen in Figure 47.

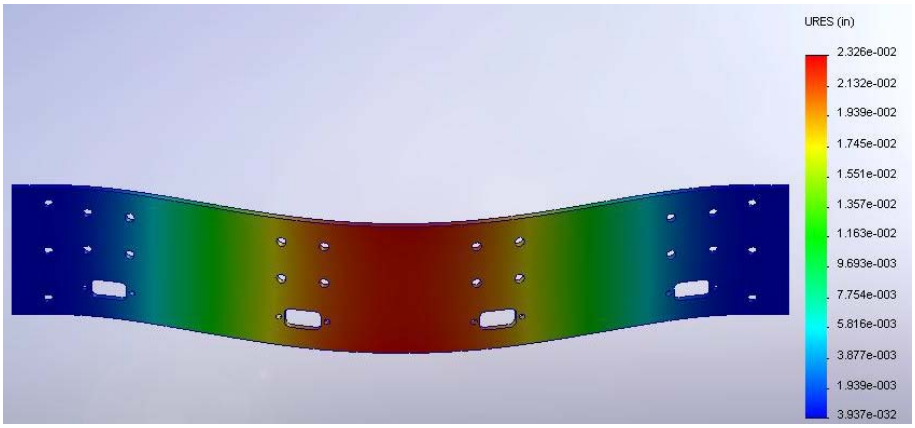

Figure 47: Resulting Displacement of the Long Chassis Plate

As a result of the testing done on the 0.125" plates, the new chassis will be constructed from the thinner material. Along with the changes made to the leg module, the revised robot will now be lighter than the current design. The revised robot weighs 15.25 lbs in a four leg configuration, while the current design weighs 25.42 lbs, a 40% overall reduction in weight.

3.2.Electrical System Observations

Overall, the electrical system performed as desired. Assembly of the boards only encountered a few problems, and the boards functioned as designed.

3.2.1. LCU PCB Construction and Issues

The completed LCU can be seen in Figure 48. No major obstacles were met in the assembly of the LCU PCB. All of the components designed specifically for this board fit as intended. There was one issue with the resistors, however. 1/2 W resistors were ordered, but the board was designed for ¼ W resistors. This did not create too much of a problem, because by purchasing one ¼ W resistor, the other ½ W resistors could be bent to fit with the other components. One other problem occurred, where connections on certain ports weren't consistent, but by resoldering those ports, all of the problems were resolved.

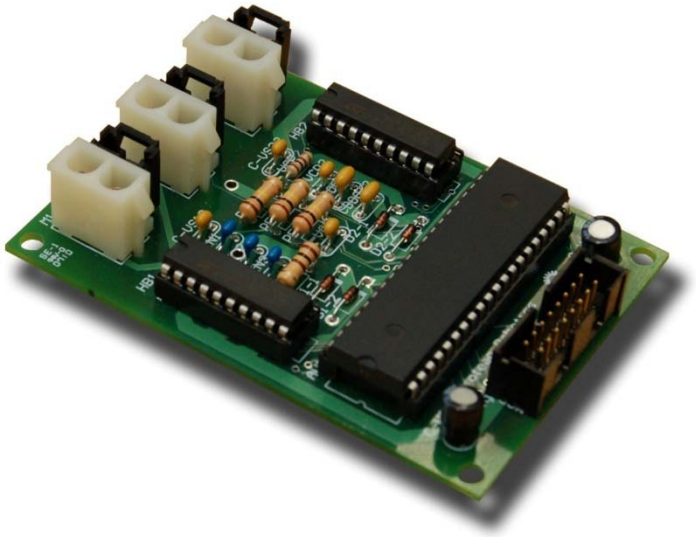

Figure 48: Assembled LCU Board

3.2.2. MCB PCB Construction and Issues

Assembly of the MCB encountered a few problems. The first of which is that the holes for the buck converters were too small. This was due to an error in translating the data sheet for the converters into a proper layout for a PCB. This issue was resolved by bending the leads for the DC-DC converter 90 degrees so that they could be mounted as surface mount. This allowed the parts that were in hand to be used as was functionally intended. The next issue was the distance between peripheral connection ports. Originally, the connection ports were designed to be 2x8 female headers, and that was what the PCBs were designed for. However, as described in Section 2.3.4.2, they were changed to a keyed shielded male header. Due to this change, the footprint of each header increased, but the PCB was not altered to match this change. Because of this increase, the headers could not fit all on the top of the PCB. Alternating headers had to be placed on the underside of the board, allowing all 15 to be placed. In doing this, the pinouts for the 2x8 to DB-15 HD cables had to be altered, so that top and bottom cables were different. Lastly, all of the pullup resistors were changed from 10K to 1K so that the luminosity of the LEDs was such that it could be seen in normal lighting conditions. Having the power LEDs use the same pullup resistor value causes them to have varying luminosity, because one is operating at 5V, and the other at 12V. In order to correct this, a 420Ω resistor would be needed for the 5V line. This is a minor issue, as they can still be seen in normal lighting conditions. Once these issues were resolved, the MCB worked as designed. The final MCB design can be seen in Figure 49.

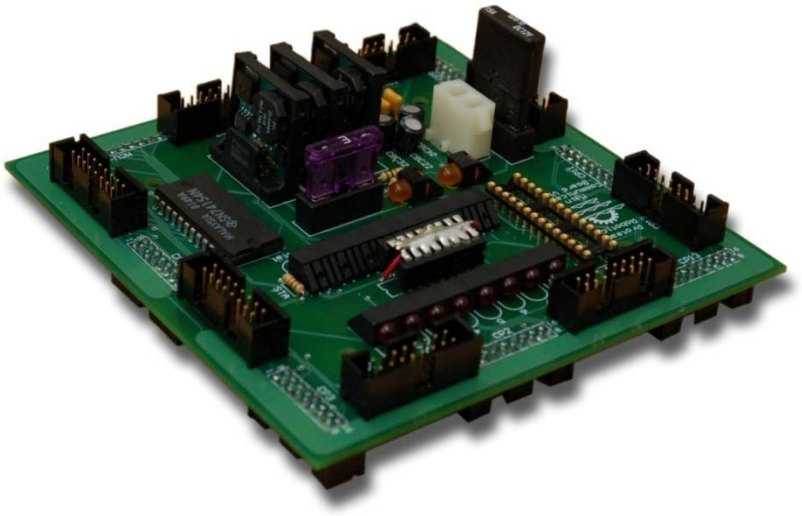

Figure 49: Assembled MCB Board

3.3.Software Timing and Effective Control Frequencies

The real-time operational characteristics of the LCU software were tested by running various functions of the LCU software in an infinite loop and toggling an output signal from the ATMega324P processor at the beginning of each iteration of this loop. An oscilloscope was then used to read this output signal. It is important to note that the frequency of the resulting square wave is that of the metered operation occurring twice. Even though a frequency is reported on the oscilloscope, it lacks the precision of the period reported by the oscilloscope (31). Therefore, to determine the frequency of any given function from the oscilloscope output, the following formula is used:

$$frequency_{(function\ )} = \frac{1}{\left(\frac{period_{(function\ )}}{2}\right)} = \frac{2}{period_{(function\ )}}$$

This formula is used to calculate the overall process time of the LCUs various functions, as well as the total expected LCU time to process a motion command from the MPU. This information, in turn, is used to calculate the expected frequency with which the MPU can delegate commands to a single LCU without incurring logical collisions.

3.3.1. PID Loop Timing

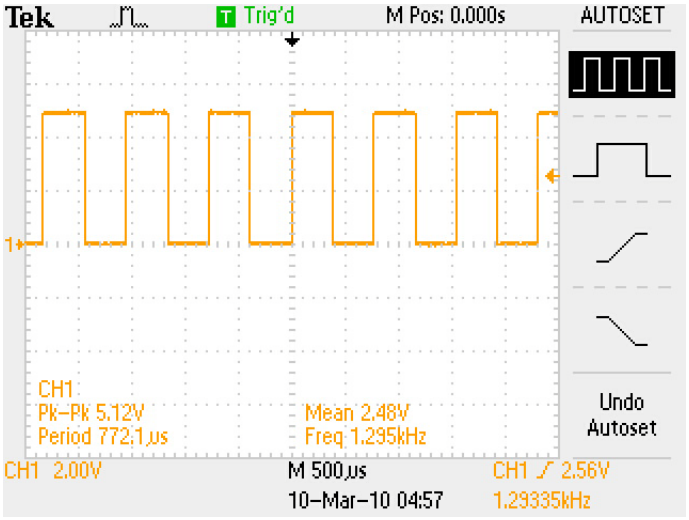

Figure 50: Single PID Loop timing

The oscilloscope-clocked period of a single PID loop in the LCU is 772.1 microseconds. The frequency of this function is then:

$$frequency_{(singlePID\ )} = \frac{2}{772.1\mu s} = 2590.34\ Hz$$

3.3.2. Total Leg PID Loop Timing

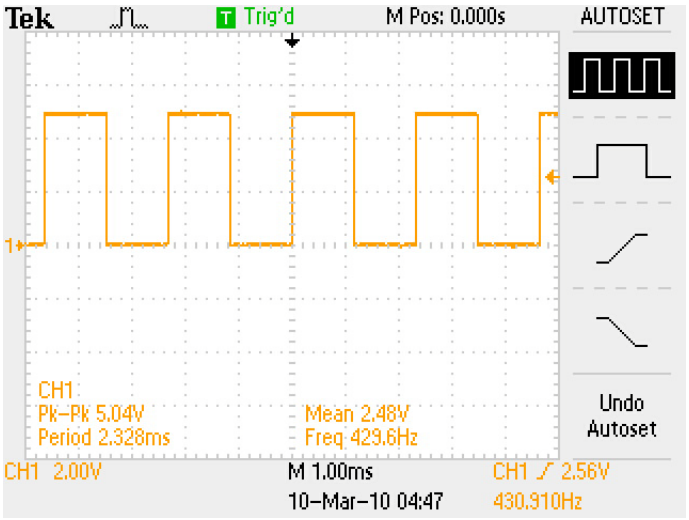

Figure 51: Total PID Loop Timing

The expected frequency of three sequential PID loops is

$$\frac{frequency_{(singlePID\ )}}{3} = \frac{2590.33\ Hz}{3} = 863.45\ Hz$$

Any difference would indicate additional overhead done in the processor between the three PID loops. The oscilloscope-clocked period of the sequential PID loops for all three leg motors in the LCU is 2.328milliseconds. The frequency of this function is then:

$$frequency_{(totalPID\ )} = \frac{2}{2.328\ ms} = 859.11\ Hz$$

This slightly lower-than-expected value indicates some minimal additional overhead in the processor, but is considered negligible as the actual and expected values are within 0.5% of each other.

3.3.3. Inverse Kinematics Timing

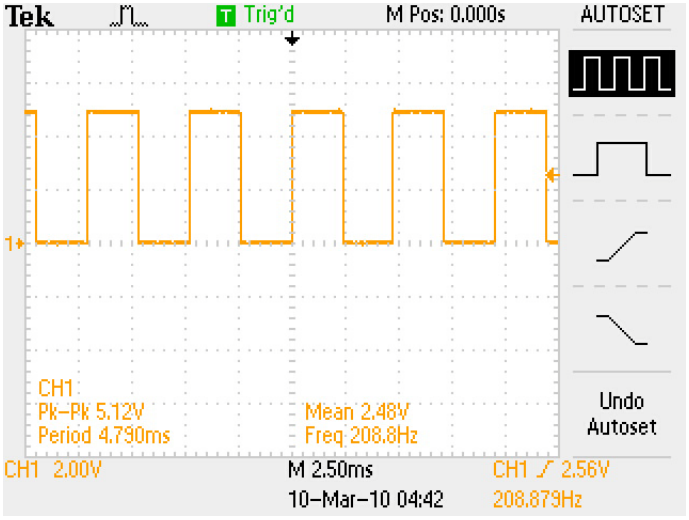

Figure 52: Inverse Kinematics Loop Timing

The oscilloscope-clocked period of the inverse kinematics in the LCU is 4.790 milliseconds. The frequency of this function is then:

$$frequency_{(inversekinematics\ )} = \frac{2}{4.79ms} = 417.54\ Hz$$

3.3.4. Forward Kinematics Timing

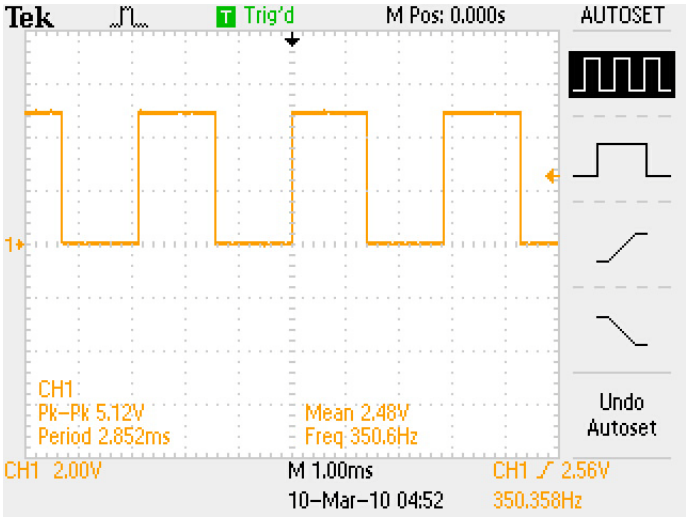

Figure 53: Forward Kinematics Loop Timing

The oscilloscope-clocked period of the forward kinematics in the LCU is 2.852 milliseconds. The frequency of this function is then:

$$frequency_{(forwardkinematics\ )} = \frac{2}{2.852ms} = 701.26\ Hz$$

3.3.5. Total LCU Command Process Timing

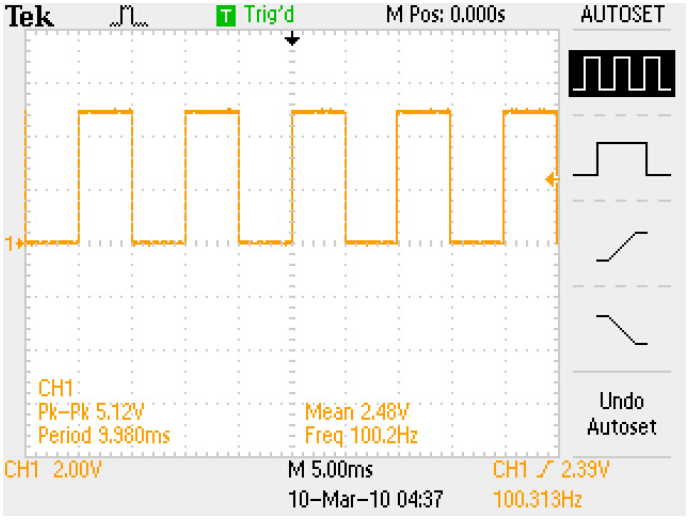

Figure 54: Complete LCU Leg Motion Command Timing

The expected frequency of the total LCU motion command, which will perform forward kinematics, one PID loop for each motor, and then inverse kinematics, can be calculated using their respective periods as:

$$frequency_{(totalmotioncommand\ )} = \frac{2}{2.852ms + 4.79ms + 2.328ms} = 200.6\ Hz$$

Again, any discrepancy between this expected value would indicate additional processing between successive functions. The oscilloscope-clocked period of the forward kinematics in the LCU is 9.98 milliseconds. The frequency of this function is then:

$$frequency_{(totalmotioncommand\ )} = \frac{2}{9.98ms} = 200.4\ Hz$$

There is a 0.1% deviation between the actual and expected value; but this is a negligible difference.

Utilizing a timing safety factor, where the minimum frequency between commands is divided by the timing safety factor to allow additional time to avoid logical collisions. Using a timing safety factor of 2, the MPU can issue motion commands to each LCU at approximately 100 Hz:

$$\frac{200.4\ Hz}{2} = 100.2\ Hz$$

Accordingly, the MPU must issue successive commands to a single LCU in time increments of no less than 0.01 seconds.

3.4.Budget

The budget is separated into mechanical components and electrical components. The small parts are grouped together to form units, such as the chassis, or an LCU.

3.4.1. Mechanical Budget

The following budget is calculated for the final mechanical design of the robot. It is separated into three distinct sections, the budget for each leg, the budget for the chassis and other onetime buys and a list of material that was not purchased due to existing stock. Table 9 shows the cost per leg.

Table 9: Mechanical Budget per Leg

Name	Cost per Unit	QTY	Total Cost	Manufacturer	Part Number
Miter Gears	47	2	94	Nordex	LHSE3030
15 Tooth Spur Gear	17	1	17	Nordex	LASC2015
30 Tooth Spur Gear	13.15	1	13.15	Nordex	LASC1030
Shaft Collars	1.25	4	5	Nordex	BACC2003
Bearings 5/8" OD	8.45	6	50.7	Nordex	ABSA5031
Bearings 1/2" OD	6	4	24	Nordex	ABSA5029
1/4-1/4 Coupler	7.5	3	22.5	Servo City	CDS-A1-5
Set Screw Hubs	5	6	30	Servo City	3463H
Motors	32	3	96	Lynxmotion	PGHM-04
1.25" #6 Spacer	0.66	4	2.64	McMaster	92510A450
1.75" #6 Spacer	1.51	4	6.04	McMaster	92510A095
5/8" #6 Spacer	0.35	4	1.4	McMaster	92510A446
1" #6 Spacer	0.45	4	1.8	McMaster	92510A449
1/16 Nylon Washer	3.86	1	3.86	McMaster	95630A242
1/32 Nylon Washer	2.44	1	2.44	McMaster	93493A234
Total Cost Per Leg			370.53		

The cost to build one leg is $370.53 and does not include metal stock as that material is covered in Table 10. The main contributors to the cost of building a leg are the miter gears and the motors. The miter gears are expensive due to the necessarily precise manufacturing needed and the fact that miter gears have to be purchased as a matched set. The motors are expensive due to their size and the high reduction of the attached planetary gearbox.

Table 10 shows the cost of one-time purchases for the robot and contains sheet metal and fasteners.

Table 10: Single Purchase Material Budget

Name	Cost per Unit	QTY	Total Cost	Manufacturer	Part Number
1"x3"x1/8 Tube Stock	7.67	1	7.67	McMaster	88935K571
1/8" Thick 6061 Alum	175	1	175	Yarde Metal	6061-T4-SH 0.1250 x 48 x 72
5-40 Pan Slotted Screws .25" Long	5.7	1	5.7	McMaster	91792A124
1/4-20 Pan Slotted Screws .25" Long	12	1	12	McMaster	91792A533
6-32 Pan Slotted Screws 2" Long	9.1	1	9.1	McMaster	91792A159
6-32 Pan Slotted Screws .25" Long	5	1	5	McMaster	91792A144
6-32 Pan Slotted Screws 1" Long	8.15	1	8.15	McMaster	91792A153
6-32 Pan Slotted Screws 1.5" Long	12	1	12	McMaster	91792A157
TOTAL COST =			234.62		

The biggest contributor to the single purchase budget is the purchase of the sheet aluminum. However this will provide enough aluminum to make the chassis and six legs. The majority of Table 10 is screws, which may be available through other means, which could save some money towards the overall cost of the robot.

The following parts will be made from existing stocks that do not have to be purchased:

- Gearboxes
- Motor to Drive Shaft Couplers
- The Hip Assembly Brackets
- The Chassis Angle Brackets

Due to the fact that there are existing stocks of material to be used, those parts are not factored into the budget for the final mechanical design.

3.4.2. Electrical Budget

The majority of the components were purchased through DigiKey. This was done so that most of the necessary components could be ordered all at once, with only a few coming from other vendors. The other vendor used was Newark, because DigiKey has a very small selection of power management ICs.

Also, blade fuse holders were purchased from Newark. The PCBs had to be custom ordered and printed, and the price listed is the cost for a single board to be printed, even though they were ordered in a bulk pack. The complete itemized budget per unit for the LCU, MCB, and MPU is shown in Table 11, Table 12, and Table 13 respectively.

Table 11: LCU Itemized budget

Component	Manufacturer	Supplier	Part Number	Price Per	Quantity	Total
ATmega164P	Atmel	Digikey	ATMEGA164P-20PU-ND	$4.73	1	$4.73
DIP40 Socket	3M	Digikey	3M5471-ND	$0.42	1	$0.42
L6205 H-Bridge	STMicroelectronics	Digikey	497-5344-5-ND	$5.44	2	$10.88
DIP20 Socket	3M	Digikey	3M5465-ND	$0.24	2	$0.48
1x2 0.25" Motor Port	Tyco Electronics	Digikey	A25313-ND	$0.36	3	$1.08
1x3 0.1" Potentiometer Port	Tyco Electronics	Digikey	A28528-ND	$0.42	3	$1.26
2x8 0.1" Main Port	Tyco Electronics	Digikey	A33164-ND	$1.62	1	$1.62
100ohm Resistor	Yageo	Digikey	100QBK-ND	$0.06	2	$0.13
100K Resistor	Stackpole Electronics	Digikey	CF1/4100KJRCT-ND	$0.08	3	$0.24
10nF Cap	Kemet	Digikey	399-4326-ND	$0.13	2	$0.26
100uF Polarized Cap	Panasonic ECG	Digikey	P833-ND	$0.01	2	$0.02
100nF Cap	Kemet	Digikey	399-4329-ND	$0.21	2	$0.42
220nF Cap	Kemet	Digikey	399-4353-ND	$0.53	2	$1.06
5.6nF Cap	TDK Corporation	Digikey	445-4747-ND	$0.28	3	$0.85
1N4148 Diode	Fairchild Semiconductor	Digikey	1N4148FS-ND	$0.08	4	$0.32
Printed Circuit Board	Imagineering Inc.		LCU V4	$25.00	1	$25.00
20 Strand Ribbon Cable	3M	Digikey	MB16R-100-ND	$0.63	1	$0.63
2x8 0.1" Ribbon Cable Conn	Tyco Electronics	Digikey	AKC16H-ND	$1.23	1	$1.23
DB-15 HD Male	Amphenol Commercial Prod	Digikey	17EHD-015-P-AA-0-0	$1.56	1	$1.56
					37	**$52.20**

Table 12: MCB Itemized Budget

Component	Manufacturer	Supplier	Part Number	Price Per	Quantity	Total
ATtiny48	Atmel	Digikey	ATTINY48-PU-ND	$2.04	1	$2.04
DIP28 Socket	3M	Digikey	3M5480-ND	$0.33	1	$0.33
SN74154N Demux	Texas Instruments	Digikey	296-8757-5-ND	$3.50	1	$3.50
TI PT5101N Buck Converter	Texas Instruments	Newark	15M7372	$13.25	3	$39.75
1x2 0.25" Battery Port	Tyco Electronics	Digikey	A25313-ND	$0.36	1	$0.36
2x8 0.1" Peripheral Port	Tyco Electronics	Digikey	A33164-ND	$1.45	15	$21.75
1x12 0.1" MPU Port	Tyco Electronics	Digikey	A26479-ND	$1.14	1	$1.14
Fuse Holder	Keystone	Newark	22M2712	$1.20	2	$2.40
15A Blade Circuit Breaker	E-T-A	Digikey	302-1243-ND	$9.09	1	$9.09
3A Blade Fuse	Littelfuse Inc.	Digikey	F996-ND	$0.63	1	$0.63
1K Resistor	Yageo	Digikey	1.0KQBK-ND	$0.06	3	$0.19
1K 15-Resistor Bussed IC	Bourns Inc.	Digikey	4116R-2-102LF-ND	$0.60	1	$0.60
100uF Polarized Cap	Panasonic ECG	Digikey	P833-ND	$0.12	3	$0.36
1uF Cap	Kemet	Digikey	399-4329-ND	$0.21	3	$0.63
Yellow LED	Avago Technologies US Inc.	Digikey	516-1764-ND	$0.72	2	$1.44
4-LED Bank	Lumex Opto/Components	Digikey	67-1285-ND	$1.26	4	$5.04
Printed Circuit Board	Imagineering Inc.		MCB V1.2	$27.50	1	$27.50
16 Strand Ribbon Cable	3M	Digikey	MB16R-100-ND	$0.63	15	$9.50
2x8 0.1" Ribbon Cable Connect	Tyco Electronics	Digikey	AKC16H-ND	$1.23	15	$18.45
DB-15 HD Female	Amphenol Commercial Produc	Digikey	17EHD-015-S-AA-0-00-N	$1.65	15	$24.71
					89	**$169.40**

Table 13: MPU Itemized Budget

Component	Manufacturer	Supplier	Part Number	Price Per	Quantity	Total
ATmega644P	Atmel	Digikey	ATMEGA644P-20PU-ND	$8.19	1	$8.19
DIP40 Socket	3M	Digikey	3M5471-ND	$0.42	1	$0.42
DB-9 Serial Port	Norcomp Inc.	Digikey	191-09FA-ND	$3.48	1	$3.48
1x12 0.1" MPU Port	Tyco Electronics	Digikey	A26479-ND	$1.14	1	$1.14
Printed Circuit Board	Imagineering Inc.		MPU V1.1	$25.00	1	$25.00
					5	**$38.23**

4. Future Work

Given the modular design of the robot, there are many potential areas for future work. The most immediate task would be the construction of the final robot design including multiple leg modules. Plans to complete this are already slated to be started following the submission of this project. The balancing algorithm can be tested to show that the robot can identify its current configuration and balance itself. From there, further work can be conducted to refine the algorithm and make it more complex. For example, the algorithm can be developed to allow the robot to balance itself regardless of the surface that the robot is standing on. The ultimate goal for the leg modules would be to allow the robot to walk using any leg configuration.

Other possible areas of future work would be the development of new modules for the robot. These modules can be generalized to include, but are not limited to, movement, manipulators and sensors. Movement modules could come in the form of wheels to enable the robot travel at fast speeds along roads, or treads for maneuvering through sand. Manipulators could come in the form of an arm, a claw or gripper module. Sensors could be range finders, localization sensors or thermal sensors. Other miscellaneous possible devices include a GPS sensor, which could be used to send the robot to a predetermined location. Also, a RF receiver module could be created to add remote control functionality to the robot. As long as the new modules follow the connection and communication protocol, there is no limit to the modules that can be created. The only thing that must be done to accommodate new modules is to program into the main processor how to handle this new module. The robot can be developed for any task with the development of new modules.

5. Conclusion

The ReMMRP serves as a proof of concept of the integration of reconfigurability, modularity, and mobility in a robotic system. The final design demonstrates effective implementation of a robot for immediate and future applications. Such a design will increase flexibility in the field of robotics, allowing the solution to a task to be viewed as a reconfiguration, not a redesign.

Additional peripherals can be designed and incorporated, as long as they conform to the connection and communication standards of the robot. Additional algorithms can be incorporated into the main software to control these new peripherals. The design features presented by this platform eliminate the need to produce an entirely new robot. Instead, focus can be shifted to the development of peripherals that will extend the capabilities of the existing platform.

Modularity of the platform makes it fault-tolerant; that is, a failure within the robot does not require replacement or repair of the entire system. Instead, modules can be replaced minimizing downtime and cost.

The reconfigurable and modular design of ReMMRP allows it to be utilized in a variety of real-world applications which would otherwise require robots of different forms and functionality. This saves time and money for the end-user of the platform, while creating jobs in the industry for designing software, mechanical, and electrical subsystems for new peripheral modules. Its low cost, flexible design, and expandability make the ReMMRP a unique robotic platform for a wide range of applications in academia and industry.

6. References

1. *Self-Reconfigurable Modular Robot -Experiments on Reconfiguration and Locomotion.* **Kamimura, Akiya, et al.** 2001. International Conference on Intellegent Robots and Systems.

2. *A Motion Planning Method for a Self-Reconfigurable Modular Robot.* **Kamimura, Akiya, et al.** Maui, Hawaii : s.n., 2003. Internatioanl Conference on Intelligent Robots and Systems.

3. *Towards Robotic Self-reassembly After Explosion.* **Dugan, Mike, et al.** 2007. IEEE/RSJ International Conference on Intelligent Robots and Systems (IROS). pp. 2767-2772.

4. **Blankespor, Kevin, et al.** *BigDog, the Rough-Terrain Quaduped Robot.* 2008.

5. **Atmel Corporation.** *ATmega 164P/324P/644P.* [Datasheet] San Jose, CA : s.n., 2009.

6. **Digi-Key Corporation.** Digi-Key ATMEGA1281-16AU-ND (Manufacturer - ATMEGA1281-16AU). *DigiKey Corp. | Electronic Components Distributor | United States Home Page.* [Online] Digi-Key Corporation. [Cited: November 18, 2009.] http://search.digikey.com/scripts/DkSearch/dksus.dll?Detail&name=ATMEGA1281-16AU-ND.

7. —. Digi-Key - ATMEGA164PV-10PU-ND (Manufacturer - ATMEGA164PV-10PU). *DigiKey Corp. | Electronic Components Distributor | United States Home Page.* [Online] Digi-Key Corporation. [Cited: November 18, 2009.] http://search.digikey.com/scripts/DkSearch/dksus.dll?Detail&name=ATMEGA164PV-10PU-ND.

8. **Atmel Corporation.** *ATmega640V/1280V/1281V/2560V/2561V.* [Datasheet] San Jose, California : s.n., 2007.

9. **Lynxmotion, Inc.** Planetary Gear Motor - 12vdc 189:1 31rpm (4mm shaft). *Lynxmotion Robotic Kits.* [Online] Lynxmotion, Inc. [Cited: November 26, 2009.] http://www.lynxmotion.com/Product.aspx?productID=308&CategoryID=71.

10. —. Planetary Gear Motor - 12.0vdc 1:231 64rpm (4mm shaft). *Lynxmotion Robot Kits.* [Online] Lynxmotion, Inc. [Cited: December 12, 2009.] http://www.lynxmotion.com/Product.aspx?productID=580&CategoryID=71.

11. **STMicroelectronics.** *L6205N DMOS Dual Full Bridge Driver.* [Datasheet] Geneva, Switzerland : s.n., 2003.

12. **Digi-Key Corporation.** *DigiKey Corp. | Electronic Components Distributor | United States Home Page.* [Online] [Cited: March 11, 2010.] http://media.digikey.com/photos/Tyco%20Amp%20Photos/HEADER%202%20CIRC%20FIG%201A.jpg.

13. —. *DigiKey Corp. | Electronic Components Distributor | United States Home Page.* [Online] [Cited: March 11, 2010.] http://media.digikey.com/photos/Tyco%20Amp%20Photos/103639-2.jpg.

14. —. *DigiKey Corp. | Electronic Components Distributor | United States Home Page.* [Online] [Cited: March 11, 2010.] http://media.digikey.com/photos/Tyco%20Amp%20Photos/5103309-3.jpg.

15. —. *DigiKey Corp. | Electronic Components Distributor | United States Home Page.* [Online] [Cited: March 11, 2010.] http://media.digikey.com/photos/Tyco%20Amp%20Photos/534237-1.jpg.

16. —. *DigiKey Corp. | Electronic Components Distributor | United States Home Page.* [Online] [Cited: March 11, 2010.] http://media.digikey.com/photos/Tyco%20Amp%20Photos/534237-6.jpg.

17. —. *DigiKey Corp. | Electronic Components Distributor | United States Home Page.* [Online] [Cited: March 11, 2010.] http://media.digikey.com/photos/Sullins%20Photos/PPTC021LFBN-RC.jpg.

18. **Bourns, Incorporated.** *51/53 - Sealed 1/2" (12.5 mm) Square Control.* [Datasheet] Riverside, California : s.n., 2009.

19. **Texas Instruments.** *SN54154, SN74154 4-Line To16-Line Decoders/Demultiplexers.* [Datasheet] Dallas, Texas : s.n., 1998.

20. **Atmel Corporation.** *ATtiny48/88.* [Datasheet] San Jose, CA : s.n., 2009.

21. **Aivaka.** *Linear or LDO Regulators & Step-Down Switching Regulators.* [Datasheet] San Jose, CA : s.n., 2007.

22. **XP Power.** *DC-DC 1 Watt IV Series.* [Datasheet] Sunnyvale, California : s.n., 2009.

23. **Texas Instruments.** *PT 5100 Series 1-A Positive Step-Down Integrated Switching Regulator.* [Datasheet] Dallas, Texas : s.n., 2001.

24. **Kugelstadt, Thomas.** Understanding the SPI bus' structure, operation. *EETimes-India.* [Online] July 28, 2009. [Cited: October 19, 2009.] http://www.eetindia.co.in/STATIC/PDF/200907/EEIOL_2009JUL29_INTD_EMS_TA_01.pdf?SOURCES=DOWNLOAD.

25. **Reed, Kenneth D.** *Introduction to Networking.* Arvada, CO : WestNet Learning Technologies, 2001.

26. **Spong, Mark W., Hutchinson, Seth and Vidyasagar, M.** *Robot Modeling and Control.* Hoboken, NJ : John Wiley & Sons, Inc., 2006.

27. **Craig, John J.** *Intorduction to Robotics.* Upper Saddle River : Pearson Education, Inc., 2005.

28. **Lathi, B. P.** *Linear Systems and Signals.* New York, NY : Oxford University Press, Inc., 2005.

29. **Kaiser, David.** *Fundamentals of Servo Motion Control.* Rohnert Park, CA : s.n., July 11, 2001.

30. *Optimum Settings for Automatic Controllers.* **Ziegler, J. G. and Nichols, N. B.** 1942, Transactions of the American Society of Mechanical Engineers, pp. 759-768.

31. **Tektronix, Inc.** *Digital Storage Oscilloscopes - TDS1000B, TDS2000B Series.* [Datasheet] Beaverton, OR : s.n., October 13, 2009.

32. **P. S. Schenker, P. Pirjanian, B. Balaram, K. S. Ali, A. Trebi-Ollennu, T. L. Huntsberger,.** *Reconifgurable Robots for all Terrain Exploration.* Pasadena : Jet Propulsion Laboratory, California Insitute of Technology, 2001.

33. **Norton, Robert L.** *Design of Machinery.* New York, New York : McGraw-Hill, 2008.

34. *Self-Adaptive Furniture with a Modular Robot.* **Ingber, Donald, et al.** Aahus, Denmark : s.n., 2008. Workshop on Imagine Future Domestic.

35. **Hibbeler, R.C.** *Enineering Mechanics: Dynamics.* Upper Saddle River, New Jersey : Pearson Prentice Hall, 2007.

36. *System of a Modular and Reconifgurable Multilegged Robot.* **Chen, Xuedong, et al.** Harbin, China : s.n., 2007. IEEE International Conference on Mechatronics and Automation.

37. **Boissonnat, Joan-Daniel, et al.** *Motion PLanning of Legged Robots: The Spider Robot Problem.* 1992.

38. *Biologically Based Distributed Control and Local Reflexes Imporve Rough Terrain Locomtoion in a Hexapod Robot.* **Beer, Randall D, et al.** 1996, Robotics and Autonomous Systems, pp. 59-64.

39. **Barry, Richard.** Multitasking on an AVR. *AVR Freaks.* [Online] March 2004. [Cited: November 16, 2009.]

40. **DARPA.** *FY2009-2034 Unmanned Systems Integrated Roadmap.* s.l. : Department of Defense, 2009.

41. **Atmel Corporation.** *AVR151: Setup and Use of the SPI.* San Jose, CA : s.n., July 21, 2008.

42. **Astrom, Karl Johan.** *Control System Design.* s.l. : Longman Higher Education, 2002.

43. **Jones, David L.** *PCB Design Tutorial.* [PDF] s.l. : Alternate Zone, 2004.

7. Appendices

7.1.LCU Schematics

(Beginning on the following page)

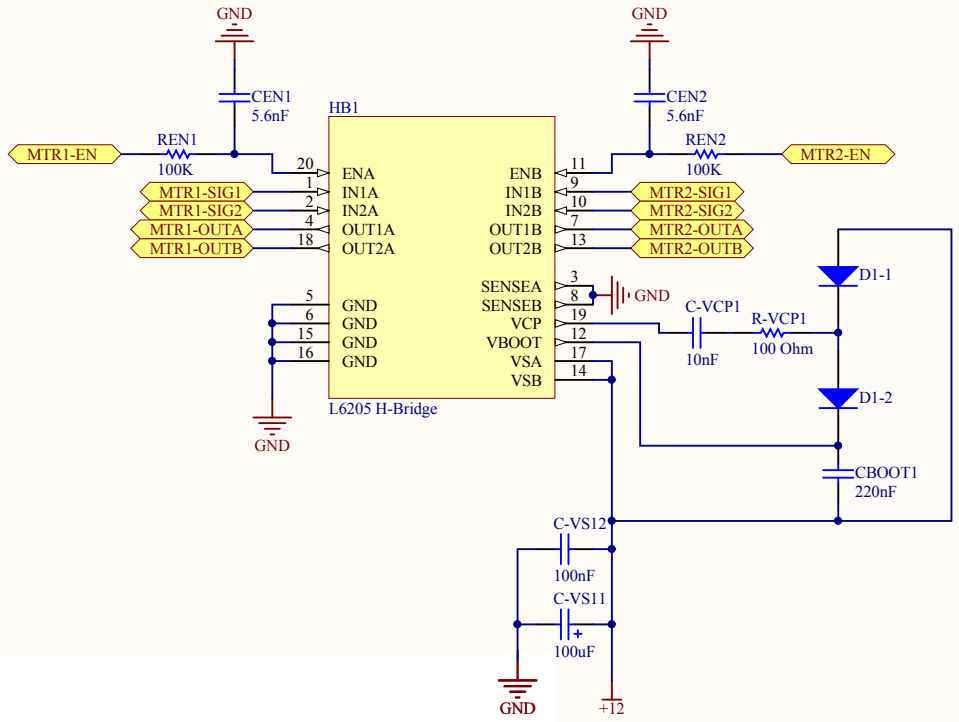

Rotean Robotics

Title: Leg Control Unit - H-Bridge 1		
Size: Letter	Number:	Revision: V4.0
Date: 2/15/2010	Sheet 2 of 4	
File: C:\Documents and Settings\..\H-Bridge 1.SchDoc	Drawn By: Matt Bienia	

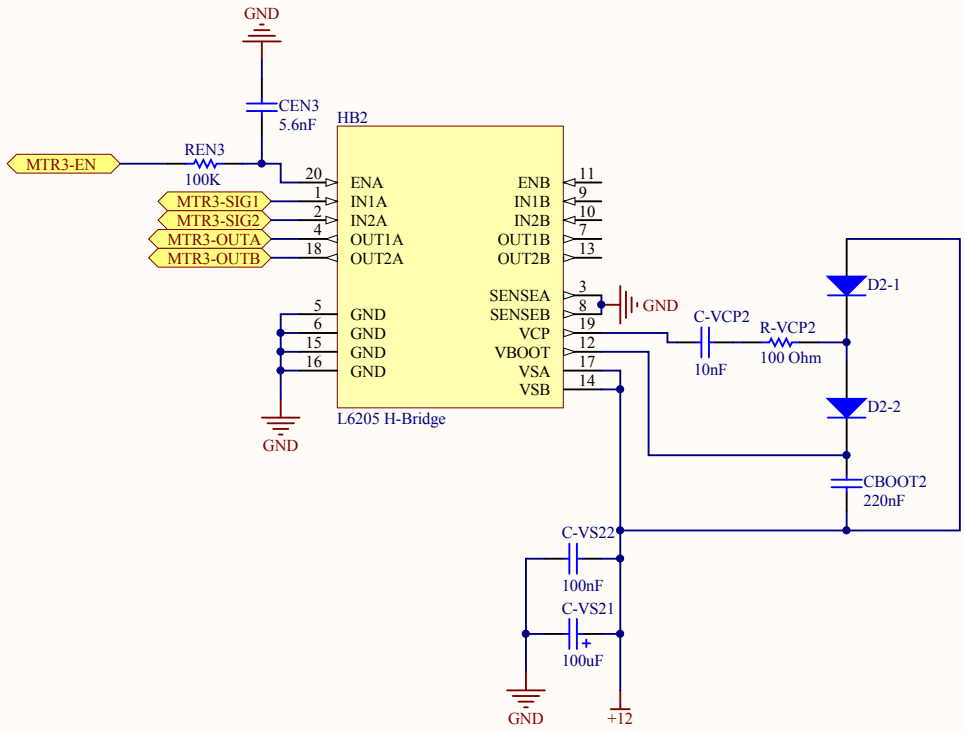

Protean Robotics

Title: Leg Control Unit - H-Bridge 2		
Size: Letter	Number:	Revision: V4.0
Date: 2/15/2010		Sheet 3 of 4
File: C:\Documents and Settings\..\H-Bridge 2.SchDoc		Drawn By: Matt Bienia

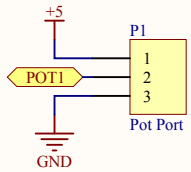

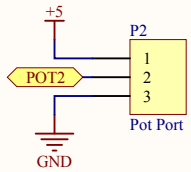

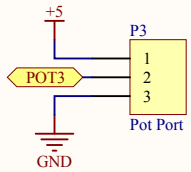

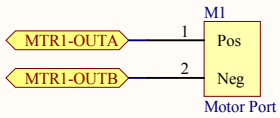

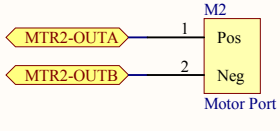

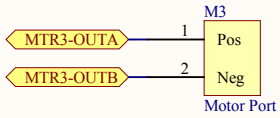

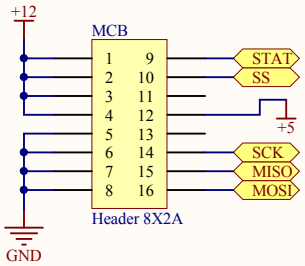

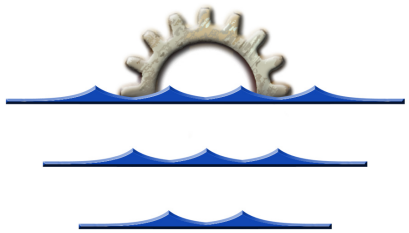

Protean Robotics

Title: Leg Control Unit - Headers		
Size: Letter	Number:	Revision: V4.0
Date: 2/15/2010		Sheet 4 of 4
File: C:\Documents and Settings\..\Headers.SchDoc		Drawn By: Matt Bienia

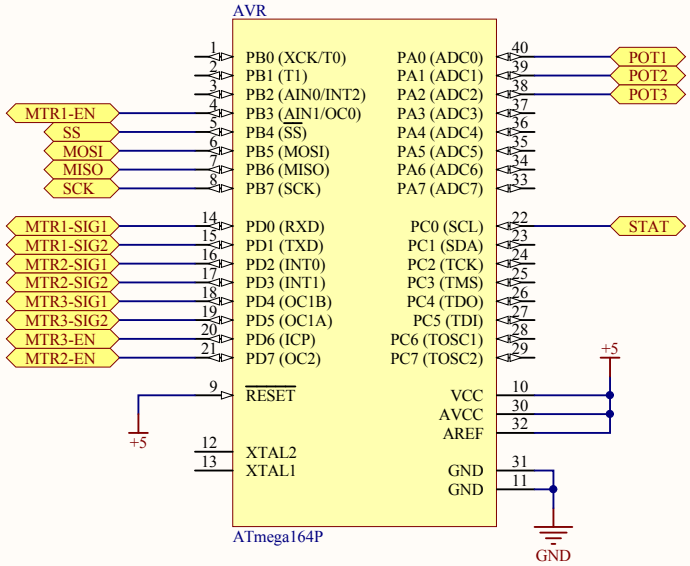

Protean Robotics

Title: Leg Control Unit - Leg Processor		
Size: Letter	Number:	Revision: V4.0
Date: 2/15/2010	Sheet 1 of 4	
File: C:\Documents and Settings\..\Leg Processor.SchDoc	Drawn By: Matt Bienia	

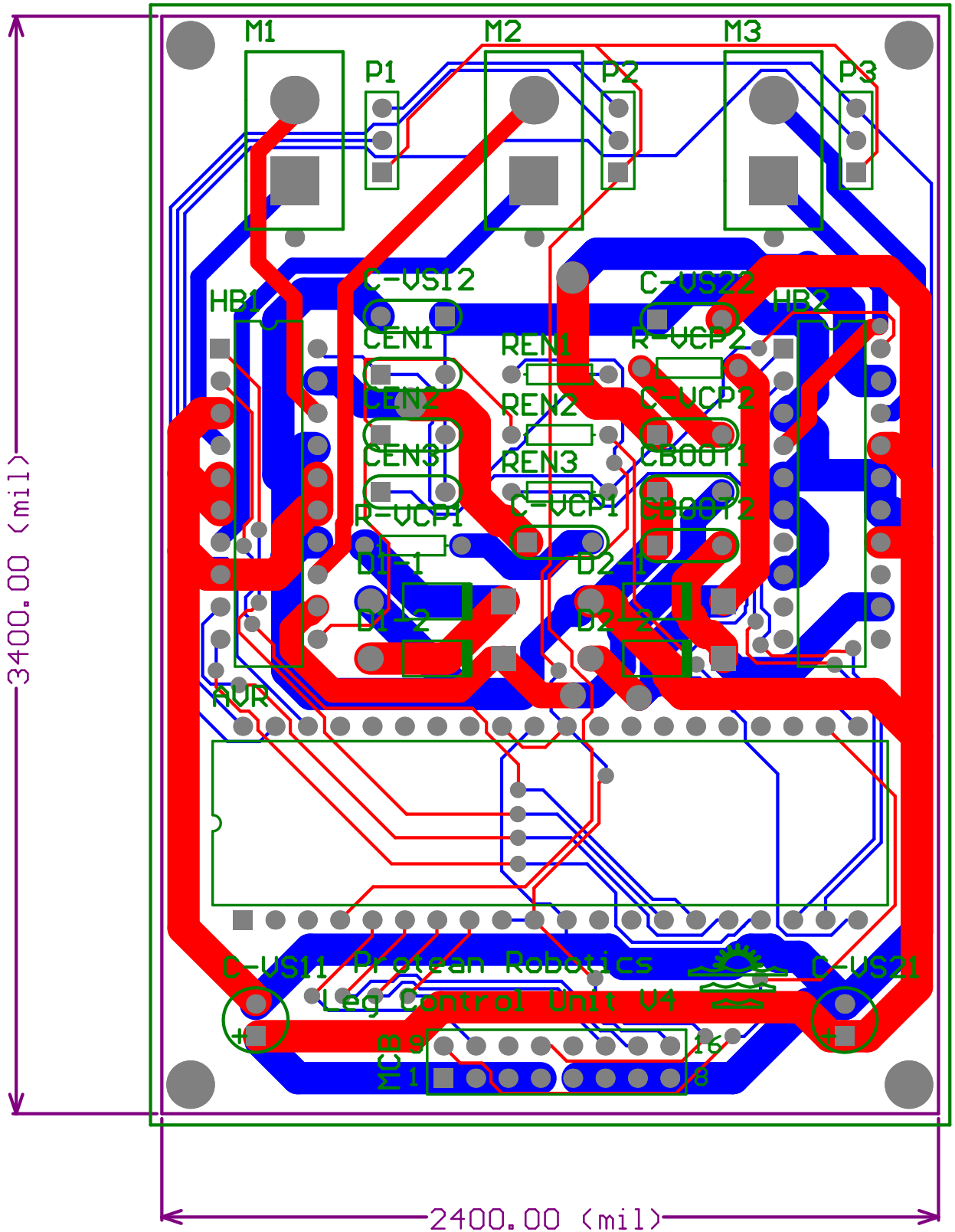
M1
M2
M3
P1
P2
P3
C-VS12
C-VS22
HB1
HB2
CEN1
REN1
R-VCP2
CEN2
REN2
C-VCP2
CEN3
REN3
CBOOT1
R-VCP1
C-VCP1
CBOOT2
D1-1
D2-1
D1-2
D2-2
AVR
C-VS11
Protean Robotics
C-VS21
Leg Control Unit V4
3400.00 (mil)
2400.00 (mil)

Comment	Description	Designator	Footprint	LibRef	Quantity
ATmega164P	8-Bit AVR Microcontroller with 16K Bytes of In-System Programmable Flash Memory	AVR	40P6	ATmega32L-8PC	1
10nF Cap	Capacitor	C-VCP1, C-VCP2	Cap 0.2	Cap	2
100uF PolCap	Polari ed Capacitor A ial	C-VS11, C-VS21	lectrolytic CAP 0.1	Cap Pol2	2
100nF Cap	Capacitor	C-VS12, C-VS22	Cap 0.2	Cap	2
220nF Cap	Capacitor	CB T1, CB T2	Cap 0.2	Cap	2
5.6nF Cap	Capacitor	C 1, C 2, C 3	Cap 0.2	Cap	3
1 4148 Diode	1 Amp eneral Purpose Rectifier	D1-1, D1-2, D2-1, D2-2	DI 10.46-5.3 2.8	Diode 1 4001	4
L6205 H-Bridge	Dual H-Bridge ith 2.8A Ma Per Channel	HB1, HB2	20P3	AT90S1200-4PC	2
Motor Port		M1, M2, M3	.250 2 1 Header	2X1 .25 Header	3
Header 8X2A	Header, 8-Pin, Dual row	MCB	HDR2X8 C	Header 8X2A	1
Pot Port	Header, 3-Pin	P1, P2, P3	HDR1X3	Header 3	3
100 R S	Resistor	R-VCP1, R-VCP2	AXIAL-0.3	Res1	2
100K R S	Resistor	R 1, R 2, R 3	AXIAL-0.3	Res1	3

7.2.MCB Schematics

(Beginning on the following page)

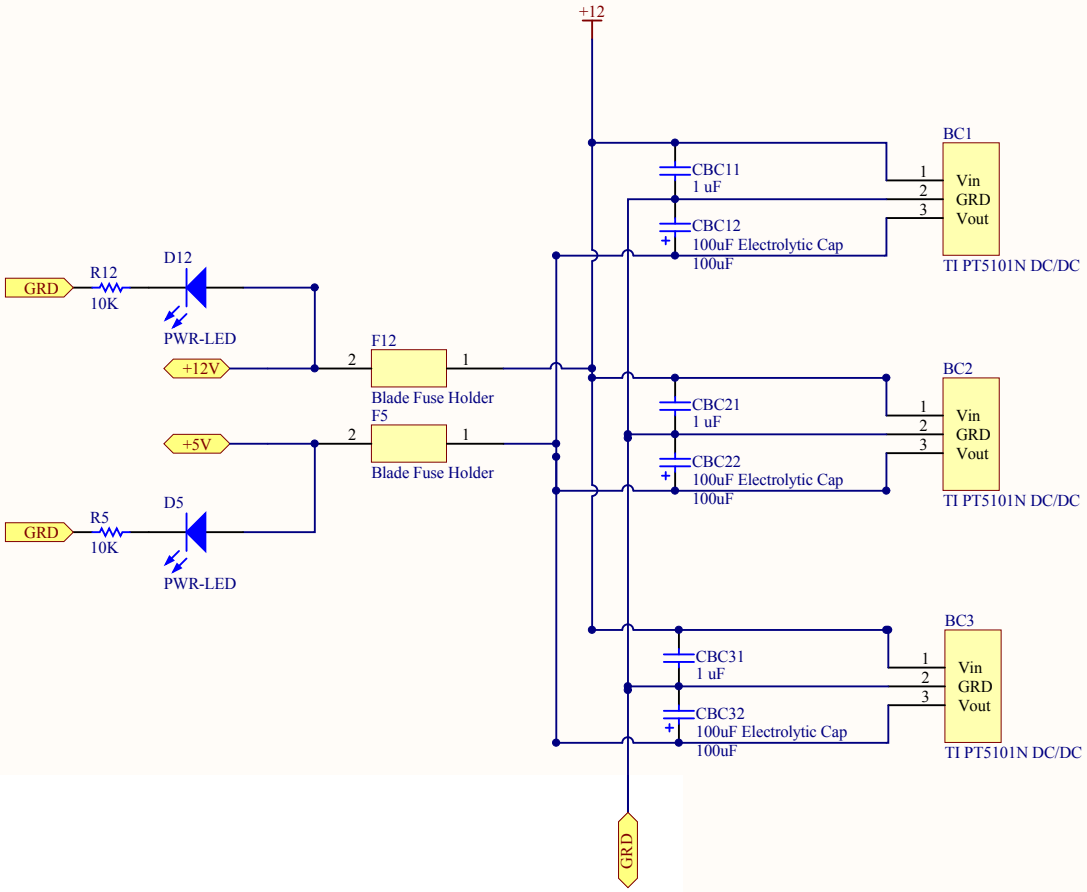

Protean Robotics

Title: Main Control Board (MCB) - Buck Converter		
Size: Letter	Number:	Revision: Version 2.0
Date: 3/10/2010	Sheet 1 of 5	
File: C:\Documents and Settings\..\Buck Converter.SchDoc	Drawn By:	Matt Bienia

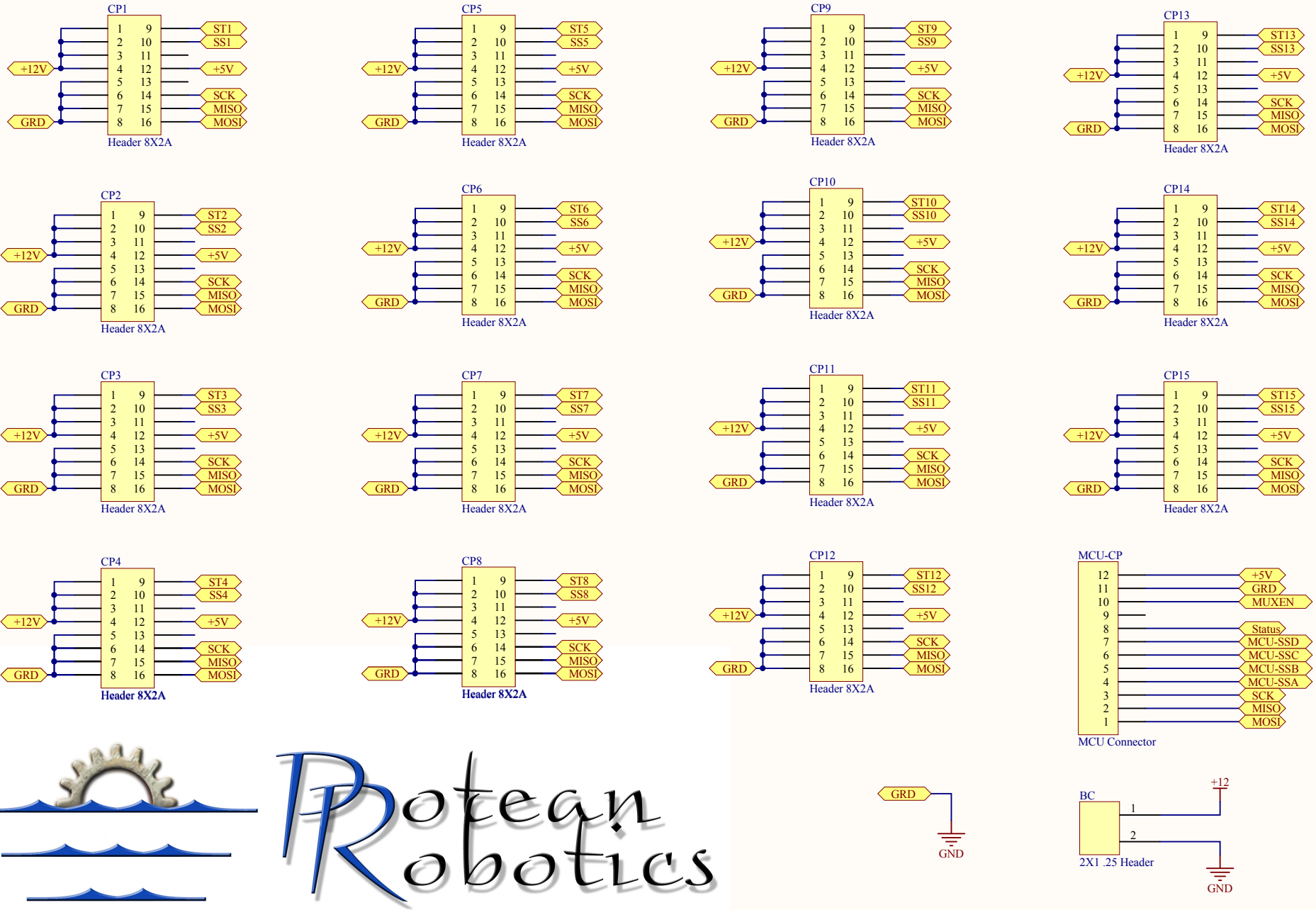

Title: Main Control Board (MCB) - Headers		
Size: Letter	Number:	Revision: Version 1.2
Date: 3/10/2010	Sheet 5 of 5	
File: C:\Documents and Settings\..\Headers.SchDoc	Drawn By: Matt Bienia	

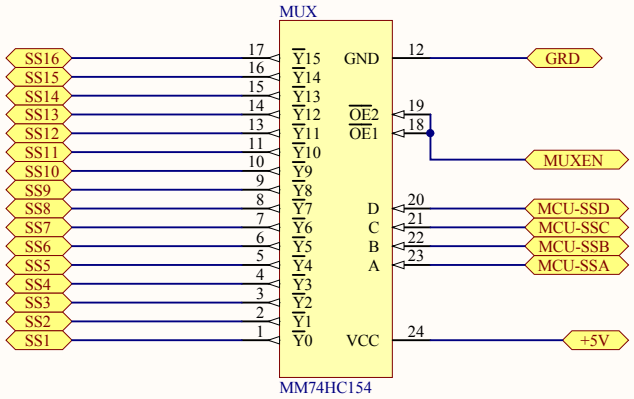

Protean Robotics

Title: Main Control Board (MCB) - Buck Converter		
Size: Letter	Number:	Revision: Version 2.0
Date: 3/10/2010		Sheet3 of 5
File: C:\Documents and Settings\..\Mux.SchDoc		Drawn By: Matt Bienia

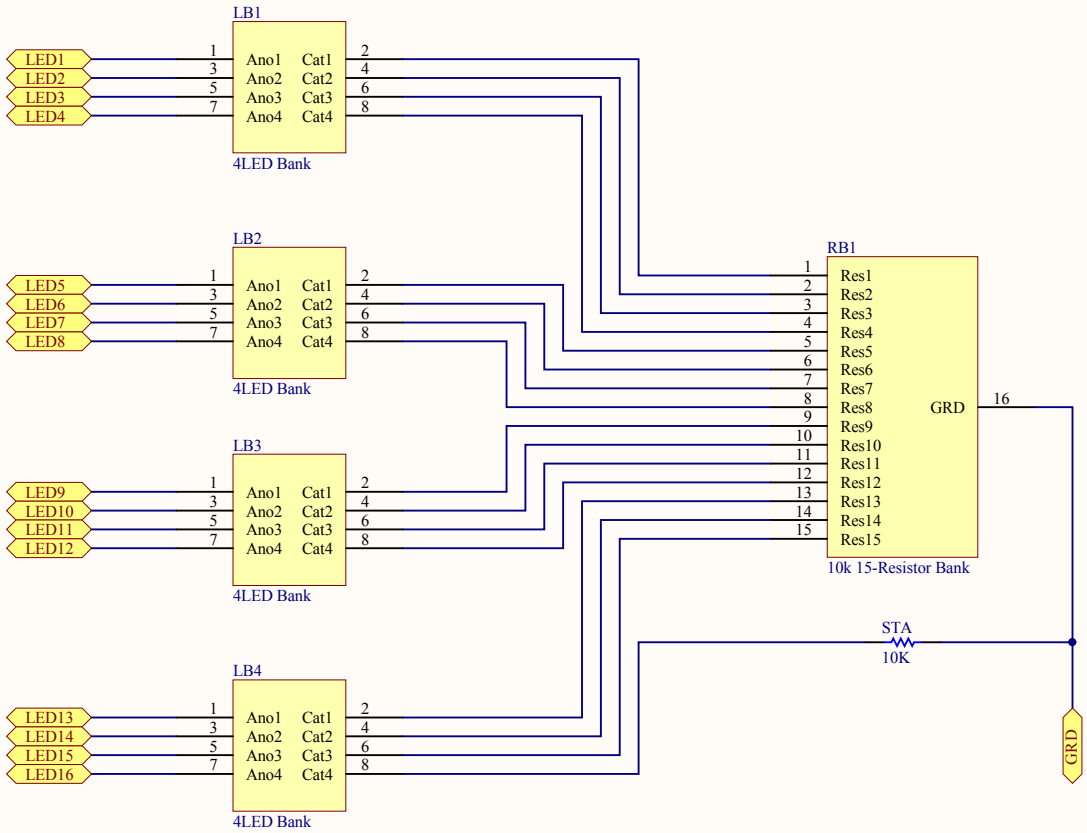

Protean Robotics

Title: Main Control Board (MCB) - Buck Converter		
Size: Letter	Number:	Revision: Version 2.0
Date: 3/10/2010	Sheet 4 of 5	
File: C:\Documents and Settings\..\Signal LEDs.SchDoc	Drawn By: Matt Bienia	

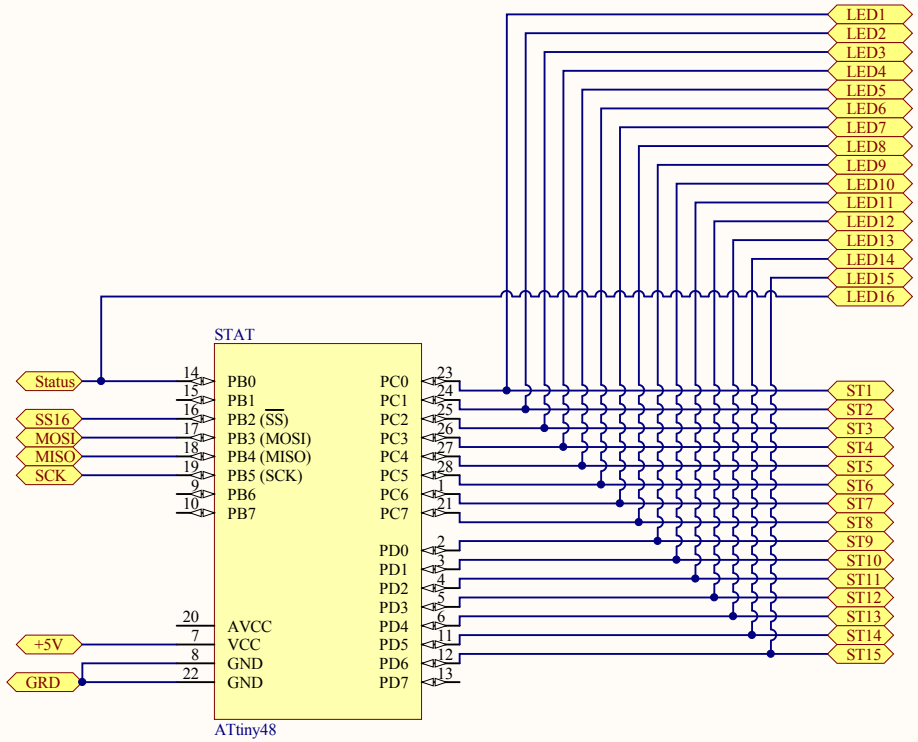

Protean Robotics

Title: Main Control Board (MCB) - Status Chip		
Size: Letter	Number:	Revision: Version 1.2
Date: 3/10/2010	Sheet 2 of 5	
File: C:\Documents and Settings\..\Status Chip.SchDoc	Drawn By: Matt Bienia	

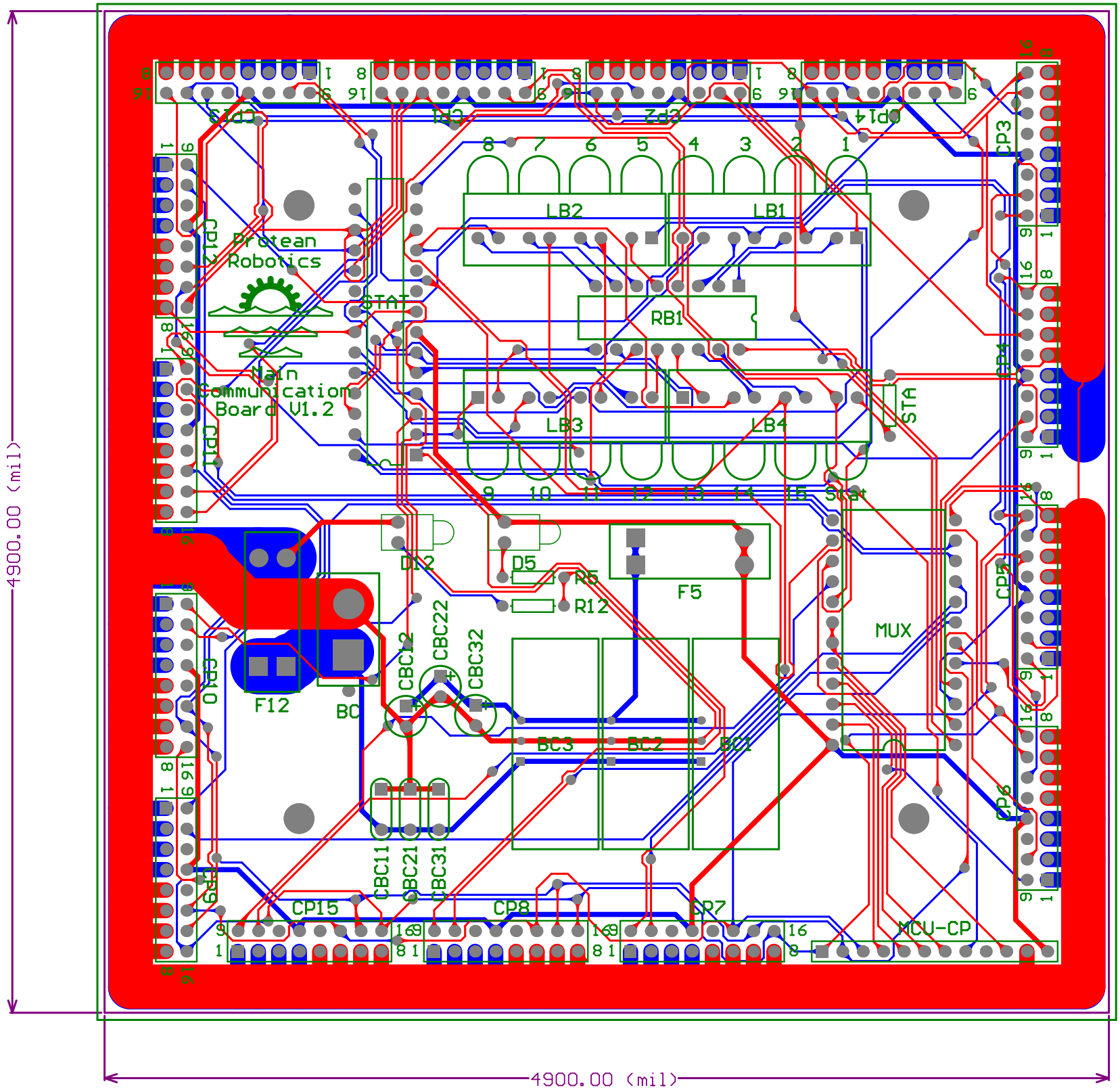
4900.00 (mil)
4900.00 (mil)
Protean
Robotics
Main
Communication
Board V1.2
LB1
LB2
LB3
LB4
RB1
STA
Stat
D12
D5
R5
R12
F5
F12
BC
BC1
BC2
BC3
MUX
CBC11
CBC12
CBC21
CBC22
CBC31
CBC32
CP15
CP8
CP7
MCU-CP

Comment	Description	Designator	Footprint	LibRef	Quantity
2X1 .25 Header		BC	.250 2 1 Header	2X1 .25 Header	1
TI PT5101 DC DC	1A 12V To 5V DC DC Buc Con erter	BC1, BC2, BC3	PT5101 DC DC	TI PT5101 9-36 DC 5DC	3
1uF Cap	Capacitor	CBC11, CBC21, CBC31	Cap 0.2	Cap	3
100uF lectrolytic Cap	Polari ed Capacitor A ial	CBC12, CBC22, CBC32	lectrolytic CAP 0.1	Cap Pol2	3
Header 8X2A	Header, 8-Pin, Dual row	CP1, CP2, CP3, CP4, CP5, CP6, CP , CP8, CP9, CP10, CP11, CP12, CP13, CP14, CP15	HDR2X8 C	Header 8X2A	15
P R-L D	Typical R D aAs L D	D5, D12	L D-1	L D1	2
Blade Fuse Holder		F5, F12	BLAD FUS H LD R	Blade Fuse Holder	2
4L D Ban		LB1, LB2, LB3, LB4	SIP8 0.1	4-5mmL D Ban	4
MCU Connector	Header, 12-Pin	MCU-CP	HDR1X12	Header 12	1
MM 4HC154	4-Line to 16-Line Decoder Demultiple er	MUX	DIP-24 600mil	DM54LS154	1
10K R S	Resistor	R5, R12, STA	AXIAL-0.3	Res1	3
10 15-Resistor Ban		RB1	DIP16 0.1	15Resis DIP16 0.1	1
ATtiny48	8-Bit AVR Microcontr	STAT	28P3	ATtiny28L-4PC	1

7.3.MPU Schematics

(Beginning on the following page)

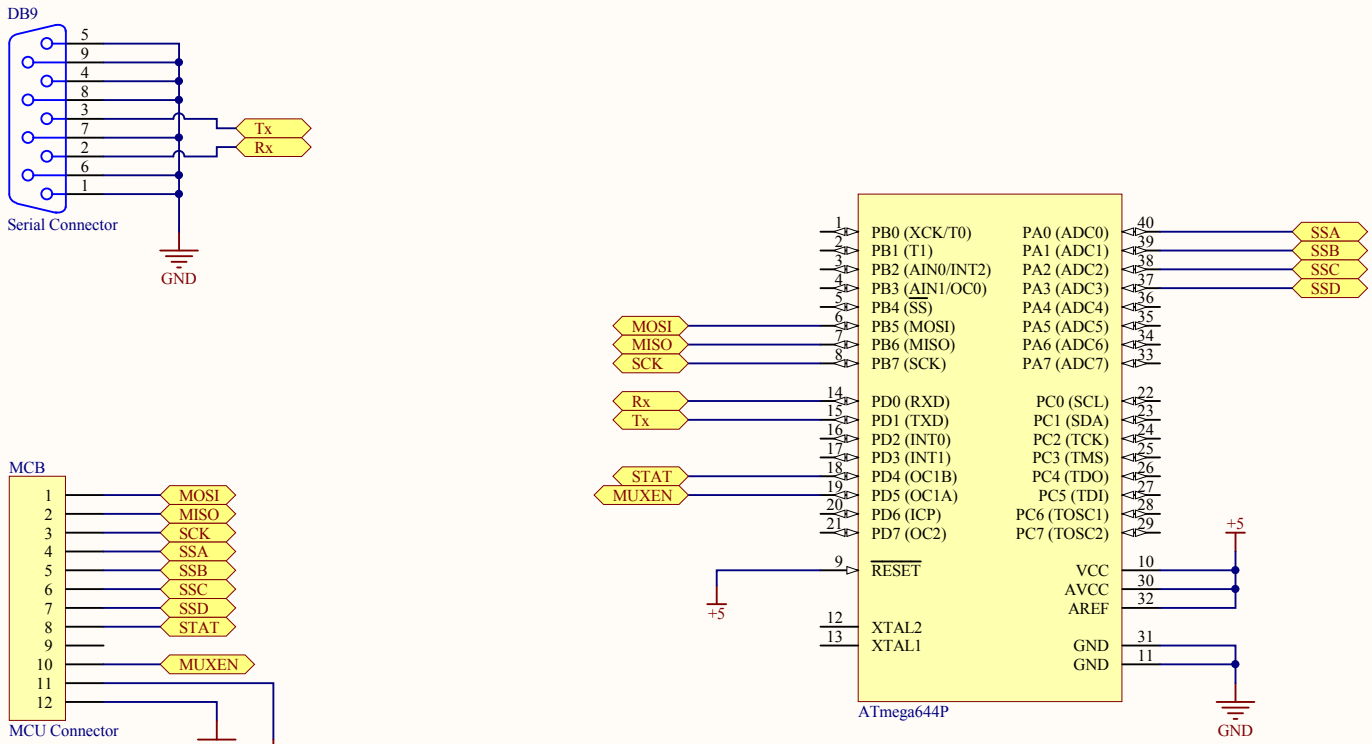

Title: Main Processing Unit		
Size: Letter	Number:	Revision: V1.1
Date: 2/8/2010		Sheet 1 of 1
File: C:\Documents and Settings\..\MCU V1-1.SchDoc		Drawn By: Matt Bienia

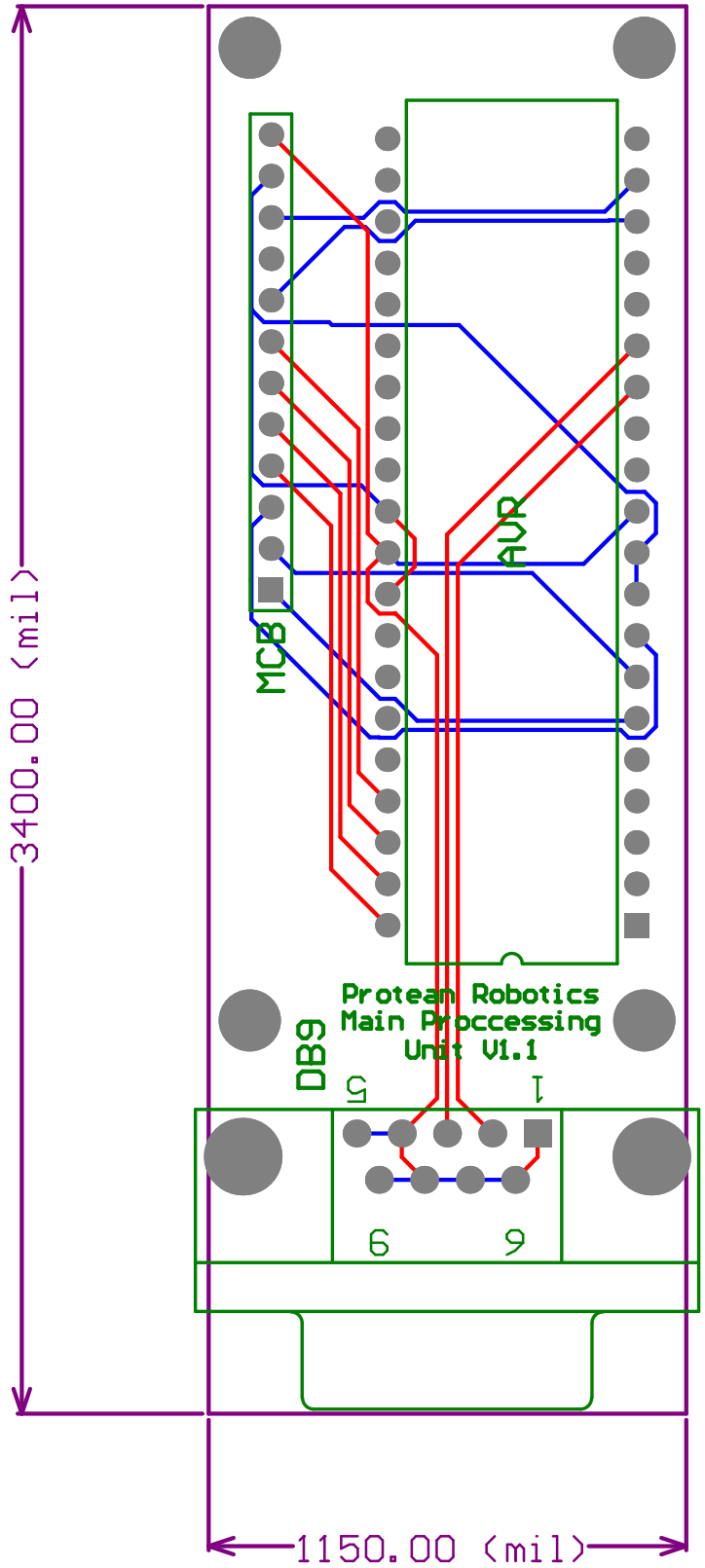
3400.00 (mil)
1150.00 (mil)
MCB
AVR
DB9
Protean Robotics
Main Proccessing
Unit V1.1
5
1
6
9

Comment	Description	Designator	Footprint	LibRef	Quantity
ATmega644P	8-Bit AVR Microcontroller with 64K Bytes of In-System Programmable Flash Memory	AVR	40P6	ATmega32L-8PC	1
Serial Connector	Receptacle Assembly, 9 Position, Right Angle	DB9	DSUB1.385-2H9	D Connector 9	1
MCU Connector	Header, 12-Pin	MCB	HDR1X12	Header 12	1